UNIVERSITÀ DEGLI STUDI DI PADOVA

DIPARTIMENTO DI MEDICINA
Direttore: Prof. Angelo Gatta
EMATOLOGIA ED IMMUNOLOGIA CLINICA
Direttore: Prof. Gianpietro Semenzato

Analysis of Protein Kinase CK2 in B-lymphopoiesis and lymphomagenesis in a mouse conditional Knockout model

Direttore della Scuola: Ch.ma. Prof. Paola Zanovello

Supervisore: Dott. Francesco Piazza

Dottorando: Fortunato Zaffino

INDEX

Results   pag. 69

ABBREVIATIONS

AA	Aminoacid
Ab	Antibody
AcMo	Monoclonal Antibody
APC	*Antigen Presenting Cells*
ATP	Adenosine triphosphate
ATF6	activating transcription factor 6
BAFF	*B-Cell Activating Factor*
BCR	*B Cell Receptor*
BCL-2	B cell lymphoma 2
BCL-6	B cell lymphoma 6
BM	bone marrow
BSA	bovine serum albumin
BTK	*Bruton's Tyrosine Kinase*
Cdc37	cell division cycle protein 37
CK2	protein kinase CK2
CK2β	β subunit of protein kinase CK2
CTRL	control
DL1	delta ligand
dNTPs	deoxyribonucleotide
dpc	*days post coitum*
DTT	Dithiothreitol
EDTA	Ethylenediaminetetraacetic acid
EGTA	ethylene glycol tetraacetic acid
FCS	fetal calf serum
floxed	flanked by loxP sites
FoB	follicular b-cells
FoI	follicular b-cells tipe I
FoII	follicular b-cells tipe II
FSC	*Forward Scatter*
Hsp90	heat shock protein 90
Ig	immunoglobulin

IL4	Interleukin 4
KO	knockout
LPS	Lipopolisaccaride
MAPK	mitogen-activated protein kinase
MDP	Macrophages-dendritic cells progenitor
MUT	Mutant
MZ	marginal zone
MZB	marginal b-cells
MZP	marginal zone precursor
NF-κB	nuclear factor kappa-light-chain-enhancer of activated B cells
N-terminale	amino terminale
PBS	phosphate buffer solution
PI3K	Phosphatidyl-inositol-3-phosphate kinase
PKB/Akt	protein kinase B/Akt
rpm	round per minute
SD	standard deviation
SDS	Sodium dodecyl sulfate
SDS-PAGE	Polyacrylamide gel electrophoresis in SDS
SP	Spleen
SRBC	Sheep Red Blood Cell
TAE	Tris-acetate-EDTA
TBS	tris buffer solution (buffer solution Tris-HCl)
TCR	T cell receptor
Tm	melting temperature
Tris	tris(hydroxymethyl)aminomethane
UPR	unfolded protein response
WB	Western Blotting
WT	wild type

AMINO ACID ABBREVIATIONS

A	Ala	Alanine
C	Cys	Cysteine
D	Asp	Aspartic acid
E	Glu	Glutamic acid
F	Phe	Phenylalanine
G	Gly	Glycine
H	His	Histidine
I	Ile	Isoleucine
K	Lys	Lysine
L	Leu	Leucine
M	Met	Methionine
N	Asn	Asparagine
P	Pro	Proline
Q	Gln	Glutamine
R	Arg	Arginine
S	Ser	Serine
T	Thr	Threonine
V	Val	Valine
W	Trp	Tryptophan
Y	Tyr	Tyrosine
X	generic amino acid	

ABSTRACT

Serine-threonine protein kinase CK2 has been recently involved in the pathogenesis of B-cell tumors, such as B acute lymphoblastic leukemia, B chronic lymphocytic leukemia, mantle cell lymphoma and multiple myeloma. CK2 acts through a "non-oncogene" addiction mechanism to propel tumor growth, protecting from apoptosis by a phosphorylation-dependent "shielding" mechanism of pro-survival molecules and stimulating oncogenic kinases by helping folding and enzymatic activity. In addition existing data on CK2 function in B-cell tumors suggest that this kinase might act as a "hub" downstream signals from surface membrane molecules, like the B-cell (BCR), growth factor and cytokine receptors, as well as from cell-intrinsic pathways – like proteotoxic and DNA-damage-related stress cascades.

To gain insights into the role of CK2 in B-lymphopoiesis and, consequently, in B-cell tumors, we generated CK2β conditional knockout (KO) mice in B-cells by crossing CK2β-Flox/Flox mice with CD19-CRE transgenic mice. CK2 kinase activity was decreased in CK2β KO B-cells. In the bone marrow (BM), CK2β KO mice displayed a reduction of B-cells, especially of the recirculating population of transitional and follicular (FO) B-cells. Pro-B and pre-B-cell progenitors were slightly reduced in number. In peripheral blood, lymph-nodes, spleen and peritoneal cavity the number of B-cells was markedly reduced. CK2β KO mice displayed lower levels of all the immunoglobulin classes in the serum. In the spleen of CK2β KO we observed an imbalance between the amount of FO and marginal zone (MZ) B-cells was found with an absolute reduction of FO B cells by approximately 2-folds and an increase of MZ B-cells and MZB cell precursors by up to three folds. Histological and immunofluorescence (IF) analysis revealed a change of size/shape of spleen follicles and a significant expansion of the inter-follicular, marginal zone areas, which appeared to invade the follicle with larger cells. *In vitro* class-switch recombination assays demonstrated impairment in IgG_1 and IgG_3 class-switch and a marked reduction of the generation of antibody-producing cells.

In vivo sheep red blood cells (SRBC) treatment (T-cell dependent response) showed a conserved up-regulation of germinal center (GC) markers, such as CD38, GL7 and

PNA. Nonetheless, the architecture of the reactive follicles was found markedly changed. The analysis of FO, GC and MZ-associated genes showed normal levels of Bcl6, elevated levels of Lrf mRNA and, more significantly, a marked up-regulation of Notch2 target genes, such as *hes*1 and *deltex*1, in CK2β KO B-cells. *In vivo* Notch2 blockage with neutralizing antibodies markedly reduced the MZB cell number in CK2β KO mice, indicating a Notch2-dependent MZB expansion associated with CK2β loss. High throughput RNAseq analysis was also performed and revealed significant alterations in FOB and MZB-regulating pathways.

Here, we found that the β subunit of protein kinase CK2 is a novel regulator of peripheral B cell differentiation. CK2β sustains a proper BCR signal, controls the GC reaction and negatively regulates Notch2 signaling, acting as a master regulator of follicular/marginal zone architecture and terminal homeostasis of FOB and MZB cells. On one side our data enrich the knowledge on the mechanisms regulating B-cell development, on the other side they inform about the potential mechanisms altered by CK2 during B-cell tumorigenesis.

RIASSUNTO

CK2 è una serin-treonin chinasi pleiotropica costituita da due subunità α catalitiche e due subunità β regolatorie. Recentemente questa proteina è stata coinvolta nella patogenesi di neoplasie delle cellule B del sistema ematopoietico, come la Leucemia Linfatica Cronica (CLL), il Linfoma Mantellare (MCL) ed il Mieloma Multiplo(MM).

CK2 agisce attraverso un meccanismo definito "*non - oncogene addiction*", favorendo la sopravvivenza delle cellule neoplastiche proteggendole dall' apoptosi, attraverso la fosforilazione di proteine pro-sopravvivenza e stimolando chinasi oncogeniche attivando, in questo modo, la loro attività enzimatica.

Alcuni studi inerenti il ruolo di CK2 nelle neoplasie di tipo B, suggeriscono che questa chinasi potrebbe agire a valle di recettori di fattori di crescita e citochine.

Sulla base di questi dati, per ottenere maggiori informazioni sul ruolo di CK2 nella B-linfopoiesi e, di conseguenza, su un suo ipotetico ruolo nello sviluppo di neoplasie B, abbiamo generato un knockout (KO) condizionale della subunità β di CK2 esclusivamente nei linfociti B, incrociando topi CK2β Flox / Flox con topi transgenici CD19 - CRE.

Mediante approfondite analisi abbiamo dimostrato che l'attività chinasica di CK2 risulta diminuita nelle cellule di topi CK2β KO. Nel midollo osseo, i topi KO evidenziano una riduzione delle cellule B, in particolare della popolazione di linfociti B ricircolanti, mentre l'analisi dei precursori dei linfociti B, cioè i pro-B e i pre-B, evidenzia che essi sono solo leggermente ridotti.

In sangue periferico, milza e cavità peritoneale si ha una marcata riduzione dei linfociti B, in più i topi CK2β KO presentano nel siero una ridotta quantità di immunoglobuline di tutte le classi (ipogammaglobulinemia).

Un'analisi approfondita dei linfociti B splenici ha evidenziato che nei topi CK2β KO si ha uno squilibrio tra la quota di linfociti B della zona follicolare (FO) ed i linfociti B della zona marginale (MZ).

L'analisi istologica e l'immunofluorescenza, effettuate su milze di topi CK2β KO, hanno rivelato entrambe un cambiamento di dimensione/forma dei follicoli ed una significativa espansione della zona marginale, che sembra invadere il follicolo stesso.

Attraverso un approccio *in vitro* abbiamo valutato lo *switch* isotipico, dimostrando che, nei topi CK2β KO, si ha una compromissione dello *switch* verso IgG1 e IgG3 ed una marcata riduzione della produzione di cellule secernenti anticorpi.

In vivo, il trattamento con globuli rossi di montone (SRBC) ha mostrato una conservata regolazione di marcatori del centro germinativo (GC), quali CD38, GL7 e PNA; tuttavia, l'architettura dei follicoli nei topi CK2β KO presenta, rispetto ai topi di controllo, un evidente cambiamento architettonico/topografico.

L'analisi, mediante *Real-Time PCR*, di geni associati alle zone follicolare e marginale, oltre che al centro germinativo, ha messo in luce, che i topi CK2β KO hanno livelli normali di bcl6 , elevati livelli di espressione di lrf e, soprattutto, una mancata up-regolazione di geni coinvolti nel *pathway* di Notch2, come *hes1* e *deltex1*.

Sulla base di quest'ultimo dato, abbiamo ritenuto risolutivo bloccare *in vivo* il recettore Notch2, mediante l'utilizzo di uno specifico anticorpo neutralizzante evidenziando, nei topi CK2β KO, una notevole riduzione del numero dei linfociti B marginali. Un'analisi *"High-Throughput"* , mediante RNA-seq, ha rivelato, nei topi CK2β KO, una significativa alterazione dei processi che regolano la formazione di MZB o FoB.

Dai risultati di questo studio si può, quindi, ipotizzare che la subunità β della protein chinasi CK2 sia un nuovo regolatore del processo di differenziamento dei linfociti B periferici. Inoltre, CK2β sembra implicata nella corretta trasmissione del segnale a valle del BCR, nella reazione di formazione del GC e nella regolazione del *pathway* di Notch2. Possiamo, perciò, definirla un nuovo "*master regulator*" del differenziamento di FoB e MZB e della definizione dell'architettura topografica della zona marginale della polpa bianca splenica.

In conclusione, i dati ottenuti con questo lavoro di tesi, da un lato arricchiscono la conoscenza dei meccanismi che regolano lo sviluppo dei linfociti B, dall'altro ci danno informazioni sui potenziali meccanismi su cui agisce CK2 durante lo sviluppo di neoplasie dei linfociti B.

1. INTRODUCTION

1.1. General characteristics of B-cells

B lymphocytes are a type of lymphocytes of the humoral immunity of the adaptive immune system. They are specialized in the production of immunoglobulins (Ig) to generate an immune response. The Ig produced can be surface or soluble antibodies and are the specific receptors for antigens. Typically, B-cells express on the plasma membrane two different forms of Ig_s with the same specificity: IgD and IgM ; only a few, express IgG , IgA or IgE.According to the Porter model of 1962 , the antibodies have four chains: two heavy (H, 50-77 kDa) and two light (L , 25 kDa) . The light chains are divided into two types (κ and λ), those heavy in five, and correspond to the respective classes of Ig_s (γ , α , μ , δ and ε). The chains possess both a constant (C) and a variable region (V). Light chains have two disulfide bonds , while, in the heavy, bridges are a total of four . Each of these links leads to the formation of a ring which represents the central portion of a larger region , defined "domain" , consisting of 110 residues . The domain constitutes the aforementioned variable region : VL for the light chains and VH for the heavy. The variable regions of the heavy and light chains associate one another to form the binding site for the antigen , whose specificity depends on the amino acids present in the chains.

Thus, antibodies with different specificities have different amino acid sequences in the V region , the diversity of which are rooted in events of " gene recombination " at the level of the *loci* for both types of chains (**Fig.1**).
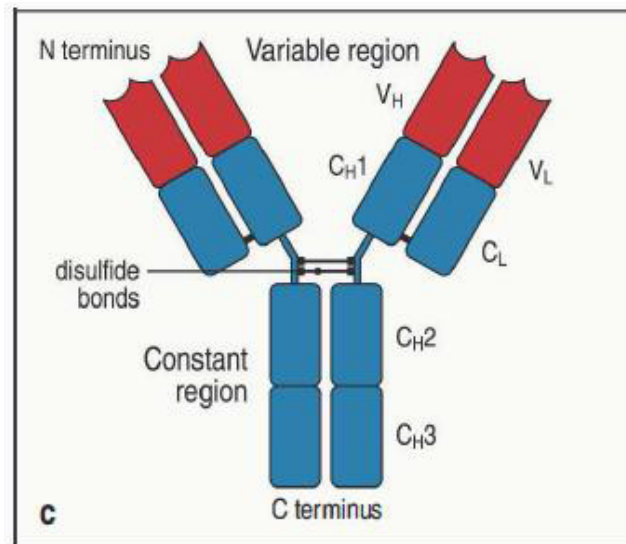
*Fig.1: **structure of antibodies** (Modified from Murphy K., Janeway's Immunobiology. 8th. Garland Science. 2012).*
The antibodies have a quaternary structure composed of two light and two heavy chains. The figure shows variable (red) and constant (blue) portions and disulfide bonds.

The B-Cell Receptor (BCR), which plays a key role in the activation of B lymphocytes , is a transmembrane receptor , constituted by an extracellular portion, which binds the antigen and an intracellular region, capable of signal transduction . This region is linked by disulfide bridges with an heterodimer , called Ig - α / Ig – β (or CD79a and CD79b). Each member of the dimer passes through the plasma membrane and has a cytoplasmic tail containing an Immunoreceptor Tyrosine-based Activation Motif (ITAM)[37].

The binding of the antigen with the BCR triggers four main processes :

1) proliferation of B lymphocytes;

2) differentiation into plasma cells (PC)

3) formation of memory cells;

4) antigen presentation to T cells [37]

BCR initiates signal transduction using Src kinases; then in the process is involved a costimulatory complex, CD21 - CD19 - CD81 - Leu13 , which implements the transduction activity. This binding causes a conformational change of the CD19 receptor and a consequent increase in the intracellular signal . Subsequently , the antigen binds the surface Igs, the B cell internalizes the Ac- Ag complex, processes and expresses antigenic epitopes in the major histocompatibility complex (MHC) and presents them to T cells (**Fig.2**).

The main function of B-cells is to produce antibodies, but they may perform other functions in the immune response through the expression of Toll Like Receptors (TLR). TLRs are membrane glycoproteins that are able to recognize a large amount of proteins derived from pathogens and the activation of TLRs triggers inflammatory responses [9]. B-cells express high levels of TLR- 9 and TLR-10, which are increased after the activation of the BCR or following the activation of the CD40 molecule.

By means of the TLR-9, B-cells may perform functions typical of the innate immune response , as the receptor recognizes un methylated CpG genomic regions, typical of bacteria with a DNA genome, and is involved in the initial responses to microorganisms. The inducible expression of TLRs in B-cells can , therefore , be a link between the innate and the acquired immune responses [8].

B-cells may also produce inflammatory cytokines (IL-6,IL-10) that induce the differentiation of naïve T cells into T helper 1 (Th1) and T helper 2 (Th2) and secrete factors that may directly mediate the destruction of pathogens . Finally, they can also function as APC , which are capable of internalizing antigens and present them in MHC-II.

B-cell development is a highly regulated process, that occurs in multiple steps during which B-cells undergo cellular and genetic changes. Firstly in the bone marrow from hematopoietic precursors to immature B-cells, then in periphery from transitional to mature B-cells.
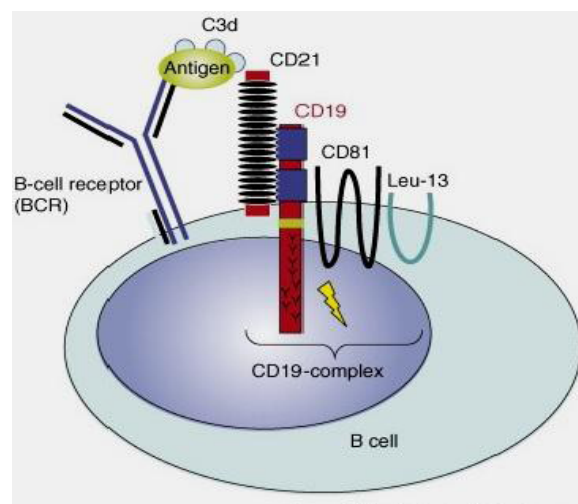

Fig. 2: Activation of the BCR complex and costimulatory molecules CD21 - CD19 - CD81 - Leu13 (Modified from Schäffer. A.A., Current Opinion in Genetics & Development;2007).

1.1.1 The bone marrow

The bone marrow (BM) is the body delegated to haematopoiesis and is crossed by a nutritive artery , which enters the cavity of the bone marrow and here divides into ascending and descending arteries (**Fig.3**). Since these are divided radial arteries, that vascularize endosteum and periosteum through a dense network of capillaries.

The capillaries converge in vascular sinuses , which are sinusoidal vessels [35].

Through the wall of the vascular sinuses mature cells, produced by the BM, go into the blood, while blood cells migrate from the blood in the bone to be removed or to perform specific functions in the processes of defense and immunity (monocytes, granulocytes, lymphocytes). The wall of the vascular sinuses is composed of three layers: endothelium , basal lamina and an incomplete adventitial layer.

The endothelial cells form a continuous foil, not being connected by specialized junctions, are separated by wide gaps , through which the cellular elements can pass in both directions. The endothelium rests on a fenestrated membrane rich in proteoglycans. Outside the basal lamina there is a third layer , which is constituted by fenestrated adventitial cells too. These cells have phagocytic activity that prevents damaged cells to go into the bloodstream.
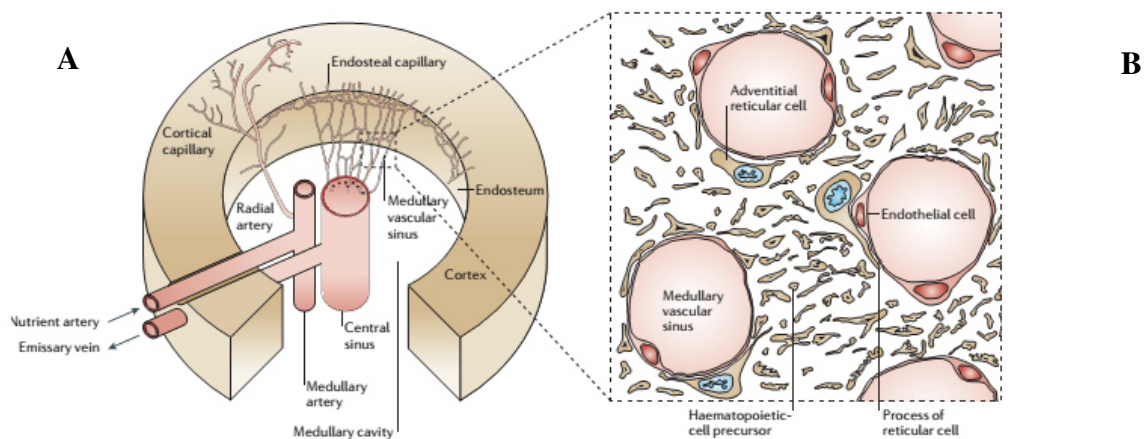
Fig. 3: Bone marrow structure (Modified from Nagasawa T., Nature Reviews Immunology 2006).
A. The main blood source to the bone marrow is provided by the nutrient artery. The nutrient artery crosses the cortex through the nutrient canal into the medullary cavity, where it divides into ascending and descending arteries, from which radial arteries. B. The medullary sinuses in the central cavity of the bone are surrounded by endothelial cells and reticular cells adventitious . The hematopoiesis occurs extravascular spaces between her breasts.

B-cells are generated from hematopoietic stem cells (HSCs) in the liver during the fetal life [20] and the same mechanism occurs in adults BM. The differentiation's pathway from HSCs to mature B-cells can be divided into several processes based on phenotype and functional characteristics that are gradually acquired by cells of the line B [30-46].

Phenotypically, HSCs express high levels of the receptor tyrosine kinase (c-KIT) and the Stem Cell Antigen 1 (SCA-1)[4]. This is a phosphatidyl inositol membrane molecule, which plays a key role in signal transduction during differentiation.

The precursor stem cells closest to the pre–pro B are the *Common Lymphoid Progenitors* (CLP), which have a low level of c-KIT and SCA1 , but a high level of IL 7R [14].

The precursors (pre-proB, proB , preB) are identified by a different expression of CD43 and CD25 (IL2Rα). CD43 is a membrane protein present from the early stages of B lymphocytes differentiation, until the end of the rearrangement of the heavy chains μ. CD43 is , therefore , the cell marker of pre - proB and proB.

In the bone marrow are also present recirculating mature B lymphocytes, and PCs expressing CD138 [28].

Differential expression of heat-stable antigen (HSA) and of the maturation marker BP-1 discriminates four fractions of pro-B cells (A, B, C, and C9). At this stage of development, DNA rearrangement begins in the Ig H chain locus. Most pro-B cells of fraction A carry Ig genes in germline configuration. DH→JH rearrangements are found in almost all cells of fraction B. VH→ DHJH rearrangement occurs in fractions C and C9. Cells in fractions B to C9 are also called pre-B I cells. As soon as mH chain proteins appear in the cytoplasm and can be assembled into a functional precursor B cell receptor (pre-BCR), pre-B I cells develop into large pre-B II cells that are c-KIT and CD43 negative. Successful rearrangement of the H chain and a correctly assembled pre-BCR associate with a functional signaling machinery that allow pre-B II cells to proliferate. [8] The pre-BCR complex plays a critical role in the clonal expansion of μ+ pro-B cells and differentiation to the pre-B cell stage. Pre-B cells undergo Ig L chain rearrangement and the resultant L chain associates with μ heavy chain to form the membrane bound IgM, in addition the signal produced by the pre - BCR receptor activates the trophic factor *Nuclear Factor kappa-light-chain-enhancer of activated B-cells* (NF-kB) [11-35].

After successful rearrangement of both heavy and light chain genes, the BCR, which includes Igα and Igβ, is assembled and expressed on the surface of B-cells. The BCR functions as an antigen-binding and signal transduction molecule during further B cell development.

At the end of this process of development, B-cells leave the bone marrow , coming out from the vascular sinuses, to complete the maturation in secondary lymphoid organs (**Fig.4**).
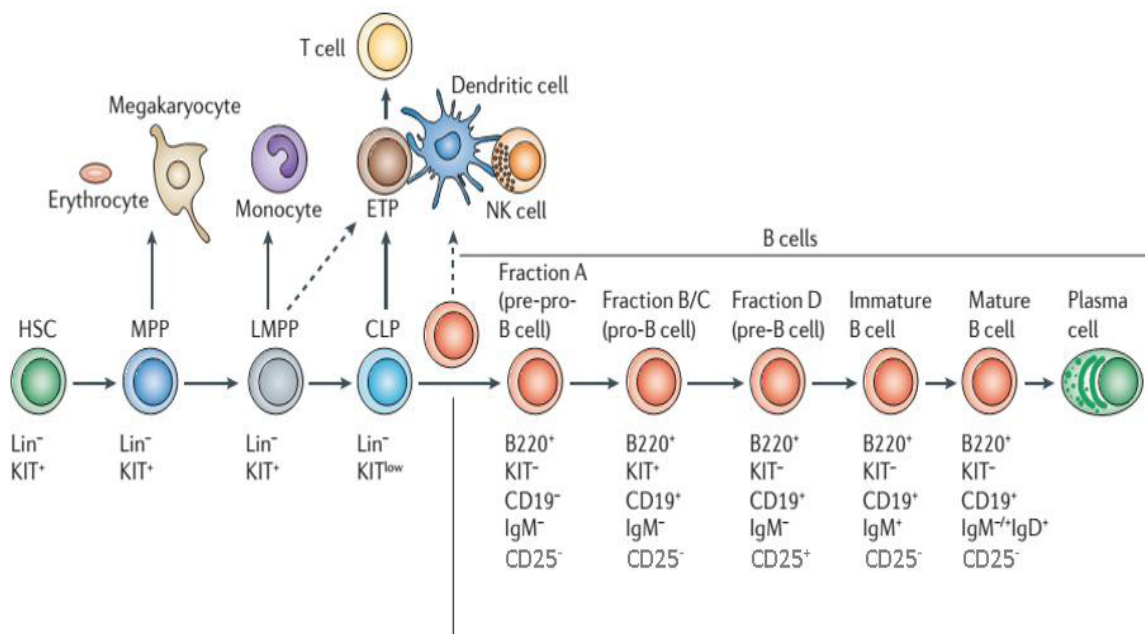
Fig.4: Steps of the B-cell differentiation (Modified from Nagasawa T., Nature Reviews Immunology 2006).
The blood cells originate from a common precursor the HSC. The stem cell with characteristics closer to the precursors of B-cells is the Common Lymphoid Progenitor (CLP). In the box are highlighted the phases of the B-cells development (pre/proB; proB; preB; immature, mature B and plasma cells) and the corresponding surface markers.

1.1.2 Lymph nodes

Lymph nodes (LN) are bean or oval shaped and are highly organized lymphoid structures placed in the sites of convergence of the vessels that are part of the lymphatic circulation. Each LN is surrounded by a fibrous capsule, and inside the LN the fibrous capsule extends to form trabeculae. LNs are divided into the outer cortex and the inner medulla. The cortex is continuous around the medulla except at the hilum, where the medulla comes in direct contact with the hilum [34].

Thin reticular fibers and elastin form a supporting meshwork called a reticular network inside the node. White blood cells (leucocytes), the most prominent ones being lymphocytes, are tightly packed in the follicles (B-cells) and the cortex (T-cells). Elsewhere in the node, there are only occasional leucocytes. As part of the reticular network there are follicular dendritic cells in the B-cell follicle and fibroblastic reticular cells in the T cell cortex. The reticular network not only provides the structural support, but also the surface for the adhesion of dendritic cells, macrophages and lymphocytes. It allows the exchange of material through high endothelial venules and provides the growth and regulatory factors necessary for the activation and maturation of immune cells (**Fig.5**). The number and composition of follicles can change especially when challenged by an antigen, when they develop a germinal center. Lymph enters the convex side of the lymph node through multiple afferent lymphatic vessels, to flow through the sinuses. A lymph sinus, which includes the subcapsular sinus, is a channel within the node, lined by endothelial cells along with fibroblastic reticular cells and this allows for the smooth flow of lymph through them. The endothelium of the subcapsular sinus is continuous with that of the afferent lymph vessel and is also with that of the similar sinuses flanking the trabeculae and within the cortex. All of these sinuses drain the filtered lymphatic fluid into the medullary sinuses, from where the lymph flows into the efferent lymph vessels to exit the node at the hilum on the concave side. These vessels are smaller and don't allow the passage of the macrophages, so that they remain contained to function within the lymph node. In the course of the lymph, lymphocytes may be activated as part of the adaptive immune response.

The LN's capsule is composed by a dense irregular connective tissue with some plain muscle fibers, and from its internal surface are given off a number of membranous

processes or trabeculae, consisting, in man, of connective tissue, with a small admixture of plain muscle fibers; but in many of the lower animals are composed almost entirely of involuntary muscle. They pass inward, radiating toward the center of the gland, for about one-third or one-fourth of the space between the circumference and the center of the node. In some animals they are sufficiently well-marked to divide the peripheral or cortical portion of the gland into a number of compartments (follicles), but in man this arrangement is not obvious. The larger trabeculae springing from the capsule break up into finer bands, and these interlace to form a mesh-work in the central or medullary portion of the gland. In these spaces formed by the interlacing trabeculae is contained the proper gland substance or lymphoid tissue. The gland pulp does not, however, completely fill the spaces, but leaves, between its outer margin and the enclosing trabeculae, a channel or space of uniform width.

This is termed the subcapsular sinus (lymph path or lymph sinus). Running across it are a number of finer trabeculæ of reticular connective tissue, the fibers of which are, for the most part, covered by ramifying cells [8].

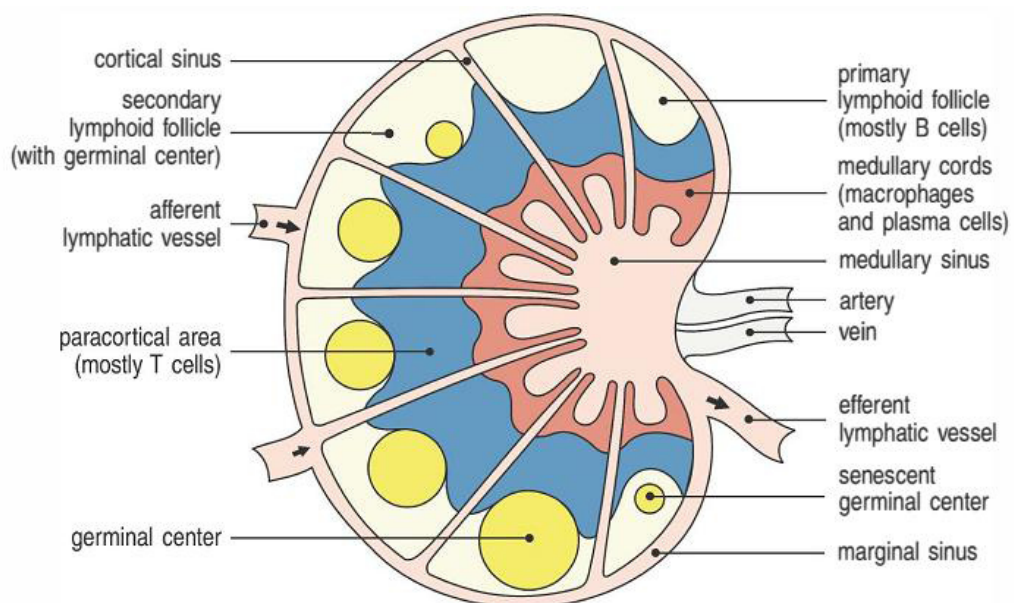*Fig.5: lymph node structure (Modified from Murphy K., Janeway's Immunobiology. 8th. Garland Science. 2012).*
A lymph node consists of a cortex and an inner medulla. The cortex is composed of a cuter cortex of B-cells organized into lymphoid follicles, and deep, or paracortical, are smade up mainly of T-cells and dendritic cells. The medulla consists of strings of macrophages and antibody secreting plasma cells.

1.1.3 The spleen

The spleen (SPL) is a lymphoid organ that is located in the abdominal cavity and is delegated to the removal of senescent erythrocytes , cell debris and micro-organisms present in the blood. It is covered by a connective tissued capsule from which originate highly vascularized trabeculae of connective tissue, which gives rigidity to the body [29]. By trabecular vessels entering the parenchyma of the organ , consisting of red pulp and white pulp (**Fig.6**).
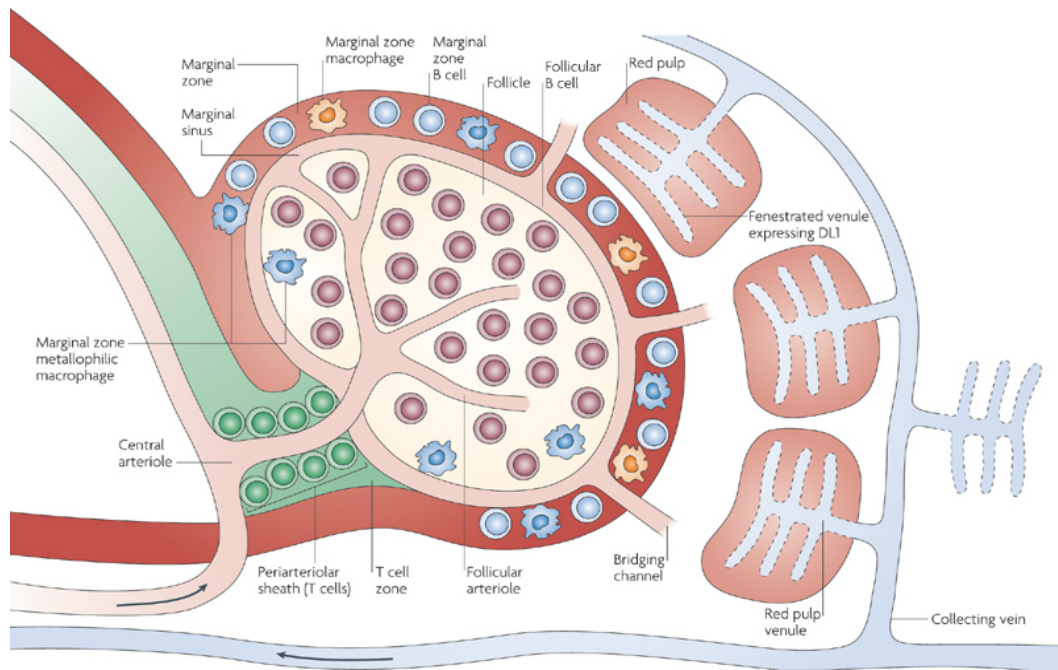
Fig.6: mouse spleen structure (Modified from Pillai and Cariappa; Nature

Reviews Immunology 2009).

The spleen is composed of red pulp and white pulp, the latter plays an immunologic function and is the site where development and differentiation of lymphocytes occurs.
In the white pulp stands a marginal zone, which separates white blood cells from the red pulp, a T-zone and a follicular zone where takes place B-cell differentiation.

Red pulp

In the red pulp of the spleen can be identified two systems : filtering the blood and recycling the iron [29].

Filtering the blood: The specialized structure of the venous system of the red pulp gives this area its unique capacity to filter the blood and remove old erythrocytes.

Arterial blood arrives into cords in the red pulp, which consists of fibroblasts and reticular fibres and forms an open blood system without an endothelial lining.

The contractility of the stress fibres might also aid in the retention of erythrocytes in the spleen thereby forming a reservoir of erythrocytes and reducing stress on the heart by reducing the viscosity of the blood during rest.

Recycling of iron: Erythrophagocytosis is important for the turnover of erythrocytes, and recycling of iron is an important task of splenic macrophages, in conjunction with those of the liver. Erythrocytes are hydrolysed in

the phagolysosome of macrophages, from which haem is released after the proteolytic degradation of haemoglobin.

In addition to such phagocytosis of erythrocytes, a considerable portion of erythrocytes are also destroyed intravascularly throughout the body, as a result of the continuous damage to their plasma membrane. This leads to the release of haemoglobin, which is bound rapidly by haptoglobin. Receptor-mediated endocytosis of CD163, an haemoglobin-specific receptor at the cell surface of macrophages, leads to scavenging of haemoglobin from the circulation in the spleen. Iron is important for survival of both the host and the bacterium.

The red pulp is also known to be the site where plasmablasts and PCs lodge. After antigen-specific differentiation in the follicles of the white pulp, plasmablasts migrate into the red pulp, initially just outside the marginal zone.

The position of plasmablasts in the red pulp resembles the localization of plasmablasts in the medullary cords of lymph nodes, and this extrafollicular antibody production leads to rapid entry of antibody into the bloodstream. The plasmablasts are attracted to the red pulp after upregulating their expression of the CXC-chemokine receptor 4 (CXCR4), which binds the CXC-chemokine ligand 12 (CXCL12), which is expressed in the red pulp. This coincides with downregulation of expression of the chemokine receptors CXCR5 and CC-chemokine receptor 7 (CCR7), which binds the homeostatic

chemokines that are present in B-cell follicles and the T-cell zone of the white pulp [32].

White pulp

The white pulp is organized as lymphoid sheaths, with T- and B-cell compartments, around the branching arterial vessels, so it closely resembles the structure of a lymph node. The correct organization and maintenance of the white pulp is controlled by specific chemokines that attract T and B-cells to their respective domains, thereby establishing specific zones within the white pulp [9].

T cells interact with dendritic cells (DCs) and passing B-cells, whereas in the B-cell follicles (also known as the B-cell zones), clonal expansion of activated B-cells, which leads to isotype switching and somatic hypermutation, can take place. CXCL13 is required by B-cells to migrate to B-cell follicles, whereas CC-chemokine ligand 19 (CCL19) and CCL21 are involved in attracting T cells and DCs to T-cell zones of the white pulp. Expression of these chemokines is controlled by lymphotoxin-$\alpha 1\beta 2$ (LT-$\alpha 1\beta 2$) and tumour necrosis factor (TNF). On the inside of the white pulp is an area in which are located activated follicular and follicular dendritic cells. In the follicles, during the humoral response , these cells generate germinal centers (GCs), which take part in the process of maturation of B lymphocytes , which ends with the formation of PCs and memory cells [28]. In GCs it is possible to distinguish a darker area, where there are proliferating B lymphocytes (centroblasts) and a lighter area , in which there are dendritic cells and where there is the selection and differentiation of the progeny (centrocytes). The outest part of the GC is the mantle zone, where there are no proliferating B-cells, which divide the inner zone of the GC from the T-zone of the white pulp (**Fig.7**) [9-29].

The marginal zone is an important transit area for cells that leave the bloodstream and enter the white pulp. It is constituted by two specific populations of macrophages (marginal zone macrophages and marginal zone metallophilic macrophages) and no recirculating B lymphocytes [28].
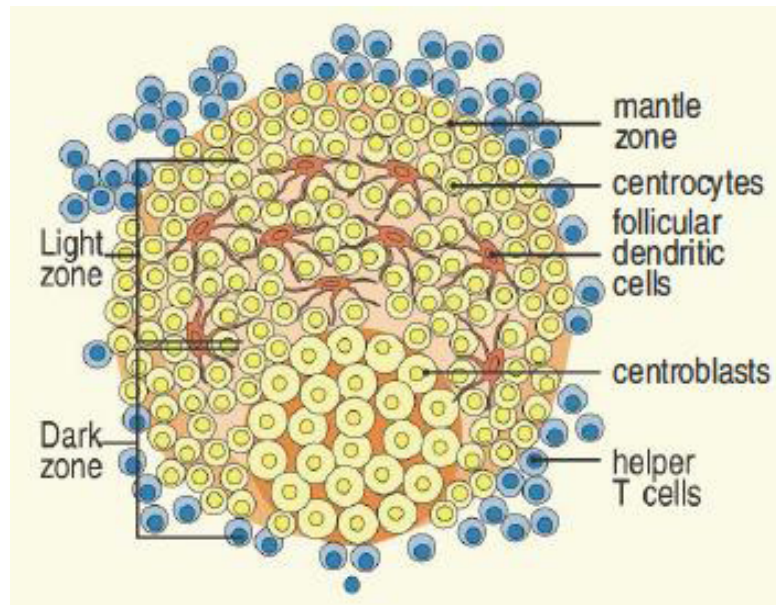
Fig.7: The germinal center (Modified from Murphy K., Janeway's Immunobiology. 8th. Garland Science. 2012)

The germinal center is divided into : mantle zone , light area and dark area . The mantle zone divides the the germinal center from the T-zone and presents especially centrocytes . The light area is composed of centrocytes and dendritic cells , while the dark area is composed of centroblasts.

1.1.4 Splenic B lymphocytes

Peripheral B-cells are lymphocytes that leave the bone marrow after the formation and expression of the BCR.

Mature B lymphocytes, newly formed, that express surface IgM but have not yet come into contact with an antigen, are defined naive B-cells. The differentiation of B lymphocytes, which leads to the formation of PCs, capable of secreting Igs, and memory cells, is in secondary lymphoid organs.

In these organs can be distinguished three main populations of B lymphocytes: transitional, follicular and marginal. Transitional B-cells are the most immature, they express markers of bone marrow precursors and may differentiate in both follicular and marginal B. Follicular B cells reside in the follicle and are responsible for the humoral response with high affinity. MZB are present in the marginal zone and are involved in innate (as APCs) and adaptive (low affinity antibody response) immunity. Based on the differential expression of a series of surface markers it is possible to distinguish different B lymphocytes' subtypes (**Table 1**) [1].

Marker/Cell	AA4.1	IgM	IgD	CD23	CD21	CD1d
T1	+	High	-	-	Low	-
T2	+	High	High	+	Low	-
Fo I	-	Low	High	+	Med	-
Fo II	Low	High	High	+	Med	-
MZP	Low	High	High	+	High	+
MZB	-	High	Low	-	High	+

Table 1: markers of peripheral B-cells (Modified from Allman D. et al., Current Opinion in Immunology. 2008).
The different classes of peripheral B-cells have different patterns of markers that define the state of maturation. AA4.1 is a midollar precursor marker and, in peripheral organs, identifies transitional B-cells. CD23 and IgD are markers of follicular B-cells, while CD21 high and CD1 are markers of marginal B-cells. IgM identifies mature B-cells.

Marginal B-cells(MZB)

In mice, MZB cells are ontogenetically distinct from follicular B cells and B-1 cells, selectively occupy the MZ, have an $IgM^{hi}IgD^{low}CD21^{hi}CD23^{-}$ $CD1d^{hi}$ phenotype and primarily express non-mutated immunoglobulin variable (IgV) genes, some of which encode polyreactive BCRs [9]. These BCRs recognize conserved molecular signatures that are often shared by foreign and autologous antigens. As a result of this promiscuous reactivity, antibodies from mouse MZB can recognize and clear bacteria from the external environment and also damaged cells from the host [28].

Mouse MZB also express high levels of TLRs, similarly to myeloid cells of the innate immune system. This dual expression pattern permits them to uniquely integrate signals from both clonally distributed and germline-encoded microorganism-recognition

receptors. Signals generated via dual BCR and TLR engagement induce the extensive production of low-affinity antibodies by MZB, which bridges the temporal gap required for the production of high-affinity antibodies by FoB cells. In mice, similar signals regulate B cell tolerance, indeed, dysregulated co-engagement of BCR and TLR molecules by self antigens contributes to the onset of autoimmunity through the pathogenic activation of autoreactive B-cells (including MZB) [9]. MZB cells are also specialized in the recognition of complement opsonins via the complement receptors CD21 and CD35 and in the recognition of microbial lipids via the MHC class I-like molecule CD1d. After recognizing a microorganism, these B-cells rapidly give rise to non-mutated antibody-secreting plasmablasts via extrafollicular TI or TD pathways. However, mouse MZ B cells can also generate long-lived PCs that secrete high-affinity antibodies via a canonical follicular TD pathway that involves the presentation of peptide–MHC class II complexes to $CD4^+T$ helper (T_H) cells, including T follicular helper cells (T_{FH} cells). Indeed, mouse MZ B cells have a high expression level of MHC class II, CD80 and CD86 molecules, which are required for the activation of T_{FH} cells.

Mouse MZ B cells are functionally versatile, as they respond to multiple types of microbial challenge, including TI carbohydrate antigens and TD protein antigens.

The development of MZB cells requires the migration of these cells to the region of the marginal sinus and their retention there until they are activated. Clearly, signals for commitment to a MZ B cell fate (through the BCR, Notch2 and the canonical NF-κB pathway) dictate the acquisition of the ability of the committed cell to migrate, differentiate further, self-renew and be retained in the marginal zone. However, a consideration of the anatomy of the spleen and the location of the ligands for Notch2 supports the notion that 'retention' is an equilibrium state [37].

The sphingosine 1-phosphate receptor (S1PR1) participates in marginal zone B-cell migration and retention *in vivo* and is crucial to overcome CXC-chemokine ligand 13 (CXCL13) mediated attraction of B-cells to the follicles. The lymphocyte function-associated antigen 1 (LFA1) and α4β1 integrins on MZ B cells bind to intercellular adhesion molecule 1 (ICAM1) and vascular cell adhesion molecule 1 (VCAM1), respectively, and contribute to the retention of MZ B cells in the marginal zone [37]. The Wiskott-Aldrich syndrome protein (WASP) is a cytoskeletal protein that connects haematopoietic cell surface receptors to the regulation of actin polymerization through the activation of the ARP2–ARP3 complex. The lymphocyte function-associated

antigen 1 (LFA1) and α4β1 integrins on MZ B-cells bind to intercellular adhesion molecule 1 (ICAM1) and vascular cell adhesion molecule 1 (VCAM1), respectively, and contribute to the retention of MZ B cells in the marginal zone [19].

Follicular B-cells (FoB)

FoB cells are the population of B lymphocytes more represented in secondary lymphoid organs. This type of recirculating lymphocytes are responsible for the high affinity antibody response.

The follicles are adjacent to the T-zone, inside of which are T helper (Th), which regulate the activation of B-cells [26]. The entry of B-cells in the follicle is regulated by a CXCL13 gradient produced by follicular dendritic cells and stromal cells. CXCL13 interacts with the receptor CXCR5 expressed by B-cells [9].

The activation of FoB lymphocytes is divided into several phases:

1. Th cells are activated in the T zone by dendritic, and after activation, T cells express CD40L [26].

2. B-cells are activated by soluble antigens or membrane antigens presented by follicular dendritic. The antigen binds to BCR and is processed and displayed on the membrane via MHC II;

3. Activated B and T cells migrate to the perifollicular level, where takes place the immunological synapse. This migration is regulated by gradients of CXCL13 and CCL19 / CCL21, which bind to CXCR5 and CCR7 respectively [28]

4. interaction CD40 / CD40L and antigen presentation results in the production by the Th lymphocytes of chemokines (IL-2, IL-4, IL21) that promote the proliferation and differentiation of B-cells and the production of transcription factors CD40 dependent, essential for the formation of GCs [26]

5. within the GC occur two processes: isotype switching and somatic hypermutation;

6. at the end of the maturation process are generated PCs and memory cells.

Fo B cells are characterized by high intensity of expression of IgD and CD23 markers, that identify recirculating B-cells. FoB cells, infact, when activated and become PCs, migrate to the the red pulp to produce the antibodies directly into the bloodstream.

19

Recirculating B-cells are also present in the bone marrow where they form the niches around the medullary sinusoidal venules [37].

There are two distinct populations of follicular cells:

Follicular type I (FoI) and Follicular type II (FoII). The difference between these two populations is the signal cascade leading to their formation. The follicular type I depend on a strong signal of BCR that activates the Bruton's Tyrosine Kinase (BTK) and inhibits the pathway of Notch2, while the follicular type II do not depend on the antigen and, therefore, the activation of the BCR . The FoII shall nevertheless be considered follicular cells, because they are independent from the activation of the Notch2 pathway (essential for the formation of MZB) and are, therefore, considered an intermediate population that can, with suitable signals, differentiate into marginal or follicular B-cells [7-17].

Transitionl B-cells

Transitional B-cells are immature B-cells that originate from the bone marrow [32].

These cells are identified through the high expression of the marker AA4.1 (CD93) [1], which regulates cell adhesion and identifies the precursors. There are three distinct populations of transitional B-cells: T1 (AA4.1 $^+$, CD23$^-$, IgM^{high}), T2 (AA4.1 $^+$, CD23 $^+$, IgM^{high}) and T3 (AA4.1 $^+$, CD23 $^+$, IgM^{low}) [1].

Transitional cells are characterized by a low ability to proliferate in the presence of stimuli(for example the anti- IgM), and their survival depends on the signal of the BCR and the trophic factor BAFF [17].

T1 cells do not express CD23 and IgD, and are considered the earliest stage in peripheral B cell maturation.

While T2 cells have follicular markers and have the capacity to recirculate, as mature cells, and, according to the stimulus, can differentiate, both in mature follicular, or in marginal cells [7-17].

T3 cells are an anergic population that expresses the same markers of T2, however, with respect to T2, have a low expression of IgM [7-17].

In fact, it was observed that the response of the BCR to self antigens in immature B lymphocytes IgM^{high}, can lead to a reduction of surface IgM, as in the case of T3[31].

Marginal B-cell precursors (MZP)

In the literature, various methods have been used to define the different populations of mature B lymphocytes, and several studies are in agreement in defining, considering the surface markers, FoB (IgM$^{med/low}$, IgD^{high}, CD23 $^{+}$, CD21^{med}, AA4.1^{-}) and MZB (IgM^{high}, IgD^{low}, CD23^{-}, CD21^{high}, AA4.1^{-}) [7-32].

Instead, it is controversial the characterization of immature cells.

The main nomenclatures are those of Loder and Allmann [1-25].

Loder defines two populations of immature B-cells, T1 and T2, distinguishing these cells by the expression of CD21, CD23, IgD and a marker of differentiation, CD24, which is lost in mature cells.

Allmann, however, distinguishes three populations of transitional cells, T1, T2 and T3, basing the analysis on the expression of AA4.1 (CD93).

The existence of a population of precursor marginal cells (MZP) was proposed by Allmann in 2005. In this study MZP were characterized by cytometry, as IgM^{high}CD21^{high} and CD23 $^{+}$, and the same area subpopulation of T2 according to the classification of Loder. MZP differ from T2 for a more intense expression of CD21 and a lower expression of AA4.1.

This result shows that MZP are immature cells, but still in a stage of maturity with respect to the following populations of T1 and T2. AA4.1, in fact, is lost with cell maturation. Moreover, it was observed in knockout mice for Notch2, a reduction of MZB and of MZP, but not a change in T2 [29-39].

From a functional point of view, recirculating MZP are cells that originate in the red pulp, where they receive the stimulation of Notch2, necessary to differentiate into marginal cells. When the marginal zone is not able to receive more cells, MZP go back in the follicle where they accumulate [7].

1.1.5 Splenic B-cell development

Newly formed or T1 B-cells arrive through the central arterioles and the marginal sinus in the white pulp of the spleen [9]. They exit the circulation through fenestrations in the marginal sinus and, in response to a CXCL13 gradient, move into splenic B-cell follicles. These transitional B-cells initially (as T1 B-cells) only require tonic BCR signals for survival but subsequently receive and require both tonic BCR signals and trophic signals from BAFF as they enter the follicle (produced by more than one cell type but mainly by follicular dendritic cells in follicles) and begin to differentiate into recirculating follicular B cells. The B-cells in the follicular zone express high levels of IgD and CD23 and intermediate levels of CD21 and acquire the ability to recirculate. Soon after their generation, these cells still express the AA4.1 marker of immaturity and are therefore defined as T2 cells [39].

An affinity-defined subset of T1 or T2 cells that recognize self antigens with high affinity, but apparently below a threshold that would induce anergy, would presumably activate BTK downstream of the BCR and differentiate into follicular type I B-cells. Another subset of T1 or T2 B-cells that express BCRs that do not recognize self antigens with sufficient affinity to activate BTK signalling, instead, if the marginal zone compartment is not 'full', when these cells encounter DL1 in the splenic red pulp they will be induced to differentiate into marginal zone precursor and MZ B-cells and migrate to and be retained in the marginal zone. The exact mechanism of sensing the pool size of the marginal zone B-cell compartment remains to be determined. The marginal zone does not contain significant numbers of IgD$^+$ or CD23$^+$cells and it therefore seems less likely that marginal zone precursor B-cells actually reside in the marginal zone; these precursor cells have never been precisely localized.

Recent study demonstrated that marginal zone precursor B-cells respond to CXCL13 and accumulate in the follicle or that they transiently occupy the red pulp as they differentiate into MZ B cells. In either case, some chemotactic signals, probably S1P, contributes in a Gα12 or Gα
13 and LSC-dependent manner to promote the differentiation of marginal zone precursor B-cells and their migration towards the marginal zone. Migration requires WASP to mediate actin reorganization in conjunction with RAC1 and RAC2 and this in

turn contributes to integrin–ligand interactions and the retention of MZB cells in the vicinity of the marginal sinus. Interactions between myeloid cells and marginal zone precursor B-cells induce canonical NF-κB signalling that collaborates with Notch2 derived signals to mediate the differentiation and maintenance of MZB cells during or after completion of the process of migration.

Perhaps, if the marginal zone B-cell compartment is 'full', a T2 B-cell that does not have sufficient avidity for self antigen to differentiate into the BTK-dependent follicular type I B-cell compartment will mature by default into a long-lived follicular type II B-cell. Different studies suggest that follicular type I B-cells are instructed not to respond to DL1, perhaps in response to BTK-derived BCR signals, as they pass through red-pulp venules, and this ensures the existence of a stable recirculating follicular B-cell compartment. As MZ B-cells might need to be regularly stimulated through Notch2, and as it is known that murine red pulp venules are fenestrated, it is probable that MZ B cells slip in and out of venules in the marginal zone to receive signals from DL1. In this model, the decision to become a marginal zone B-cell might be initiated at the T1, T2 or follicular type II B-cell stage. We assume that only self antigens available through the circulation in the bone marrow or the spleen can contribute to the decision to drive a developing B-cell into a follicular type I-B-cell fate. However, if the developing B-cell lacks the ability to become a follicular type I B cell, it might then be induced to assume a MZB cell fate in the red pulp or the marginal zone through weak BCR signals, Notch ligands and BAFF. Based on anatomical considerations we assume that the temporal order of events that drive marginal zone B-cell development is as follows: weak BCR signalling, followed by inductive signals from DL1 and BAFF, followed then by chemotactic signals by either a poorly understood mechanism including S1PR1 or an unknown Gα12- or Gα13-linked receptor, and followed finally by a migration and retention event that involves the activation of integrins. By comparing BCR repertoires of transitional, Fo and MZ B cells, it has been argued that marginal zone B-cells could be derived from T1 B cells (**Fig.8**).
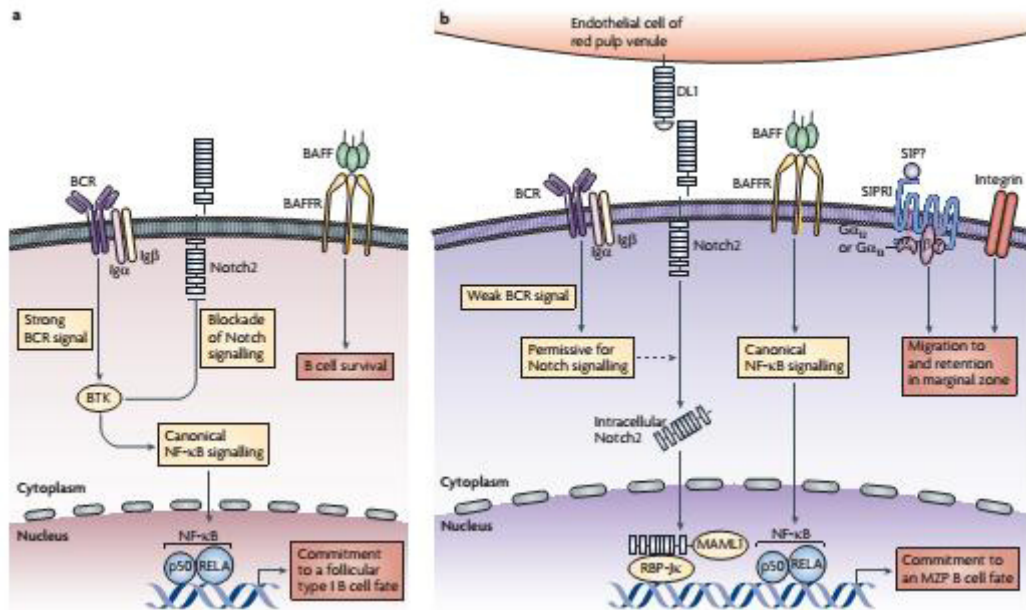
Fig. 8: signals required for the B-cell commitment *(Modified from Pillai and Cariappa Nature Reviews Immunology 2009).*

a. Strong signalling through the B cell receptor (BCR) activates Bruton's tyrosine kinase (BTK), which in turn activates the canonical nuclear factor-κB (NF-κB) signalling pathway and might instruct B-cells not to respond to signals through Notch2 receptor. Signals through the B cell-activating factor receptor (BAFFR) are required for B cell survival but not for the commitment to follicular type I B cell fate.

 b. Although weak BCR signalling is the initial event driving commitment, acquisition of the marginal zone B cell phenotype also requires further signalling pathways. Signals resulting from the interaction of delta-like 1 (DL1) expressed by endothelial cells of red pulp venules with Notch2 on developing B-cells leads to activation of the transcription factors Mastermind-like 1 (MAML1) and RBP-Jκ. Signals resulting from the interaction of BAFF with BAFFR activate NF-κB through the canonical pathway.

1.1.6 Notch2 and MZB commitment

The requirement of Notch2 for the generation of both precursor and mature marginal zone B-cells has led to some intriguing insights about the follicular versus marginal zone B-cell transition (**Fig.8**) [37-9-7]. Whereas Notch1 drives the development of αβ T cells at the expense of   B-cells, Notch2 is required for marginal zone B-cell

development during B-cell maturation in the spleen. In the Notch signalling pathway, intracellular Notch, RBP-Jκ (recombining binding protein suppressor of hairless) and Mastermind proteins form a ternary complex that activates Notch target genes. Knockout mice lacking Notch2 or RBP-Jκ in B-cells, Mastermind-like 1 (MAML1) or the Notch ligand DL1 have all defects in marginal zone B-cell development. Mice in which MSX2-interacting protein (MINT), a suppressor of Notch signalling, is inactivated have an increased number of marginal zone B-cells, which indicates that increased Notch signalling favours an increase in marginal zone B-cell development. [37-7] It is unclear exactly how Notch-mediated gene regulation contributes to marginal zone B-cell development, but it is possible a link between Notch signalling and known helix–loop–helix proteins. The helix–loop–helix transcription factor E2A and the ID2 and ID3 proteins that oppose E2A activity have a remarkable reciprocal relationship in regulating follicular versus marginal zone B-cell development, and these proteins are also indirectly linked to the Notch pathway. Decreasing E2A and increasing ID2 and ID3 levels facilitates marginal zone B-cell development at the expense of follicular B cell development. The transcription factor FLI1 regulates the levels of E2A and ID2 and ID3[7]. In FLI1-deficient mice, there are lower numbers of splenic follicular B-cells but higher numbers of marginal zone B-cells than in wild-type mice. Interestingly, Notch signalling induces the degradation of both E12 and E47 differentially spliced isoforms of E2A and could therefore contribute to marginal zone B cell development primarily by regulating the availability of E12 and E47 transcriptional regulators [7-9].

The physiologically relevant ligand for the activation of Notch2, DL1, is expressed on the luminal face of venules found mainly in the red pulp of the spleen but also in the marginal zone. There is a weak interaction between Notch2 and DL1 that is strengthened by the lunatic fringe and manic fringe glycosyltransferases, which enhance Notch2 signalling by adding N-acetyl glucosamine moieties to O-linked fucose residues on Notch2 [37].

1.1.7 Peritoneal mouse B-cells

The peritoneal cavity is a membrane-bound and fluid-filled abdominal cavity of mammals, which contains liver, spleen, most of the gastro-intestinal tract and other viscera. It harbors a number of immune cells including macrophages, B-cells and T cells.[52] The presence of a high number of naive macrophages in the peritoneal cavity makes it a preferred site for the collection of naive tissue resident macrophages. The peritoneal cavity is also important to study B-cells because of the presence of a unique peritoneal cavity resident B-cell subset, known as B1 cells, in addition to conventional B2 cells. B2 cells, also known as conventional or Fo B-cells, are abundant in spleen, lymph nodes and peripheral blood of mice, and arise continually from bone marrow precursors. They cooperate with T cells in the GC and undergo somatic hypermutation of their immunoglobulin genes to produce high-affinity antibody during humoral immune responses. B1 cells arise early from fetal and neonatal progenitors, and are enriched in peritoneal and pleural cavities of mice.

B1 cells are subdivided into B1a and B1b, which can be distinguished by surface expression of CD11b and CD5 molecules. B1 cells are an important source of natural IgM providing early protection from a variety of pathogens. These cells are autoreactive in nature, however, the mechanism through which they are controlled to prevent autoimmunity is still not completely understood [52].

CD5$^+$ B1a cells possess some regulatory properties by virtue of their IL-10 producing capacity. Therefore, peritoneal cavity B1 cells are interesting to be studied because of their diverse functions and unaddressed questions, associated with their development and regulation.

1.2 Protein kinase CK2

CK2 is a highly conserved and expressed serine/threonine kinase. It is now abundantly clear that it is a promiscuous enzyme as a diverse and somewhat bewildering array of more than 300 potential substrates have been identified. CK2 partecipates in many cellular process including cell proliferation, survival and differentiation [38]. There is an increasing body of evidence indicating that CK2 is involved in protein kinase networks controlling cell cycle progression and cellular responses to stress including ultraviolet light, heat schock, TNFα. Furthermore, abnormally high levels of CK2 have been observed in various types of cancer both solid tumours (breast, prostate, lung, kidney, neck and head) and hematological malignancies (Multiple Myeloma, Burkitt Lymphoma, Mantel cell Lymphoma and Diffuse Large B-Cell Lymphoma). Based on this involvement in trasformation and tumorigenesis, CK2 has recently attracted attention as a potential therapeutic target.

1.2.1 CK2 structure

CK2 has typically been viewed as tetrameric complex consisting of two catalytic subunits (38-42 kDa) and two regulatory subunits (27 kDa) (**Fig.9**). However the catalytic subunits can perform its activity also as monomer in the absence of the regulatory counterpart. CK2 was distinguished among other protein kinase for its ability to phosporylate serine or threonine residues that are proximal to acidic amino acids. Pinna defined a minimal consensus sequence for phosphorylation by CK2, however there are sites that are efficiently phosphorylated by CK2 despite the absence of this consensus sequence. CK2 has also the ability to phosphorylate tyrosine residues, although the kinetic parameters for this phosphorylation are much less favourable than those in ser/thr residues [24].
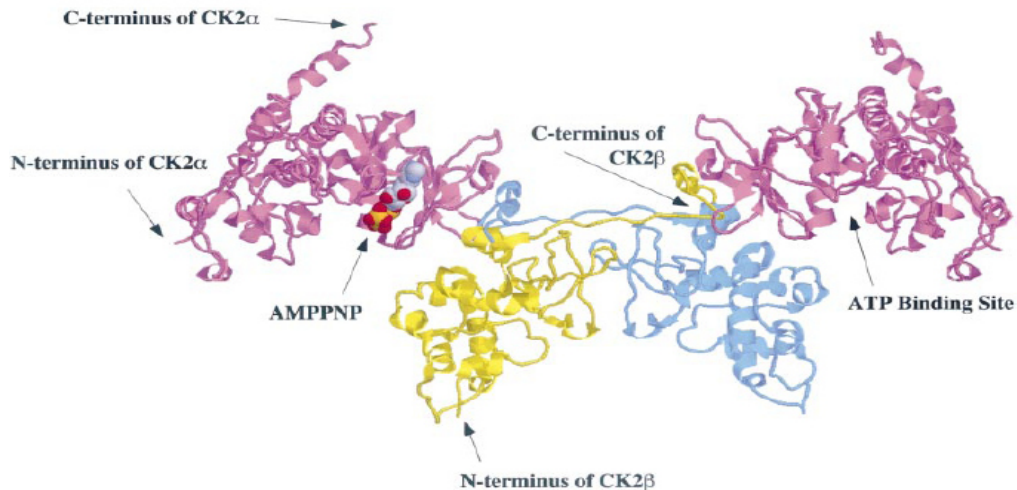
Fig.9: Ribbon diagram illustrating the high-resolution structure of tetrameric CK2.

While consideration of CK2 as a tetrameric complex remains relevant, significant evidence has emerged to challenge the view that its individual subunits exist exclusively within these complexes. Indeed, a lot of data indicate that the regulatory β subunit exists and performs functions independently of tetramers. In particular:

-X-ray crystallography revealed that the CK2α and CK2β interface is relatively small and flexible; this result raises the possibility that CK2 tetramers are subjected to disassembly and reassembly.

-Expression of CK2. Relatively little is known about how either CK2α or CK2β expression is regulated. Earlier studies had shown that CK2β protein was synthesized in excess of the catalytic subunit, underling a lack of coordinated expression. Several reports have also revealed an unbalanced expression of the two subunits in different tissues. For example the level of CK2β in testis was significantly higher in comparison to the level of CK2α.

The intriguing demonstration that aberrantly high levels of CK2β have also been observed in tumors, highlights the importance of understanding the dynamic role of CK2β both within the context of the holoenzyme and as an independent protein.

-Localization of CK2 subunits.

Immunofluorescence studies confirmed that catalytic and regulatory subunits of CK2 are not exclusively co-localized. While the majority of both subunits are localized to nuclear fractions, a major proportion of CK2α was tightly bound to nuclear components whereas CK2β was only loosely associated with other nuclear components. In addition, it was demonstrated in mammalian cells that all the three subunits of CK2 were localized to the smooth endoplasmic reticulum and the Golgi complex, instead only CK2α and CK2α' could be detected in the rough endoplasmic reticulum. In addition to confirm the predominantly nuclear and moderately cytoplasmic localization of both CK2α and CK2β, these studies showed that nuclear import and export of CK2 subunits are regulated independently and can result in rapid changes of their steady-state distribution. However, when associated in a stable holoenzyme complex, the two subunits are dynamically retargeted in the cytoplasm. Moreover, they demonstrated that the binding of fibroblast growth factor 2 (FGF-2) to the holoenzyme provokes its nuclear accumulation, supporting the concept of a signal-mediated localization, which may result in a sophisticated regulation of the kinase**.**

CK2α

In humans, two different forms of the catalytic subunits (designated CK2α and CK2α') which are encoded by distinct genes, were initially characterized. With the exception of their unrelated C-terminal domains, these two isoforms are very similar to one another, exhibiting approximately 90% identity within their catalytic domain. Recently, a third isoform, CK2α'', almost completely identical to CK2α, was identified; the only distinguishing feature lies in the completely distinct C-terminal domain. It is known that the different CK2 isoforms are closely related and show considerable functional overlap; indeed, knocking out the gene encoding CK2α' in mice results in variable offspring when heterozigous mice are bred to homozygosity, suggesting that CK2α has the capacity to compensate for CK2α' in the context of viability. However the male are sterile and display defects in speramatogenesis, demonstrating that the functional compensation is not absolute. There is also evidence for functional specialization of the individual CK2 isoforms in yeast, mice and mammals and there may also be differences in the subcellular localization of CK2α andCK2α' [24].

CK2β

In contrast to the catalytic isoforms of CK2, only one known form of the regulatory subunit β has been identified in mammals, but multiple forms have been identified in other organisms, such as *Saccharomyces cerevisiae*. CK2β is remarkably conserved among species and x-ray crystallography studies have determined that a dimer of CK2β subunits forms the core of the CK2 tetramer [24].

A large portion of CK2β has been shown to be phosphorylated at an autophosphorylation site consisting of serine 2, 3 and 4 at its N-terminus.
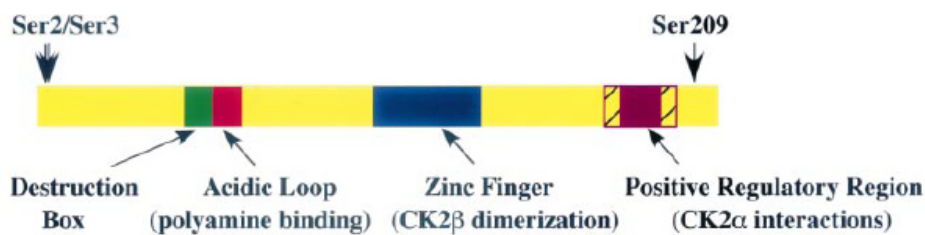

Fig.10: the regulatory CK2β subunit.
Linear representation of CK2β, illustrating the main elements within its amino acid sequence.

It was hypothesized that this autophosphorylation could be mediated by an intermolecular reaction through the formation of higher order CK2 structures and it could enhance CK2β stability. CK2β is also phosphorylated at S^{209} near its C-terminus, a residue which is phosphorylated in a cell-cycle dependent manner by p34[cdc2](**Fig.10**) .

> -It is particularly intriguing that CK2β has motifs that have been previously characterized as motifs that regulate cyclin degradation. Indeed, this sequence is similar to the amino acid motif called destruction box that plays a key role in the specific degradation of cyclin B at the end of mitosis [24].

X-ray crystallography revealed the importance of the zinc-finger region: this sequence is characterized by four cysteine residues which mediate the interaction allowing the CK2β dimer to form the core of the holoenzyme. CK2β dimerization precedes catalytic subunits binding and it is a prerequisite for CK2 tetramer formation.

30

-C-terminal region is responsible for the ability of CK2β to enhance and stabilize CK2 activity.

-One additional important sequence is the acidic loop: it has been identified as the site on CK2 that binds polyamines which are known to stimulate CK2 activity *in vitro* [24].

Over the last decade a plethora of CK2β-specific interaction partners have been identified through studies performed *in vitro* and *in vivo*. Some of these proteins have undergone more extensive validation allowing for their classification as either CK2 dependent or CK2 independent partners of CK2β.

-CK2-dependent binding partners are proteins that interact with tetrameric CK2 through binding sites on CK2β. Within CK2 complex a major role for CK2β appears to be substrate docking or recruitment where it brings the substrate protein and the catalytic subunit close enough to facilitate the phosphorylation reaction. A second function of CK2β appears to involve transmission of regulatory signals provided by other proteins in manner that could be analogous to that seen with polyamines. FGF-2 exemplifies this, as binding of FGF-2 to CK2β stimulates CK2 activity.

Thus, these two functions of CK2β modulate the ability of CK2 to phosphorylate specific cellular targets.

- CK2β independent binding partners are proteins that interact with CK2β in the absence of catalytic subunits. These proteins include A-Raf, c-Mos, and Chk1, that are ser/thr protein kinases containing sequences reminiscent of the CK2β binding region present in the CK2 catalytic subunit. In the case of A-Raf-CK2β interaction it was demonstrated that the presence of CK2α abolishes the activation observed with CK2β, suggesting that CK2α was competing with A-Raf for binding to CK2β. Interestingly, while in the case of c-Mos, the interaction with CK2β leads to down-regulation of the latter, inducing mitotic arrest in rapidly dividing embryonic cells; in the case of A-Raf and Chk1, the kinase activity is enhanced upon interaction with CK2β [24].

1.2.2 Regulation of CK2 in cells

The traditional view of CK2 looks at this protein as a constitutive active [84] and unregulated kinase, nevertheless, several studies support the idea that there are distinct mechanisms contributing to the physiological regulation of CK2:

- the first one is represented by the CK2β subunit that influences CK2 recruitment of the substrate and CK2 localization; moreover, it was demonstrated that the presence of the destruction box in CK2β, and consequently its degradation through proteasome, determines the oscillation of CK2 activity during cell cycle [24].

- Phosphorylation of CK2: several works indicate that phosphorylation is not absolutely required to activate CK2 in a manner analogous to that seen with MAP kinases. However they do not exclude the possibility that phosphorylation partecipates to some degree in aspects of CK2 regulation. Examination of CK2, isolated from mammal cells, has led to the identification of a number of physiological phosphorylation sites on both CK2α and CK2β. Indeed CK2β is phosphorylated at its autophosphorylation site and at Ser^{209}, a residue that is phosphorylated in a cell-cycle dependent manner. Autophosphorylation of CK2β could indirectly regulate CK2 activity. CK2α is phosphorylated in a cell-cycle dependent manner at four sites within its unique c-terminal domain even if these sites do not appear to effect a dramatic change in the catalytic activity of the kinase. CK2 can also be phosphorylated by the Src tyrosine kinases, by c-Abl tyrosine kinase and by the pathological counterpart Bcr-Abl fusion protein (typical of chronic myeloid leukemia). In this last context CK2 activity is inhibited by phosphorylation. [16].

- Protein-protein interaction: it has been shown that CK2 interacts with proteins such as FGF-1, FGF-2, HSP90 (heat shock protein 90) and the cochaperonine cdc37 that may directly alter or stabilize its catalytic activity. CK2 also interacts with tubulin, FAF-1 and cKIP-1, that could be involved in the targeting of CK2 to specific sites or structures within cells. There are three tumor suppressors that bind and inhibit CK2 activity: p53 interacts with the β subunit affecting its

function; in a similar way also p21WAF1 binds to CK2 β; adenomatous polyposis coli protein (APC) inhibits CK2 through the interaction with α subunits [18].

- Role of small molecules in CK2 regulation: CK2 is inhibited by negatively charged compounds such as heparin and activated by positively charged compounds, including polyamine [24].

1.2.3 CK2 functions

CK2 always behaves as an antiapoptotic agent implying on different cellular functions, signalling pathways and biochemical reactions which ultimately cooperate to promote cell survival (Fig.11).

- CK2 is a multisite regulator of different signalling pathways that are potentiated by phosphorylation:

  -NFkB: this transcription factor is normally sequestered in the cytosol by the binding to its inhibitor IkB. CK2 acts at different levels: it phosphorylates IkB promoting its degradation through proteasome, increases the expression of IKK kinases, phosphorylates p65 subunit of NF-kB increasing its transcriptional capability.

  -Wnt pathway: in the presence of Wnt, the destruction complex which targets β-catenin to the proteasome is inhibited by the stabilizing protein dishevelled (Dvl). CK2 phosphorylates Dvl and β-catenin promoting their stabilization, and TCF/LEF, facilitating its association to partner molecules;

  -PI3K/Akt: here again CK2 operates as a multisite regulator: a first level is represented by the tumor suppressor PTEN, the phosphatase which dephosphorylates PIP3 (phosphatidylinositol 3, 4, 5 triphosphate), thus maintaining the PI3K/Akt signal down, under resting conditions; it has been demonstrated that the constitutive phosphorylation of PTEN by CK2, while regulating the PTEN protein stability, has an inhibitory effect on its phosphatase activity as well, with the final effect of stimulating Akt-dependent signalling. A second level of CK2 intervention on this pathway is represented by Akt itself:

beside a physical interaction between the two kinases, a direct phosphorylation of Akt on Ser 129 by CK2 has been found, which promotes an hyper-activated state of Akt. [10]   There is moreover an indirect effect of this CK2-mediated phosphorylation, since it contributes to maintain an high level of phospho Thr-308, by ensuring a stable association with the chaperone protein Hsp90, known to protect Thr308 from dephosphorylation.
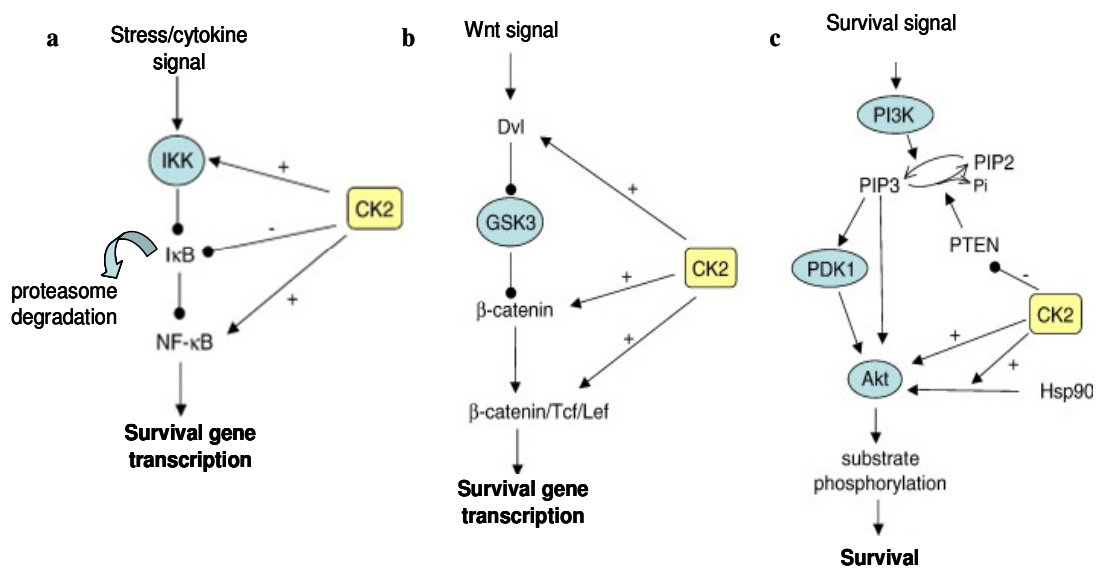

Fig.11: CK2 –dependent multisite regulation of NF-kB (a), β-catenin (b), and Akt (c) signaling.

- Jak-Stat pathway: Zheng and co-workers provided the first evidence that ser/thr kinase CK2 binds and phosphorylates Jak2 and these events are critical for the activation of Jak2-Stat signalling pathway [50].
- CK2 and apoptotic signalling: the caspase inhibitor ARC is phosphorylated and activated by CK2 while survivin, a member of the inhibitor of apoptosis protein

(IAP) family, is upregulated whenever CK2 expression is increased. Other CK2 targets are Bid, Max, HS1, presenilin, connexin, whose previous phosphorylation generates caspase resistant sites. Caspase 9 itself falls in this category, since its phosphorylation by CK2 protects caspase 9 from caspase 8 cleavage [27].

- CK2 participates in the regulation of proteins that have important functions associated with cell cycle progression: topoisomerase II, p34, cdc34, $p27^{kip}$, MDM2, p21WAF/CIP and p53 [27].

- CK2 cooperates also with proto-oncogenes such as c-Myc, c-Myb, c-Jun, Ha-Ras and A-Raf [38].

- The RNA polymerase I and RNA polymerase II complexes were among the first substrates to be discovered. Then RNA polymerase III was also shown to be target of CK2. Phosphorylation by CK2 of the TATA-binding protein (TBP), a subunit of TFIIIB (the core component of the Pol III transcriptional machinery), promotes a remarkable increase in Pol III activity, favouring the synthesis of tRNA and 5SrRNA. Thus CK2 enhances rRNA and tRNA biogenesis [38].

- Y. Miyata and colleagues demonstrated that the cochaperone cdc37 is a CK2 target. Cdc37 is involved in the folding process of several protein kinases in tight collaboration with Hsp90; however, cdc37 shows molecular chaperone activity *per se*. Phosphorylation of cdc37 by CK2 is essential for the proper function of the chaperone, moreover, CK2 itself operates in a cdc37-dependent manner being directly associated with the latter one. Thus CK2 may control many growth-related protein kinases simultaneously via cdc37 phosphorylation (**Fig.12**) [27].
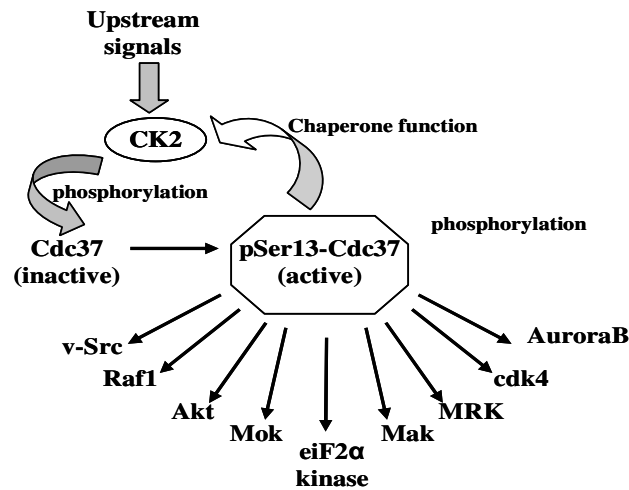
Fig. 12: Cdc37 as substrate of CK2.
CK2 and Cdc37 cooperate to create a positive feedback to control a number of important kinases.

1.2.4 CK2 and cancer

A number of genetic alterations can occur which bypass the physiological way of a kinase to be activated, giving rise to a constitutively active enzyme no more subjected to its physiological mechanism of control. The molecular alterations that interfere with protein kinase activities and are causative of cancer may be several, including gain/ loss of function, gene deletion, translocation with generation of fusion proteins. However CK2 does not conform to this general paradigm, merely because only active forms of it apparently exist. In addition, mutations of CK2 have never been reported, while its physiological concentration is one of the highest found, suggesting that CK2 is one of the most represented kinases. Remarkably, CK2 levels have been found to be invariably higher in malignant cells than in normal cells of the same type. There is also a correlation between the grading of the malignancy and the level of CK2: the higher this latter, the worse the prognosis [48]. It is felt now-a-days that such elevated CK2 is neither the cause nor the consequence of neoplastic transformation while it may well reflect the tendency of the tumour, regardless the genetic alterations causing it, to preferentially colonize those cells where CK2 is higher. Ruzzene and Pinna introduced the concept of "non-oncogene addiction" in order to explain the role of CK2 in ensuring survival of a variety of cancer cells, where its elevated activity seems to be relied to epigenetic events. They propose a model: assuming that stochastically such high CK2 level occurs only in a little part of the cell population, its contribution to the overall

tissue phenotype will be almost null. Any oncogenic mutation occurring in these cells will be counteracted by a number of opposing mechanisms in the majority of cells, where CK2 is normally represented; in contrast it will find a more favourable environment in the few cells were CK2 is abnormally elevated which are predisposed to evade apoptosis, to stabilize the onco-kinome, to develop drug resistance etc..(Fig.14) These cells are destined to proportionally increase in number, conferring to the tissue a malignant phenotype which will be associated and maintained by elevated CK2. At this stage it can be said that the tumour has become "addicted" to CK2 (**Fig.13**)**.**

There is the possibility that tumor cells more strictly rely on CK2 functionality for their survival than normal cells do.

This concept is supported by the observation that, when primary tumor cells are treated with CK2 inhibitors, their susceptibility to cell death tends to be higher than in the case of normal precursor cells. This has been found e.g. for MM**,** for T-ALL, and MCL[21].
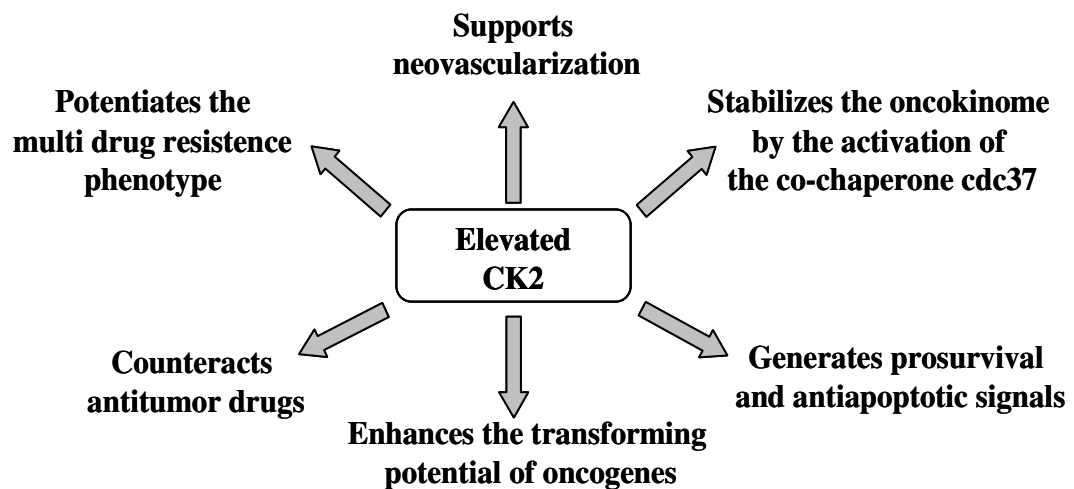

Fig.13: CK2 as a cancer driver. Effects promoted by abnormally high CK2 levels.

1.2.5 CK2 in lymphoid tumors

The first evidence of a pro-survival role for CK2 in lymphocytes came from *in vivo* mouse models of lymphomagenesis that were prompted by previous demonstration of CK2 involvement in lymphomas in the cattle. CK2α-overexpression favored T-cell lymphomagenesis in T-ALL-transgenic mice. MRL-lpr/lpr mice bearing a Fas receptor mutation develop a lymphoproliferative disease and autoimmuity resembling systemic erythematous lupus. Double MRL-lpr/lpr CK2-transgenic mice displayed an accelerated tumor phenotype characterized by massive enlargement of lymphoid organs due to proliferation of aberrant, though polyclonal, T-lymphocytes. Parallel and subsequent work demonstrated in this model that CK2 cooperates both with loss of the tumor suppressor p53 and with overexpression of the oncogene c-myc in causing lymphocyte proliferation and clonal expansion. These initial studies established a proliferative and apoptosis-protective role for CK2 in T lymphocyte in the mouse. However, a more straightforward role of this kinase in lymphocyte oncogenesis has been recently suggested by studies in human lymphoid tumors, both arising from precursor cells and from mature lymphocytes [36].

CK2 in LLC

In addition to having a role in immature lymphoid precursor derived blood tumors, CK2 has recently been implicated also in the pathogenesis of B-chronic lymphocytic leukemia (B-CLL).

The group of Jaeger et al. found elevated CK2β phospho-Ser209 levels in primary samples from 44 B-CLL patients.

Remarkably, CK2 inhibition with apigenin or TBB caused a reduction in the phosphorylation of PTEN at Ser380 and of AKT at Ser473 and was associated to B-CLL cell apoptosis. Remarkably, the combination of CK2 and

PI3K inhibitors (LY294002) was shown to produce a synergistic cytotoxic effect on B-CLL cells. Importantly, parallel work confirmed the pro-survival function of CK2 in the growth of B-CLL cells. Martins et al. showed that both CK2α and CK2β subunits are elevated in primary B-CLL from patients and CK2 inhibition in B-CLL cells is coupled with inactivation of protein kinase C, increased PTEN activity and apoptosis.

Interestingly, the cytotoxic effect of CK2 inhibition was more pronounced on B-CLL cells isolated from advanced stage (Binet B or C) patients. Normal

T and B lymphocytes were slightly affected by the treatment with CK2 inhibitors.

 Of note, in this work the authors used the novel compound CX-4945 as a CK2 inhibitor, which is currently under investigation in phase-I clinical trials in cancer patients [36].

CK2 in MM

CK2 has also been implicated in the pathogenesis of MM. Our group described that CK2 is crucial for malignant plasma cell survival demonstrating that this protein kinase positively regulates STAT3 and NF-kB-dependent signalling (**Fig.14**). CK2 activity and CK2a and b protein levels were found upregulated in MM cell lines and primary cells. CK2a knockdown or CK2 inhibition with TBB and TBB-derived agents caused MM cell apoptosis, which was not counteracted by the addition of growth factors, such as interleukin-6 and insulin-like growth factor-I. We also found that CK2 inhibitors made MM cells more sensitive to the cytotoxic effect of melphalan. Remarkably, CK2 silencing or inhibition was associated to IkBa stabilization and decreased NF-kB transcriptional activity. Similarly, our group demonstrated that CK2 inhibition caused a reduction in STAT3 phospho-Tyr705 and phospho-Ser727 levels, implying this kinase as a positive regulator of two critical pro-survival pathways in MM. Moreover, CK2 could be instrumental for the modulation of MM cell sensitivity to novel therapeutic agents. A recent study has reported that CK2 could represent a central kinase downstream inhibition of the proteasome with bortezomib, thus influencing

the cell phosphoproteome and many signaling pathways upon treatment with this central, widely employed therapeutic agent [36].
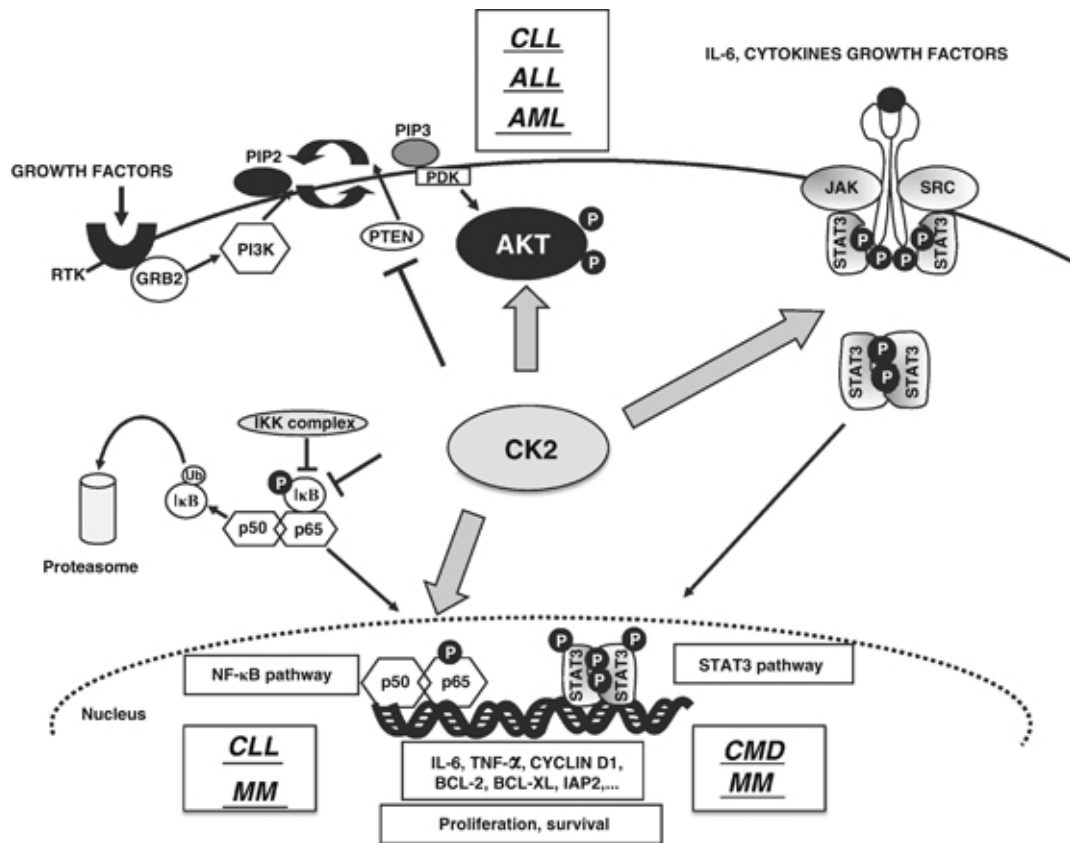
Fig.14:involvement of protein kinase CK2 in blood tumor-associated signaling pathways(Piazza F.,Leukemia 2012).

Among the several signaling pathways regulated by CK2, the modulation of the AKT/PKB/PI3K/PTEN cascade may be critical for the survival and proliferation of ALL, CLL and AML tumor cells; in CMD and in MM. CK2 regulates the extent of JAK/STAT activation downstream of cytokine/growth factor signaling; CK2-mediated phosphorylation of IκBα in its PEST domain leads to IκBα inhibition through proteasome degradation and CK2 phosphorylation of NF-κB p65 on Ser529 causes the activation of the NF-κB pathway and this could be important for CLL and MM cell survival and resistance to cytotoxic therapies

1.3 GENERATION OF A CONDITIONAL KO MICE MODEL

Conditional mutagenesis is a critical tool to study pleiotropic genes, that exert their functions in several organs and tissues during embryogenesis and adult life.

For this reason, several mouse models have been generated in order to obtain the conditional activation of gene expression in one or more cell types (spatial control) or in specific developmental stages (temporal control). One of the principal strategies used for these purposes, combines the homologous recombination with the properties of the Cre recombinase.

Cre Recombinase is a tyrosine recombinase enzyme derived from the P1 Bacteriophage. The enzyme uses a topoisomerase I like mechanism to carry out site specific recombination events. The enzyme (38kDa) is a member of the Integrase family of site specific recombinase and it is known to catalyse site specific recombination between two DNA recognition sites (loxP sites). This 34 base pair (bp) loxP recognition site consists of two 13 bp palindromic sequences which flank an 8bp spacer region. The products of Cre-mediated recombination at loxP sites are dependent upon the location and relative orientation of the loxP sites. Two separate DNA species both containing loxP sites can undergo fusion as the result of Cre mediated recombination. DNA sequences found between two loxP sites are said to be "floxed". In this case the products of Cre mediated recombination depends upon the orientation of the loxP sites. DNA found between two loxP sites oriented in the same direction will be excised as a circular loop of DNA whilst intervening DNA between two loxP sites that are oppposingly orientated will be inverted. The enzyme requires no additional cofactors (such as ATP) or accessory proteins for its function (**FIG.15**).

The enzyme plays important roles in the life cycle of the P1 Bacteriophage such as cyclization of the linear genome and resolution of dimeric chromosomes that form after DNA replication [21-3].
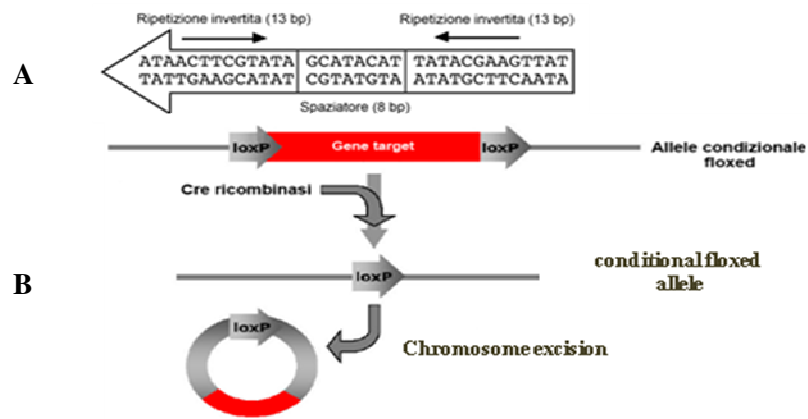
Fig.15: A. *Canonic loxP sequence (Modified from Araki K et al., BMC Biotechnology 2010);*
B. Conditional genetic inactivation through the loxP system (Modified from Kim JE,
Journal of Korean Endocrine Society 2006).

Using the combination of gene targeting and site-specific recombination techniques, it is possible to generate *KO* mice in a desired specific tissue or cell line. The rationale consists in using a target vector to insert two loxP sites flanking the gene of interest or a sequence included within the open reading frame (ORF), maintaining its correct expression [6]. The embryo or the homozygous mice that possess both alleles flanked by loxP sites, and transgenic for the expression of Cre recombinase will be characterized by a normal gene function for the tissue or cell type of interest. With the term gene targeting we identify the manipulation of the murine genome based on the homologous recombination. Linear DNA molecules represent the preferred substrate for the homologous recombination, which is more frequent during the S phase of cell cycle. The targeting vector is studied to introduce loxP sites in the desired genomic site in embryonic stem cells (ES). The selection of the recombined ES cells is carried out through a marker gene (generally a gene that confers a drug resistance) inserted in the targeting vector. For example, the gene that codifies the neomycin phosphotransferase (*neo*): only cells that have correctly made the recombination are able to survive when in their culture medium is present G418, as this drug is lethal for cells that don't bear the neo cassette. The negative selection eliminates ES cells that have incorporated the vector through a mechanism of non-homologous recombination. A marker gene is usually insert externally to the vector region included in the genome. The timidine kinase, isolated from the herpes virus (HSV-tk) constitute an example: if the vector incorporation happens through the linearized far ends, HSV-tk gene is inserted together

with *neo* gene. Adding the 2'-fluoro-2'-deoxy-1beta-D-arabinofuranosyl-5-iodouracil (*FIAU*) occurs the negative selection of HSV-tk^{+} cells. After the enrichment of ES cells that bear the correct modified genetic locus, the next step is to generate chimeric mice, that are able to pass on the offspring the mutant gene. For this reason, ES mutant cells are injected in a host blastocyst that originates the chimeric mice after being transplanted in a foster mother. In order to make easier the isolation of mice bearing the mutant gene, ES cells and the host blastocyst derive from mice that express distinguishable pigmentation alleles [6].

Finally, to obtain mice with conditional deletion of the target gene, it is necessary to cross mice that bear the floxed gene with mice that express the Cre recombinase under the control of a tissue or cell type specific promoter (**Fig.16**) [21-3].
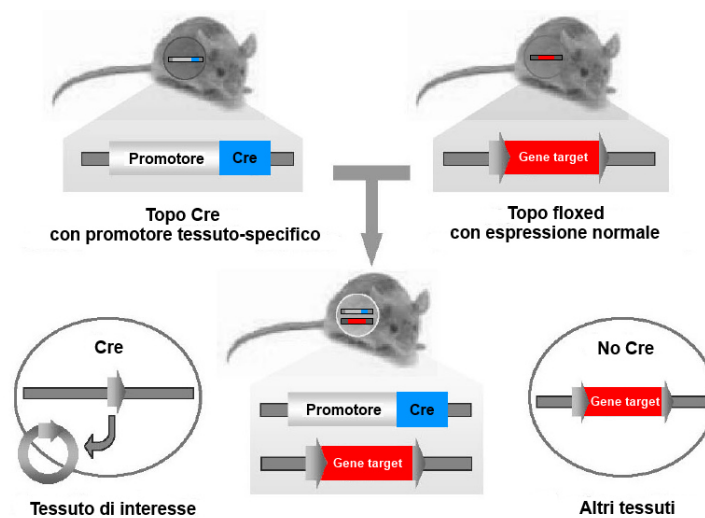

Fig. 16: Tissue specific conditional mutagenesis (Modified from Kim JE, Journal of Korean Endocrine Society 2006).

Target gene is excised by Cre recombinase, selectively expressed in floxed mice. Arrows indicate the orientation of the loxP sites.

The offspring will have the gene deleted only in the cells that express the integrase. Another accurate control of recombination is possible if these mice are transgenic also for a reporter gene, the expression of which is activated by Cre recombinase. A common example is the β galactosidase gene (LacZ), included in ROSA26 locus, that is

active only after the excision of a floxed STOP codon. The efficiency of recombination can be site-dependent, for this reason the recombination pattern obtained is not necessary comparable for different genes. Another important parameter is the control of potential phenotypes generated by the only presence of the Cre transgene.

2. AIM OF THE STUDY

Protein kinase CK2 is a highly conserved, acidophilic serine-threonine kinase whose central role in several cellular processes has abundantly been described. The essential role of CK2 for cells and organisms is underscored by the lethal phenotype of its inactivation in the mouse: both CK2β and CK2α KO result in *in utero* death and multiple embryonic alterations. CK2 participates in many developmental pathways, of which particularly relevant for hemo-lymphopoiesis are those dependent on Wnt/β-Catenin, Hedgehog, NF-κB and STAT3, which regulate cell differentiation, proliferation, self-renewal as well as lineage choice commitment.

Moreover, recent studies, including those from our group, have shown that CK2 is involved and overexpressed in a wide variety of B-cell derived tumors, such as Multiple Myeloma, Marginal Zone B-cell Lymphoma and Diffuse Large B-Cell Lymphoma.

Since CK2β KO is lethal *in utero*, to elucidate the physiological and pathogenetic role of CK2 in B-lymphocytes, we generated CK2β B-cell specific conditional KO mice, were we studied the effects of CK2β deletion during normal B-cell development and the role of CK2β downstream of B-cell receptor and Notch2 receptor, which activate signalling pathways crucial for B-cell development and proliferation.

3. MATERIALS AND METHODS

3.1 Generation of conditional CK2β KO mice in the hematopoietic compartment

CK2β KO mice in hematopoietic cells were generated through several sequential crossings.

The first cross was made between C57BL6 mice homozygous for the *Csnk2b floxed* (CK2β$^{Fl/Fl}$) allele (C. Cochet, Grenoble), with C57BL6 mice hemizygous for the transgene *Cd19-Cre* (Cd19$^{+/Cre}$) (Jackson laboratories). This cross originates mice with the genotype CK2β$^{+/Fl}$ Cd19$^{+/Cre}$ (heterozygous mice). To obtain KO mice, heterozygous mice were then crossed with CK2β$^{Fl/Fl}$ mice. The genotype of our KO mouse model possesses the following genotype CK2β$^{Fl/Fl}$ Cd19$^{+/Cre}$.

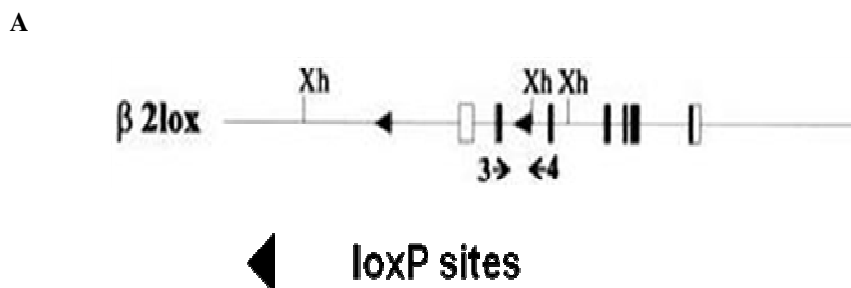Figure 17 shows CK2β^{Fl} and Cd19^{Cre} alleles.

A

Fig.17: A. CK2β^{Fl} allele.

Rectangles represent the exons of the *Csnk2b* gene. The first exon is indicated by the white rectangle, with an arrow that indicates the transcription initiation site. LoxP sites are indicated by black arrowheads. The promoter (not highlighted in the picture) is located between the first loxP site and the first exon.

B
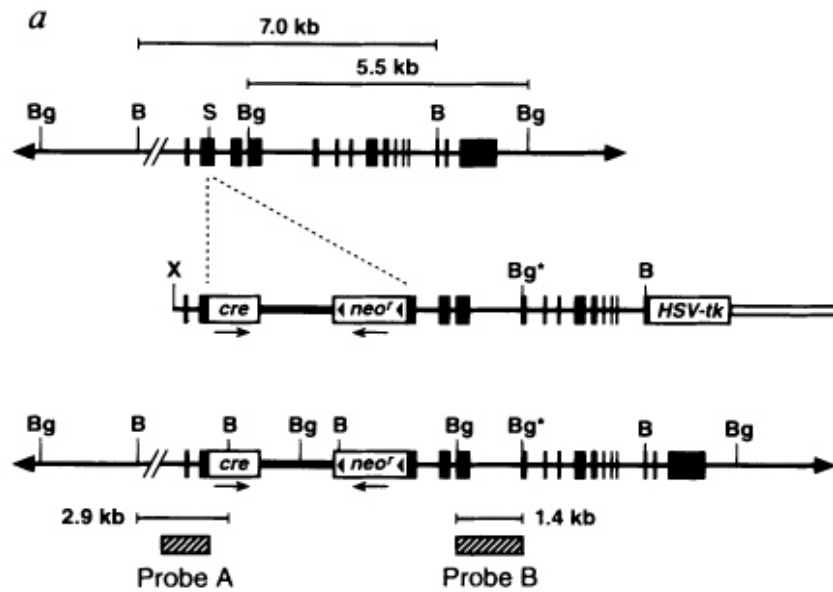
B) Cd19-Cre transgene.

A targeting vector containing Cre recombinase, the rabbit beta-globin intron /poly A signal sequence, and an FRT-flanked neomycin resistance gene, was used to disrupt exon 2 of the Cd19 gene and to express cre under the regulation of the endogenous promoter. Herpes simplex virus thymidine kinase gene was placed at 3' of the Cd19 sequence to allow for the selection against random integration. The construct was transfected into 129P2/OlaHsd-derived E14-1 embryonic stem cells. Correctly targeted ES cells were injected into 129/Sv blastocysts. The resulting chimeric animals were backcrossed to BALB/c IgHb congenics for a number of generations and then backcrossed to C57BL/6 for 10 generations.

3.2 Isolation of genomic DNA from mice tales

The far ends of tails of adult mice were digested for 3 to 4 hours at 55°C, after having been resuspended in 500μl of a suitable lysis buffer, the composition of which is described below:

- 250 μL of *mouse tail* 2X lysis buffer,
- 25 μL di Proteinase K 10 mg/mL (Ambion, Life Technologies, Carlsbad, USA),
- 25 μL of SDS 10% w/v,
- H_2O Milli-Q to 500 μL.

mouse tail 2X lysis buffer contains:

- Urea 8M,
- EDTA (pH 8.0) 20 mM,
- SDS 1% w/v,
- Tris-HCl (pH 8.0) 1M,
- NaCl 5M.

Each sample was subsequently centrifuged at 13,000 rpm for 10 minutes at 4°C and the supernatant was collected and transferred to a new eppendorf containing 1ml of absolute ethanol and mixed vigorously.

This leads to the formation of a white precipitate that corresponds to genomic DNA. Samples were centrifuged at 13,000 rpm for 30 minutes at 4°C, supernatant was discarded and pellet dried up at room temperature for 10 minutes.

DNA was then rehydrated with 500μl of H_2O and stored at 4°C till usage.

3.3 Protocol for mouse genotyping

Amplification of the CK2β^{Fl} allele

The presence of the CK2β^{Fl} allele was determined through PCR using the following primers (F = Forward; R = Reverse):

- F (BB3): 5´-CTAGCTCGAGATGAGTAGCTCTGAGGAGGTG-3´
- R (BB4): 5´-GGATAGCAAACTCTCTGAG-3'

The reaction mix for one sample is composed by:

- 12.5 μL ofREDTaq® ReadyMix™ (Sigma-Aldrich, Steinheim, Germania), containing Tris-HCl (20mM, pH 8.3), KCl (100 mM), $MgCl_2$ (3 mM), gelatine (0.002%), dNTPs and DNA *Taq* polimerase (0.006 Units/μL),
- 1.0 μL of each primer (20 pmol/μL),
- 8.5 μL of H_2O, included in the commercial kit,
- 2.0 μL of purified genomic DNA.

The thermal protocol of the PCR reaction is listed below

Amplification protocol		
94°C	5min	Initial denaturation
94°C	30sec	Denaturation
55°C	30sec	annealing of primers to genomic DNA
72°C	2min	Extension
72°C	7min	Final extention
4°C	endless	Hold
denaturation, annealing and extension: 40 repeats		

The amplification products were separated by gel electrophoresis on a 1.5% agarose gel. The size expected for the amplification products are between 400 and 600 bp.

Detection of the *Cd19-Cre* transgene

The CD19-Cre knock-in/knock-out allele has the Cre recombinase gene inserted into the first coding exon of the CD19 gene; abolishing endogenous Cd19-gene function and placing cre expression under the control of endogenous Cd19 promoter/enhancer elements. Cre recombinase expression is directed at the earliest stages and throughout B-lymphocytes development and differentiation.

PCR reaction is carried out using the following primers (F = Forward; R= Reverse):

- Primer for transgene allele:
    - F: 5'-GCG GTC TGG CAG TAA AAA CTA TC-3'
    - R: 5'-GTG AAA CAG CAT TGC TGT CAC TT-3'

- Primer for wild type allele:
    - F: 5'- CCT CTC CCT GTC TCC TTC CT-3'
    - R: 5'-TGG TCT GAG ACA TTG ACA ATC A-3'

The reaction mix for one sample is composed by:

- 12.5 μL of REDTaq® ReadyMix™ (Sigma-Aldrich, Steinheim, Germany), comtaining Tris-HCl (20mM, pH 8.3), KCl (100 mM), $MgCl_2$ (3 mM), gelatine (0.002%), dNTPs and DNA *Taq* polimerase (0.006 Units/μL),
- 1.0 μL of each primer (20 pmol/μL),
- 6.5 μL di H_2O, included in the commercial kit,
- 2.0 μL of genomic DNA.

The thermal protocol of the PCR reaction is listed below:

Amplification Protocol		
94°C	3min	Initial denaturation
94°C	30sec	Denaturation
62°C	1min	annealing primers-genomic DNA
72°C	1min	Etesio
72°C	2min	Final extension
10°C	endless	Hold
denaturation, annealing and extension: 35 repeats		

The size of the expected amplification products are: 477 bp for the *wild type* allele and 100 bp for the *transgene*. In heterozygous mice are present both amplification products. The amplification products were separated by gel electrophoresis on a 1.5% agarose gel.

3.4 Isolation of hematopoietic organs

Spleen, thymus, lymph nodes were isolated from CK2β KO and CTRL mice 8-12 weeks old. Organs were extracted and put in a dish containing PBS.

They were disrupted through pipetting and the solution obtained was filtered with a cell strainer of 70 μm (Becton Dickinson, Milan, Italy) posed on the top of a 50ml Falcon tube.

Cell strainers were washed several times with RPMI-1640 supplemented with 1% v/v (100 U/μl) antibiotics (penicillin/streptomycin, Euroclone, Italy) and 10% v/v of fetal bovine serum (FBS, Euroclone, Italy).

After this passage, tubes were centrifuged at 1200 rpm for 5 minutes at 4°C. The supernatant is discarded and cells resuspended in PBS 1X without Calcium and Magnesium.

To analyze bone marrow cells, femurs and tibiae were carefully cleaned from adherent soft tissue. The tip of each bone was removed with a rongeur and the marrow was harvested by inserting a syringe needle into one end of the bone and flushing with RPMI. Bone marrow cells were filtered with a cell strainer of 40 μm (Becton Dickinson, Milan, Italy) on the top of a 50ml Falcon tube. Cells were counted after staining with trypan-blue dye.

3.5 Splenic B-cells purification

Splenic B-cells from CK2β KO and CTRL mice were purified using EasySep™ Mouse B Cell Isolation Kit (Stemcell).

EasySep™ Mouse B Cell Isolation Kit is designed to isolate B-cells from single cell suspensions of splenocytes by negative selection. Unwanted cells are targeted for removal with biotinylated antibodies directed against non-B-cells (CD4, CD8, CD11b, CD43, CD49b, CD90.2, Ly-6C/G (Gr-1), TER119) and streptavidin-coated magnetic particles (RapidSpheres). Labeled cells are separated using an EasySep magnet without the use of columns. Desired cells are poured off into a new tube.

This procedure is used to process 0.25 - 2 mL of sample (up to 2 x 10^8 cells).

1. Cell suspension was prepared at a concentration of 1 x 10^8 cells/mL in recommended medium (PBS + 2% FBS with 1 mM EDTA) in a 5 mL polystyrene tube to properly fit into the EasySep Magnet. Normal Rat Serum was then added (50 µL/mL) to cells.

2. EasySep Mouse B Cell Isolation Cocktail was then added (50 µL/mL) and cells were incubated at room temperature for 10 minutes.

3. EasySep Streptavidin RapidSpheres (75 µL/mL), previously vortexed for 30s'', were added to cells and incubated at room temperature for 2.5 minutes.

4. Cell suspension was brought up to a total volume of 2.5 mL by adding recommended medium. The tube was inserted into the magnet at room temperature for 2.5 minutes.

5. In one continuous motion magnet and tube were inverted, pouring off the desired fraction into a new 5 mL polystyrene tube. The magnetically labeled unwanted cells will remain bound inside the original tube, held by the magnetic field of the EasySep Magnet (**Fig**.18).
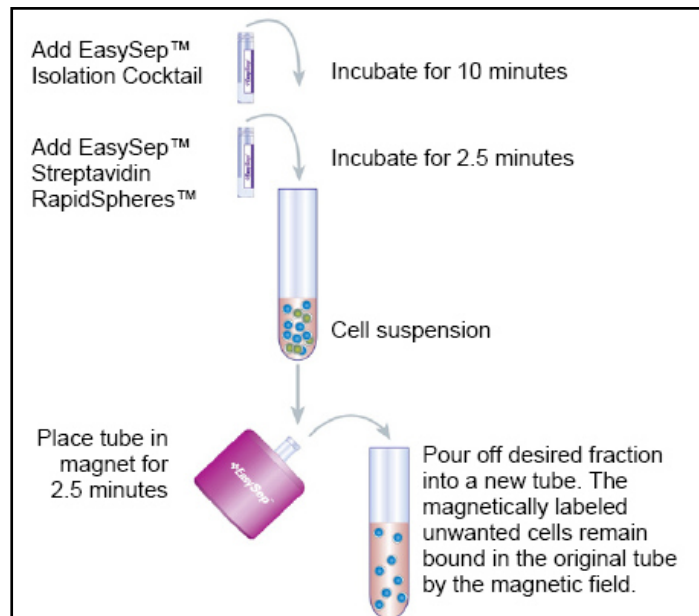

Fig.18 Manual Easysep protocol diagram

3.6 B-cells culture

B-cells purified from the spleen of CK2β KO and CTRL mice were coltured at a density of 10^6 cells/ml in RPMI medium plus 10% FBS and 2-mercaptoethanol for 36 h with 1 µg/ml anti–mouse CD40 (clone HM40-3; BD) +/- 15 µg/ml goat anti–mouse IgM F(ab′)2 fragments (Jackson ImmunoResearch Laboratories, Inc.) +/- 10ng/ml murine IL-4 (Sigma).

3.7 Splenic B-cells stimulation

For *in vitro* class switch assays, B-cells were cultured at 10^6 cells/ml with 20ug of Lipopolysaccharide (LPS; Sigma-Aldrich) and recombinant murine IL-4 at 10ng/ml to induce switching to IgG1 or with LPS alone to induce switching to IgG3.

The percentage of IgG1 or IgG3 expression was measured by flow cytometric analysis after 3 days of stimulation and using anti-mouse IgG1, IgG3 and anti-B220.

3.8 Flow citometry

To investigate the role of CK2β during lymphopoiesis, 500,000 cells from spleen, thymus, bone marrow, peripheral blood, lymph nodes and peritoneal cavity of KO and CTRL mice, sacrificed between 8 and 12 weeks, were stained.

The staining was performed in 5 ml tubes in a maximum volume of 100 ul of Phosphate Buffered Saline (PBS) without Calcium and Magnesium. Prior to the staining, cells were incubated in the dark for 5 minutes, at 4°C, with CD16/CD32 Antibodies (FcBlock, BD Bioscences).

Then cells were stained with the following antibodies:

ANTIBODY	FLUOROCHROM	COMPANY
CD21/CD35	FITC	BD Biosciences
CD43	FITC	BD Biosciences
CD3	FITC	BD Biosciences

IgD	FITC	BD Biosciences
Gr-1 (Ly6GELY-6C)	FITC	BD Biosciences
B220/CD45R	FITC	BD Biosciences
CD19	PE	BD Biosciences
Mac-1(CD11B)	PE	BD Biosciences
IgM	PE	BD Biosciences
CD23	PE	BD Biosciences
CD8	PerCP-Cy5.5	BD Biosciences
CD19	PerCP-Cy5.5	BD Biosciences
Streptavidin	PerCP-Cy5.5	BD Biosciences
CD25	APC	BD Biosciences
B220/CD45R	APC	BD Biosciences
CD21/CD35	APC	BD Biosciences
IgG1	APC	BD Biosciences
IgM	PE-Cy7	BD Biosciences
cKit(CD117)	PE-Cy7	BD Biosciences
B220/CD45R	APC-Cy7	BD Biosciences
IgD	V450	BD Biosciences
biotin IgG3		BD Biosciences
CD138	PE	BD Biosciences
PNA	FITC	SIGMA
GL7	UNCONJUGATED	eBIOSCENCE
CD38	PE	BD Biosciences
CD95	PE-CY7	BD Biosciences

After the staining, cells were acquired through FACSAria III (BD Biosciences, NY, USA).

The analysis of dot plots was carried out with FlowJo software (TreeStar).

3.9 Protein extraction

Whole cell protein extraction

All steps were performed at 4°C. Cells (1-5x10^6) were collected and washed in PBS. Pellets were resuspended with 30-50µl of lysis buffer composed of:

-Triton	0,5% v/v
-Okadaic acid	1µM (Sigma)
-phosphatase inhibitor cocktail (100X)	1X (Thermo scientific)
-DTT	1mM (Sigma)
-PMSF	1mM (Sigma)
-Protease inhibitors (100X)	1X (Sigma)

-Buffer made up of TRIS (pH7.5) 20mM, NaCl 150mM, EDTA 2mM, EGTA 2mM to final volume.

Samples were incubated for 30', vortexed every 5' and centrifuged for 10' at 13000 rpm. Supernatants were collected and stored at -20°C.

Protein quantification

To measure the concentration of proteins in solution we used the Bradford (Sigma) protein assay. It is based on an absorbance shift of the dye Comassie Brilliant Blue G-250 in which under acidic conditions the red form of the dye is converted into its bluer form to bind to the protein being assayed. The bound form of the dye has an absorption spectrum maximum at 595 nm. The binding of the dye to the protein stabilizes the blue anionic form. The increase of absorbance at 595 nm is proportional to the amount of bound dye, and thus, to the amount (concentration) of proteins present in the sample.

Bradford was diluted 1:2 in distilled water and 1-2µl of cell lysate was added; the solution was mixed and incubated 4' in the dark; absorbance was performed using a spectrophotometer (Ultrospec 1100pro; Amersham).

Concentration values were obtained applying the Lambert-Beer law:

$$A = \varepsilon \times c \qquad \varepsilon = \text{molar extinction coefficient}$$

Molar extinction coefficient was calculated from a calibration curve, obtained using rising concentrations of BSA.

SDS-PAGE

Sodium dodecyl sulfate polyacrylamide gel electrophoresis (SDS-PAGE) is a method that allows to separate proteins according to their size and no other physical feature.

SDS is a detergent that can dissolve hydrophobic molecules but also has a negative charge (sulfate) attached to it. SDS can disrupt hydrophobic areas and coat proteins with many negative charges which overwhelm any positive charge the protein has. The resulting protein is denatured by SDS (reduced to its primary structure) and, as a result, is linearized. Moreover all proteins, having a large negative charge, will all migrate towards the positive pole when placed in an electric field.

When polyacrylamide, which is a polymer of acrylamide monomers, undergoes the process of polymerization, it turns into a gel and we will use electricity to pull the proteins through it. The acrylamide concentration of the gel can be varied, generally in the range from 5% to 25%. Lower percentage gels are better to resolve very high molecular weight proteins, while much higher percentages are needed to resolve smaller proteins. Polyacrylamide gel is not solid but is made of a labyrinth of tunnels through a meshwork of fibers. Small molecules can move through the polyacrylamide mesh faster than big molecules.

Sample preparation:

12-25µg of protein lysates are mixed with sample buffer (1:4 v/v) composed by SDS 20%p/v, Tris (pH6.8) 1,5M, bromophenol blu 0,05% v/v, DTT 6% v/v, and β-mercaptoethanol 1:20 v/v. Samples are heated at 100°C for 3' to favour denaturation.

Preparing acrylamide gel:

The gel is composed of two different phases: the upper phase called stacking gel (pH6.8) and the lower phase called separating gel. The first one allows proteins to compact and makes them enter the separating gel simultaneously. The last one allows the real separation of proteins according to their size. In this work we used both fixed concentration of acrylamide (10% v/v for separating gel; 5% for stacking gel) or precast gradient gels with a concentration of acrylamide increasing from 4% to 20% (Thermo Scientific) for the separating gel. Gradient is best suited to show high and low molecular weight proteins in the same gel; it still helps resolution in a couple of ways: first, by

getting more and more restrictive as the protein moves down the gel, it helps maintain stacking. Sharper bands will not overlap as much. Second, by engineering the gradient properly one can enhance the separation of closely moving bands.

Protein samples and a standard sample, as molecular weight reference (Seeblue Plus2 Prestained Standard 1X-Invitrogen), are loaded into the gel at 25mA. We used Amersham electrophoretic chambers and a specific saline running buffer (pH 8.3) (25 mM Tris, 192 mM glycine, 0.1% SDS).

Western blot (WB)

Following electrophoresis, proteins must be transferred from the electrophoresis gel to a membrane. The transfer method that is most commonly used is an electrophoretic transfer: this method involves placing a protein-containing polyacrylamide gel in direct contact with a piece of PVDF or other suitable, protein-binding support and "sandwiching" this between two electrodes submerged in a conducting solution. The sandwich is composed into a grid in the following manner: sponge, watman paper, PVDF, gel, paper, sponge. When an electric field is applied, proteins move out of the polyacrylamide gel onto the surface of the membrane, where proteins become tightly attached. The result is a membrane with a copy of the protein pattern that was originally in the polyacrylamide gel. The transfer was done in specific saline buffer containing (Tris 250mM, glycine 1.92M and methanol 20%v/v in deionized water).

After the transfer it is important to block the remaining surface of the membrane to prevent unspecific binding of the detection antibodies during subsequent steps. Saturation is performed for 1 hour in a solution composed of non fatty milk 5% v/v and TBS (tris buffer saline) supplemented with tween-20 0,05% (Sigma).

Saturation is followed by washing steps in TBS plus Tween-20 0,05% v/v in order to remove unbound reagents and reduce background.

The membrane is incubated for 1 hour with a primary antibody that recognizes a specific protein or epitope on a group of proteins. The primary antibody is not directly detectable. Therefore, tagged secondary antibodies are used as means of ultimately detecting the target antigen (indirect detection). Our secondary antibodies were enzymatically labelled with Horseradish peroxidase (HRP), which is conjugated to the antibodies. After a final series of washes, antibodies on the membranes are ready to be

detected. An appropriate chemiluminescent substrate, which produces light as a bioproduct, is then added to the membrane. The light output can be captured using ImageQuant LAS500 machine (GE Healthcare Life Sciences). The intensity of the signal should correlate with the abundance of the antigen on the membrane. We used different chemiluminescent substrates:

-Pierce ECL western blotting substrate (Thermo Scientific);

-LiteAblot PLUS Enhanced Chemioluminescent Substrate (EuroClone);

-LiteAblot EXTEND Long Lasting Chemiluminescent Substrate (EuroClone);

-LiteAblot Turbo Extra Sensitive Chemioluminescent Substrate (EuroClone).

In order to detect more antibodies with the same specificity and similar molecular weight it is necessary to strip the membrane. Stripping buffer (Thermo scientific) allows the cleaning and the efficient removal of primary and secondary antibodies from immunoblots without removing or damaging the immobilized antigen. This allows blots to be re-probed with new antibodies. Membranes are covered with this buffer and incubated for 10'-15' at room temperature; some washes in TBS are then performed and finally the membrane can be saturated again with milk.

Antibodies

We used antibodies directed against the following proteins:

Primary antibodies: anti-rabbit CK2α provided by Dr. S. Sarno, University of Padova, Italy; anti-CK2β (Abcam,USA); anti-p65 (Abcam), anti-phospho-p65 ser259 (SantaCruz, California, USA), anti-IRF4 (SantaCruz, California, USA); anti-BLIMP1 (SantaCruz, California, USA); anti-GAPDH (Ambion). Secondary antibodies: anti-rabbit IgG HRP-linked antibody (Cell Signaling Technology, Beverly, MA, USA); HRP labeled goat anti-mouse IgG (KPL, Gaithersburg, MD, USA).

3.10 RNA purification

RNA was purified using RNeasy mini kit (Quiagen). This procedure represents a well-established technology that combines the selective binding properties of a silica-based membrane with the speed of microspin technology. A specialized high-salt buffer

system allows up to 100ug RNA longer than 200 bases to bind to the RNeasy silica membrane. Biological samples are first lysed and homogenized in the presence of a highly denaturing guanidine-thiocyanate-containing buffer, which immediately inactivates RNases to ensure purification of intact RNA. Ethanol is added to provide appropriate binding conditions, and sample is then applied to an RNeasy Mini spin column, where total RNA binds to the membrane and contaminants are efficiently washed away. RNA is then eluted in water. The procedure provides enrichment for mRNA since most RNAs <200 nucleotides are excluded.

Protocol:

Cells are collected and washed, removing the medium; then the appropriate volume of RLT lysis buffer, that contains guanidine-thiocyanate, is added (350 µl for <5x10^6 cells, 600 µl for 5-9x10^6 cells). RLT is supplemented with β-mercaptoethanol 1:100 v/v, which inhibits RNases further. Samples are homogenized by vortexing and then 70% ethanol is added. After pipetting, lysed samples are transferred to RNeasy spin columns and centrifuged at 11000rpm for 1', discarding the flow-through. RNA bound to the silica membrane is washed with buffer RW1 and centrifuged at 1000rpm for 1'; a mix of DNase and buffer RDD (10µl and 70 µl respectively) are then added directly on the membrane and kept in incubation for 15'-30', in order to remove contaminant DNA. Afterwards a series of washes are performed, first of all with buffer RW1 (700µl) and then with buffer RPE (500µl) (containing ethanol). Samples are centrifuged at 12800 rpm for 2'. At the end RNA is eluted using 30µl of RNase free water.
RNA was quantified by means of Nanodrop 1000 (Thermo Scientific).

RNA reverse transcription
Reverse transcription is a reaction exploited by an RNA-dependent polymerase that is capable to synthesize a complementary strand of DNA, called cDNA, using an RNA strand as a template.
RNA is reverse transcribed to cDNA by means of Promega system (USA). AMV, namely *Avian myeloblastoma virus,* is the reverse transcriptase enzyme used. AMV sythesizes single stranded cDNA from total or poly(A) isolated RNA; it shows polymerase activity from 5' to 3' and RnaseH activity from 3' to 5', degrading the RNA

strand when the hybrid cDNA/RNA is formed. The reaction takes place in 20μl of final volume. For each RNA the following mix has been used:

-MgCl$_2$ (25mM)   4μl

-reverse transcription 10X buffer   2μl

-dNTPs mix (10mM)   2μl

-Oligo dT primer (0,5mg/ml)   1μl

-RNasin RNase inhibitor   0,5μl

-AMV Reverse Transcriptase   0,75μl

-RNase free H$_2$0 to final volume of   20μl

Then samples underwent the following thermal protocol:

42°C for 15'

95°C for 5'

4°C maintenance

3.11 Real-time PCR (qRT-PCR)

Real-time PCR is a method to quantify nucleic acid characterized by high sensibility and specificity. It is called "real-time" because it allows the scientist to actually view the increase in the amount of DNA as it is amplified. This is possible because it detects and quantifies fluorescent molecules: these compounds bind the amplified DNA and emit a signal that increases in a proportional way with the rise of amplified products. The result is an amplification curve where cycle numbers are found in abscissa and fluorescence, normalized on an internal fluorophore, in ordinate. At the beginning of the reaction there are only little changes in fluorescence and this is called "baseline region"; the increasing of fluorescence above this threshold underlines amplified product formation. From this point on the reaction performs an exponential course that degenerates in plateau at the end of the reaction.

In the midway cycles the curve has a linear course: this represents the most important phase since in this stage the amount of amplified DNA is correlated with the amount of cDNA expressed at the beginning in the sample. In this linear region a threshold of fluorescence is chosen: from this value it is possible to obtain the Ct (threshold cycle),

namely the cycle necessary, for the sample, to reach that threshold of emission (Figure 20). If the amount of cDNA present at the beginning is high, the curve will rise earlier and Ct values will be smaller.
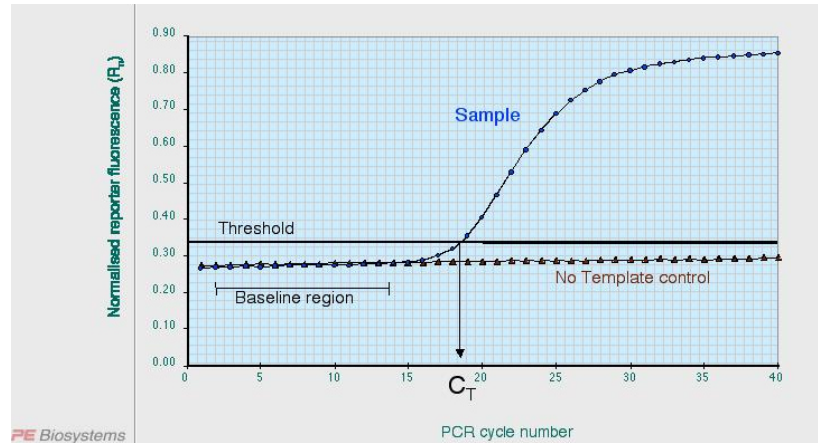

Figure 20. Amplification curve. Cycle numbers are found in abscissa and fluorescence normalized on internal fluorophore in ordinate.

As detector we used SYBR GREEN: its molecules emit low levels of fluorescence if present in solution, on the contrary the signal becomes stronger if the dye binds to double strand DNA. However, SYBR GREEN is not a selective dye and binds to all DNA, even to primer dimers. For this reason it is recommended the introduction of a further step after amplification, that is the "dissociation protocol": temperature rises gradually until all the DNA double strands are denaturated; this method allows the identification of contaminants or unspecific amplification products since they show different melting temperatures. There is also a second dye called ROX, which works as an internal reference used by the instrument to normalize the SYBR GREEN fluorescence. For the evaluation of gene expression we chose a relative quantification method, using the $\Delta\Delta$Ct formula:

1) ΔCt= Ct (target gene) - Ct (reference gene)
2) $\Delta\Delta$ Ct= ΔCt (of treated sample) - ΔCt (of untreated sample, the internal calibrator)
3) $2^{\wedge -\Delta\Delta Ct}$

61

The "2" value in the last formula represents the higher efficiency for the reaction that means a doubling of the product at every cycle of amplification.

The thermalcycler used is the Sequence Detection System 7000 (Applied Biosystem) and the software is ABI PRISM 7000.

The reagents of the following reaction mix are provided by Invitrogen:

-Platinum SYBR GREEN supermix	6,25µl
-ROX	0,25µl
-Forward primer (10pmol/ µl)	1µl
-Reverse primer (10pmol/ µl)	1µl
-H$_2$O	4,7µl
-MgCl$_2$	0,3µl
-cDNA	1,5µl
Final volume	20µl

Platinum SYBR GREEN supermix contains:

-SYBR GREEN fluorochrome;

-the Uracil DNA Glycosylase enzyme (UDG), that allows the removal of contaminant DNA (carryover) coming from previous amplifications. Indeed, UDG recognizes deossiuridine residues, that commonly substitute timidine residues in dNTPs mix and degrades this carryover DNA, preserving cDNA. UDG is activated at 50°C and this step precedes the amplification protocol; then it is inactivated at 95°C.

-Platinum Taq DNA Polymerase is an hot start polymerase.

Amplification protocol:

-UDG activation	50°C 2'	
-Polymerase activation	95°C 10'	
-Denaturation	95°C 30'	for 40 cycles
-Annealing and amplification	60°C 60''	

-Dissociation protocol: increasing temperature from 60°C to 95°C.

The sequences of primers, used in Real-Time PCR, were found using Primer Express program (Applied Biosystem).

Table 1: NOTCH target genes

MOUSE PRIMER	FORWARD	REVERSE
deltex-1	5'-CATCAGTTCCGGCAAGAC -3'	5'-GATGGTGATGCAGATGTCC -3'
hes-1	5'-CCAGCCAGTGTCAACACGA-3'	5'-AATGCCGGGAGCTATCTTTCT -3'
Notch-2	5'-ATGTGGACGAGTGTCTGTTGC -3'	5'-GGAAGCATAGGCACAGTCATC-3'
Notch-1	5'-TGCCTTCTGTGAGGAGGACATCAA-3'	5'-AGGTGTGTTGTTCTCGCAGTGGAT-3'

Table 2: Primers for CK2α and CK2β subunits

MOUSE PRIMER	FORWARD	REVERSE
CK2α	5'-ACACACACAGACCCCGAGAGT-3'	5'-TCATCTTGATTCCCCCATTCC-3'
Ck2β	5'-AGAGCTGGAAGACAACCCCAA-3'	5'-CCAACATTTGTGCGATGCC -3'

Table 3: Gene used to normalize the reaction

MOUSE PRIMER	FORWARD	REVERSE
gapdh	5'-CACCATCTTCCAGGAGCGAG-3'	5'-CCTTCTCCATGGTGGTGAAGAC-3'

3.12 Enzyme-Linked Immunosorbent Assay (ELISA)

For the ELISA test we utilized the Mouse Immunoglobulin Isotyping ELISA KIT (BD Pharmigen). This kit employs a direct horseradish peroxidase-labeled system and the assay format eliminates the need for coating the plate with an antigen.

Each kit supplies: 8 mouse immunoglobulin isotype-specific rat monoclonal antibodies, a horseradish peroxidase (HRP)-conjugated rat anti-mouse Ig antibody, substrate/stop solutions, coating/blocking buffers and a positive reference antigen mixture. The positive reference antigen mixture is a mixture of purified monoclonal mouse immunoglobulins of nine Ig heavy-and light-chain isotype combinations (IgG1κ, IgG1λ, IgG2aκ, IgG2aλ, IgG2bκ, IgG3κ, IgMκ, IgAκ, and IgAλ).

Reagent Preparation:

1. All reagents were brought to room temperature before use.

2. Coating Buffer (1X PBS) was prepared by diluting required quantity of 10X PBS with deionized water.

3. Blocking Buffer: was prepared by diluting required quantity of 10% BSA 1:10 with 1X PBS.

4. Positive reference antigen was diluted 1:50 with Blocking Buffer.

5. HRP-labeled rat anti-mouse Ig Ab was diluted 1:100 with Blocking Buffer.

6. Isotype-specific rat anti-mouse purified monoclonal antibody was diluted in Coating Buffer and delivered 50 µl of eachreagent to applicable rows.

8. Tap plate gently to ensure even distribution of antibody solution on the bottom of wells.

9. The plate was incubated, covered, at 37°C for 1 hour.

10. Plate contents were washed out using a washing solution (0.05% Tween-20 in PBS), for 3 times.

11. 200 µl of Blocking Buffer were added to each well, and incubated at room temperature for 30 minutes.

13. 100 microliters of each sample were pipetted to the appropriate columns plate and incubated for 1 hour at room temperature.

15. After, 100 µl of HRP-labeled rat anti-mouse Ig mAb solution were pipetted to each well, and incubated at room temperature for 1 hour.

16. Washed 6X, soaking the wells for 30 seconds to 1 minute on each wash.

17. 100 µl of prepared Substrate Solution were added to each well and incubated plate for 3 - 10 minutes at room temperature. Positive reaction wells will develop a greenish-blue color. Negative wells will be colorless.

18. 50µl of Stop Solution were pipetted to each well.

19 The plates were read in the spectrophotometer at 450 nm.

3.13 CK2 kinase activity assay

CK2 activity in whole cell lysates was measured using Casein Kinase 2 Assay Kit (Millipore). The assay is designed to measure the phosphotransferase activity of CK2 and is based on the phosphorylation of a specific substrate peptide using the transfer of the gamma-phosphate of [γ-32P]ATP by CK2. The phosphorylated substrate is then separated from the residual [γ-32P]ATP using P81 phosphocellulose paper and quantitated using a scintillation counter. The assay is linear for incubation times of up to 30 minutes and incorporation of up to 20% of total ATP. Further incubation or incorporation may not be linear and may therefore not be a true indication of CK2 activity in the sample extract.

<u>**Assay Protocol Summary**</u>:

1. Bradford quantification of whole cell lysates.

2. Addiction of 7µL of ADBI, 5 µL of the substrate peptide EIF2β (200µM final concentration), 5 µL of PKA inhibitor cocktail, 5 µL of cell lysates (2,5ug), 3 µL of the diluted [γ-32P]ATP to a microcentrifuge tube

3. Incubation for 35' minutes at 30°C

4. Stop the reaction by placing each tube for 10 min on ice

5. Transfer 25 µL on numbered P81 paper squares

6. Immersion of the paper in 0.75% phosphoric acid and mix gently on a rotator for 1h.

7. Washing of the squares in 20 mL of acetone for 10 min.

8. Allow to dry, transfer to a scintillation vial and add 3 mL of scintillation cocktail.

9. Read in a scintillation counter.

CPM of enzyme samples were compared to CPM of control samples that contain no enzyme (background control). Suitable blanks were performed to correct for non-specific binding of [γ-32P]ATP and its breakdown products to the P81 paper. Controls for endogenous phosphorylation of proteins in the sample extracts can be performed by substituting assay dilution buffer with substrate cocktail.

3.14 Immunofluorescence (IF)

Spleens of CK2β KO and CTRL mice were fixed with 4% paraformaldehyde (PFA) for 3h. Spleens were then washed in PBS to remove residues of PFA and left overnight in 20% sucrose to dishidrate. The day after 10 um thick-sections were cut, permeabilized with PBS plus 0,1% Triton for 20 min and blocked with PBS plus 0,5% BSA and 10% FCS for 30 min. After washing in PBS they were stained with rabbit anti-NOTCH2 (D76A6; Cell Signaling Technology), FITC-conjugated anti-CD169 (MOMA1; AbD Serotec), PE-conjugated anti-IgM (BD bioscence), V450-conjugated-IgD (BD bioscence), FITC-conjugated-PNA (Sigma) and GL7 (eBioscence).

Slides were then washed and the following secondary antibodies were used: ALEXA-FLUOR 594 goat anti-rabbit IgG (Invitrogen), PEanti-rat IgM (eBioscence). At the end sections were stained with a Fluoromount aqueos mounting medium without DAPI (Sigma). Images were acquired at Zeiss LSM700 and merged in three-color images with ImageJ software.

3.15 Immunohistochemistry (IHC)

Spleens of CK2β KO and CTRL mice were explanted and processed to achieve formalin fixation and paraffin embedding. Sections 2–3 µm in thickness were cut and

stained with hematoxylin/eosin and BCL6 antibody (Vector Laboratories) to evaluate the formation of GCs in basal conditions and after stimulation with SRBC.

3.16 *In vivo* immunization

CTRL and KO mice (10 weeks old) were immunized intra peritoneally (i.p.) with 200 ul of Sheep Red Blood Cells (SRBC; Microbiol) diluted 1:10 in PBS, as a control were inoculated 200ul of PBS only.

Peripheral blood and spleens were removed after 14 days for immunoistochemical and cytometric analysis.

To evaluate the formation of germinal centers (GC), splenocytes were stained with anti-B220, anti-CD19, anti-CD95, anti-CD38, anti-PNA (Sigma).

3.17 *In vivo* inhibition of Notch2 activation

CK2β KO and CTRL mice were injected i.p. with 15 mg/kg α-NRR2 (synthesized and kindly provided by Dr. Christian W. Siebel, Genentech , Department of Discovery Oncology) or IgG (Jackson ImmunoResearch Laboratories, Inc.) as a control. Mice were analyzed 72h after injection of a single dose of α-NRR2, through a cytometric and immunophenotypic analysis.

3.18 Whole transcriptome sequencing

RNA isolated from purified B-cells from CK2β KO and CTRL mice (3+3) was used for RNA seq analysis. The analysis was conducted through a collaboration with Prof.Giorgio Valle (CRIBI Biotechnology Center, University of Padua). For the transcriptome analysis, they used the SOLiD 5500 (Lifetechnologies) , and results were analyzed by the use of a special software by dott.Nicola Vitulo (CRIBI Biotechnology Center, University of Padua).

3.19 Statistical analysis

Experiments were performed at least three times. We used t-test to analyze data as appropriate. We considered p values < 0,05 as significant. Analyses were performed using Excel (Microsoft Office) or Origene 7.0 software.

3.20 Software

Sono stati utilizzati per l'acquisizione e l'analisi dei dati citoflorimetrici *BD Cell Quest Pro*, *BD FACSDiva*, *FlowJo* v.X.

I grafici di dispersione e gli istogrammi sono stati realizzati con *GraphPad Prism* v.VI e con *Microsoft Office Excel*.

4. RESULTS

4.1 Generation of CD19 conditional CK2β KO mice

In order to obtain a conditional knockout mice for CK2β, we performed crossings of CK2β Flox / Flox mice (generated by Dr. B.Boldyreff , Grenoble) with CD19Cre / Cre mice (Jackson Lab) .

The first generation of mice obtained were heterozygous for the two loci.

Heterozygotes mice were crossed with each other , generating Flox / Flox , Cre / + (KO) and + / + , Cre / + (CTRL) mice.

 For the experiments we only used CD19 Cre/+ mice , because CD19 Cre/Cre mice have an abnormal phenotype in the development of B lymphocytes. Mice obtained were viable, fertile and had a normal phenotype. Mice genotype was verified by a PCR (**FIG.19**).

A   **B**   **PCR CK2β Floxed**

PCR CD19 MUT

PCR CD19 WT

🟨 CK2β Flox/Flox; CD19 Cre/+ (KO)
🟥 CK2β +/+; CD19 Cre/+ (CTRL)
🟩 Positive control
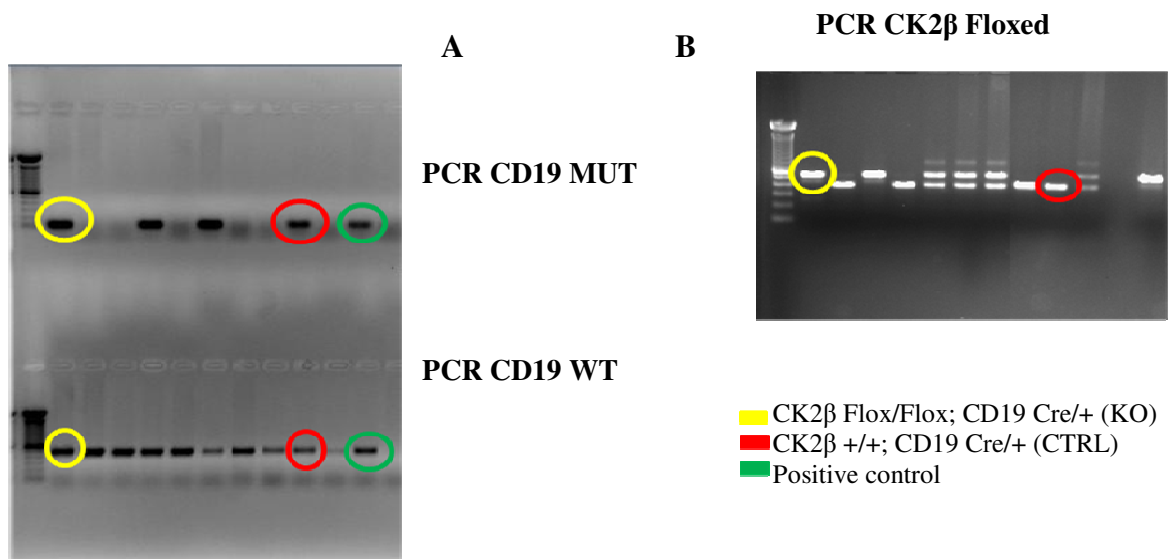
Fig.19: mice genotyping.

A. PCR for CD19 mutated and CD19 wt
B. PCR for the site CK2β. The positive control (C +) is a CK2βFlox / Flox mouse.

The PCR to determine the presence of the WT CD19 gene, provides a 477 bp fragment, while the mutant CD19 provides a 100 bp fragment. In the PCR for CK2β gene, product of 550 bp and 400 bp are expected for Flox and WT, respectively.

In Figure 19 are shown the PCR products of 10 mice, generated with the previously described crossings.

4.2 CK2β KO mice present an evident splenomegaly

CK2β KO and CTRL mice were sacrificed between 8 and 12 weeks.

During the isolation of organs, the spleen of CK2β KO mice showed an increase in size and weight (splenomegaly) (**Fig.20**), while the remaining hematopoietic organs did not show any phenotypic alteration.

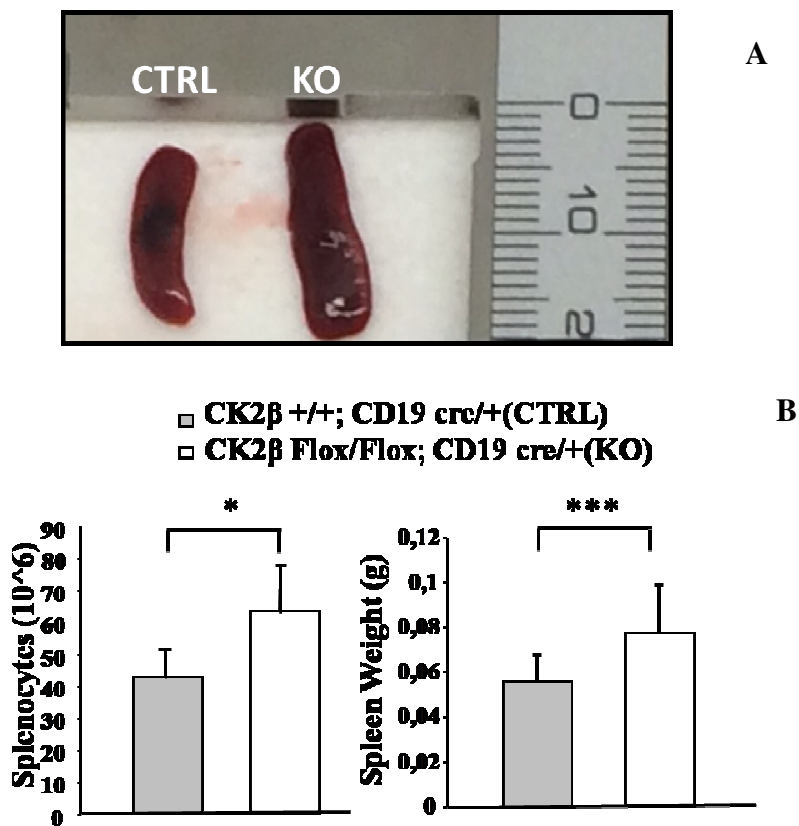In addition, the staining with the trypan-blue dye, showed, an increase in cell count in CK2β KO mice (**Fig.20**).

Fig.20: CK2β KO mice are characterized by a marked splenomegaly.
A. CK2β KO mice showed a phenotypic alteration (splenomegaly) when compared to CTRL mice.
B. Histograms summarizing the increase in cellularity and weight of spleens in CK2β KO mice compared to CTRL mice.

4.3 CK2β KO is confirmed by quantification of mRNA and protein levels

In order to verify if the excision of the floxed sequence in the Csnk2β in the KO mice determines a reduction of mRNA and protein levels of CK2β, we have performed qRT- PCR and WB experiments (**Fig.20**).

To this purpose, total proteins and mRNA were extracted from splenic and bone marrow B-cell collected from CK2β KO and CTRL mice.
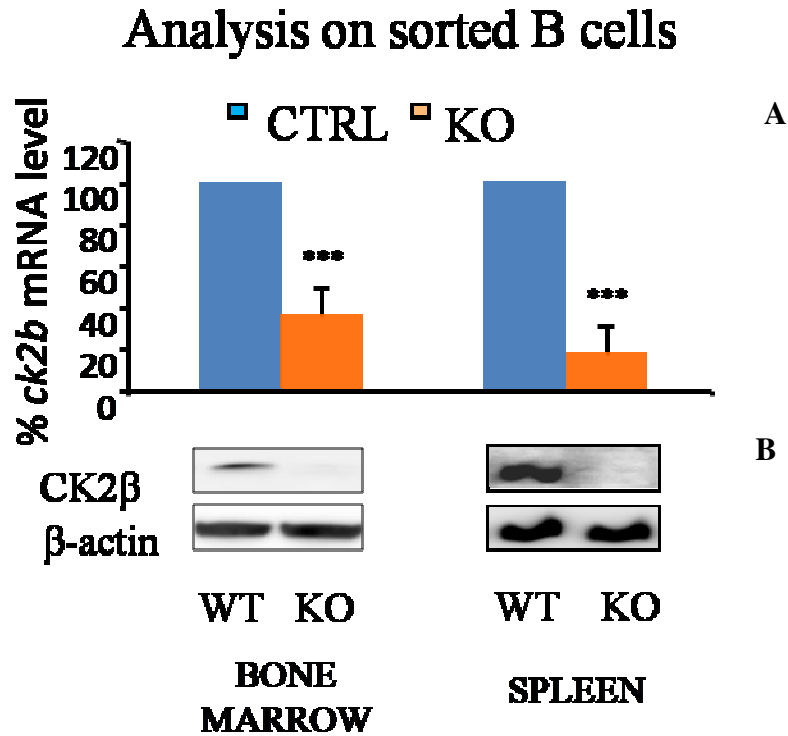

Figure 20: Quantification of CK2β mRNA and protein levels in spleen and bone marrow: **A)** results of the qRT-PCR analysis of B-cells conducted in mice sacrified after 8 weeks; **B)** results of the WB analysis of B-cells of mice sacrified after 8 weeks.

As shown in figure 20, mRNA levels correlate with protein quantity, showing an almost complete disappearance of CK2β in spleen and bone marrow of CK2β KO mice as compared to control mice.

Thus, this analysis demonstrates that our KO system is effective.

4.4 Kinase activity

Since our KO model regards only CK2 regulatory subunits, we decided to check CK2 catalitic subunits status carrying out a kinase assay using purified B-cells from CTRL and KO mice (**Fig.21**).

KO mice displayed a reduction in CK2 catalytic activity, towards a β specific peptide, compared to CTRL mice, whereas no significant difference could be detected

considering a peptide that can be phosphorilated by the holoenzyme or by the catalytic subunits alone. A further confirmation of CK2 kinase activity reduction, has been demonstrated with the reduction of phosphorylation of p65 in ser 529 in WB, which is a direct target of CK2 (**Fig.21**).
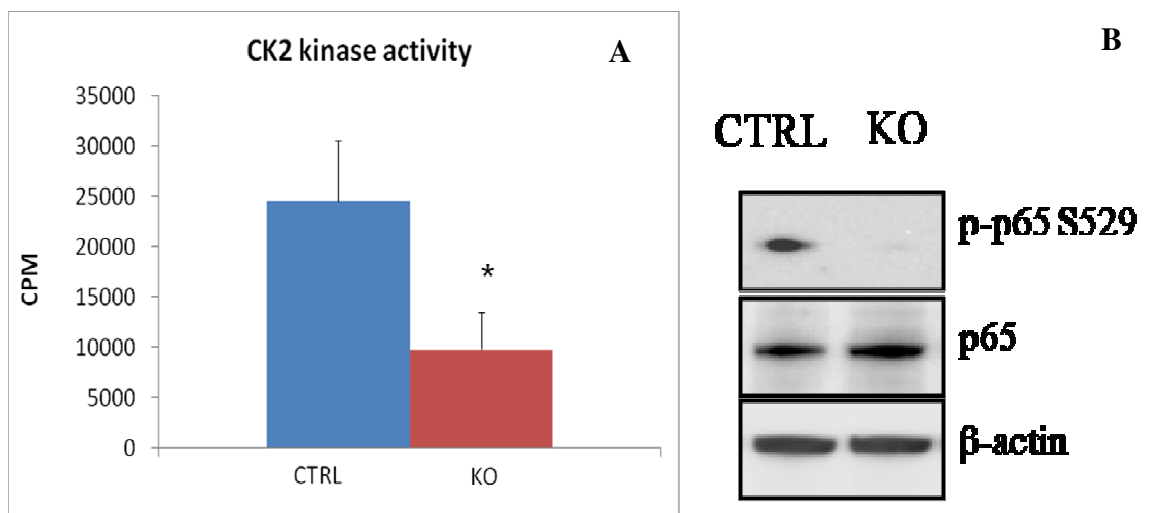

Fig. 21: CK2 kinase activity was decreased in CK2β KO B-cells.
A.Graphs showing the Kinase activity of spleen B-cells of CTRL and CK2β KO mice. The graphs represent the mean and standard deviation. Numerosity: (CTRL = 3, KO = 3). * P <0.05. B. The WB analysis of NF-κB p65 phosphorylation at the CK2 target site Ser529 revealed that absence of CK2β in B lymphocytes was associated with a near complete disappearance of phosphorylated p65, indicating a critical role for CK2β in the phosphorylation of this target site

4.4. Quantification of total B-cells

In order to assess potential differences in the percentage of B-cells present in the hematopoietic organs of CK2β KO and CTRL mice, flow cytometryc analysis was performed using fluorescent antibodies that recognize specific markers for these cells: CD19 and B220.

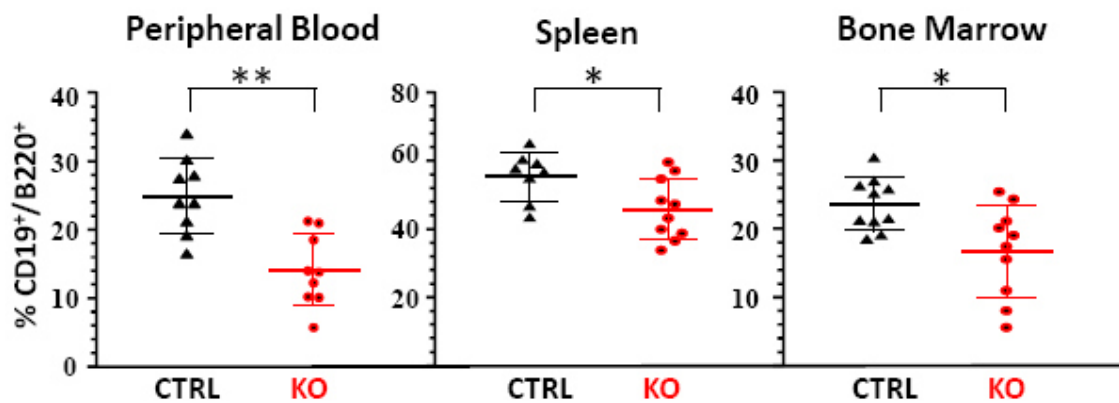We analyzed bone marrow, spleen, and peripheral blood (**Fig.22**).

Fig. 22: percentage of B-cells in CK2β KO and CTRL mice.
The analysis was performed with FACSCalibur, using CD19 and B220 markers in peripheral blood, spleens and bone marrow. Graphs show mean and standard deviation (SD). Numerosity: peripheral blood (CTRL = 8, KO = 9); spleen (CTRL = 8, KO = 10); bone marrow (CTRL = 10, KO = 10). * p <0.05, ** p <0.01, *** p <0.001.

As observed in figure 22, in peripheral blood, spleen and BM, there is a significant reduction in B-cells (p <0.05) in CK2β KO when compared to CTRL mice.

There is no variation of B lymphocytes in the lymph nodes (data not shown).

The most significant varation was observed in peripheral blood (p = 0.00155), indicating a possible reduction of the recirculating B-cell population.

4.5. Analysis of recirculating B lymphocytes

After quantification of total B-cells, we analyzed the populations of naive B-cells (CD19$^+$/B220$^+$), newly formed lymphocytes, and recirculating B lymphocytes (CD19^{high}/B220^{high}), the most mature component of B lymphocytes. Flow cytometric analysis showed a reduction of the (CD19^{high}/B220^{high}) in KO mice, in particular in the bone marrow (**Fig.23**).
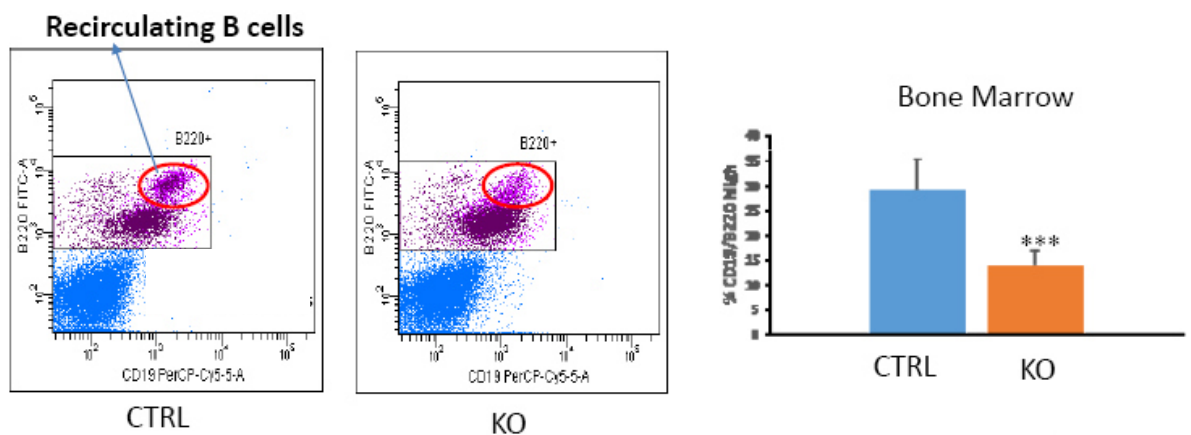

Figure 23: reduction of recirculating B lymphocytes in KO mice.
The analysi was performed with FACSCalibur flow cytometric for the markers CD19 and B220 in the peripheral blood, spleen, bone marrow. The graphs show the mean and standard deviation (SD). Numerosity: peripheral blood (CTRL = 8, KO = 9); spleen (CTRL = 8, KO = 10); bone marrow (CTRL = 10, KO = 10). * P <0.05, ** p <0.01, *** p <0.001

To confirm the reduction of recirculating B lymphocytes, we used two specific markers IgM and IgD, which allow to discriminate *naïve* B-cells (IgM$^+$/IgD$^-$) and recirculating B lymphocytes (IgM$^+$/IgD$^+$) (**Fig.24**).
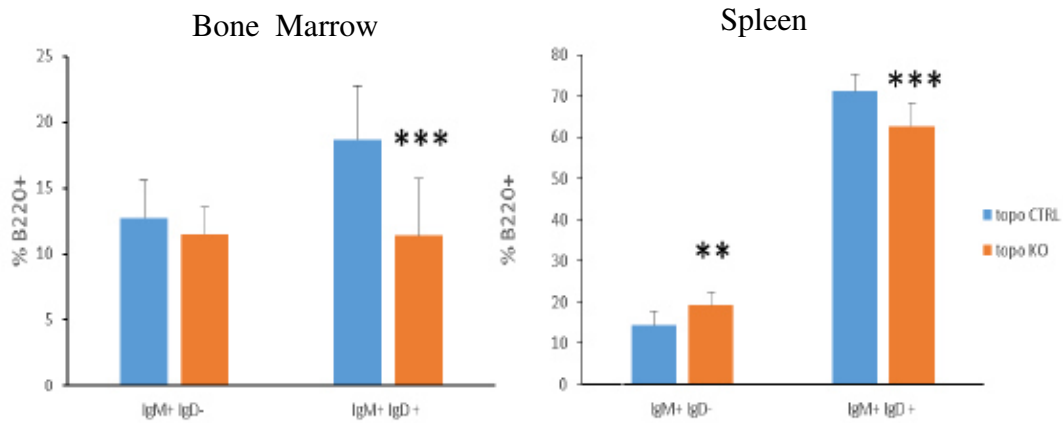
Fig.24: analysis of IgM and IgD markers in spleen and bone marrow.
Analysis B220/IgM /IgD on B-cells of BM and SP. Graphs show means and SD. Numerosity: BM (CTRL = 10, KO = 11); SP (CTRL = 11, KO = 11). *** p <0.001; ** p <0.01.

Figure 24 showed no significant variation of naive B-cells (IgM$^+$/IgD$^-$) in the bone marrow, while these increase significantly (p<0.01) in the spleen of KO when compared to CTRL mice.

In addition there is a reduction of recirculating B-cells (IgM $^+$/IgD$^+$), both in the bone marrow and spleen of KO, compared to CTRL mice. Confirming previous result obtained with (CD19^{high}/B220^{high}) staining.

4.6 Analysis of BM precursors

To evaluate a possible reduction of B-cells during their development , we analyzed the bone marrow precursors proB (CD19$^+$, B220$^+$, IgM$^-$, CD25$^-$, CKIT $^+$) and preB (CD19 $^+$, B220$^+$, IgM$^-$, CD25$^+$, cKit$^-$) .

For this analysis we stained cells of bone marrow with the following fluorochromes: B220-FITC, IgM-PE, CD19-PerCPCy5.5, CD25-APC, CKIT-PECy7. During this analysis were considered B220 and CD19 markers of B cell line, and in particular we analyzed the population B220$^+$, because it is expressed earlier than CD19 (**Fig.25**).
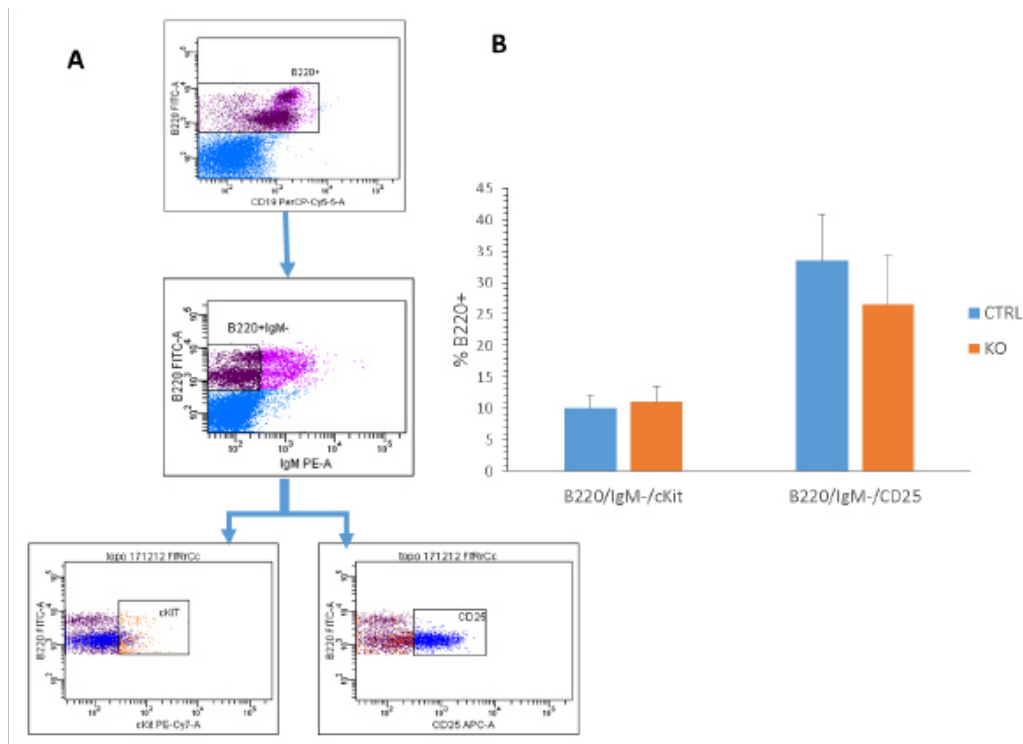
Fig. 25: analysis of preB and proB in BM.
A.summary cytograms of flow cytometric analysis. only the cells B220 were selected. Among the B220[+] IgM were excluded. Finally among the B220 [+]/ IgM[-] we selected CKIT [+] (PROB) and CD25 [+] (preb). B. histogram of populations B220 [+]/ IgM[-] / CKIT [+] (PROB) and B220 [+]/ IgM[-] / CD25 [+] (preb). Numerosity: BM (CTRL = 7, KO = 10). The graphs show the mean ± SD.

Statistical analysis shows that the proB lymphocytes do not have a significant variation between KO and CTRL mice, while preB lymphocytes have a tendency of reduction in KO mice (p 0.08).

4.7. Characterization of peripheral B lymphocytes

After analyzing in detail the B-cells of the bone marrow and their precursors, we analyzed peripheral B lymphocytes. We stained the spleen cells with specific markers of follicular and marginal B lymphocytes, which are the most represented classes of splenic B-cells. Over the two line markers CD19 and B220, we added CD21 and CD23. CD23 is expressed in lymphocytes that enter in the follicle, and is a marker of recirculating B-cells. CD21 is expressed at high intensity in MZB is a marker of proteins complement (C3b and C3d) and is part of the BCR coreceptor.

B-cells were divided into FoB ($CD19^+$, $B220^+$, $CD21^-$, $CD23^+$) and MZB ($CD19^+$, $B220^+$, $CD21^+$, $CD23^-$). The plots of the acquisition are described in detail in Figure 26. The results of this analysis show that, in the spleen of KO mice, there is a marked reduction of follicular B-cells when compared to CTRL mice ($p < 0.001$). This reduction was offset by an accumulation of MZB in KO mice.
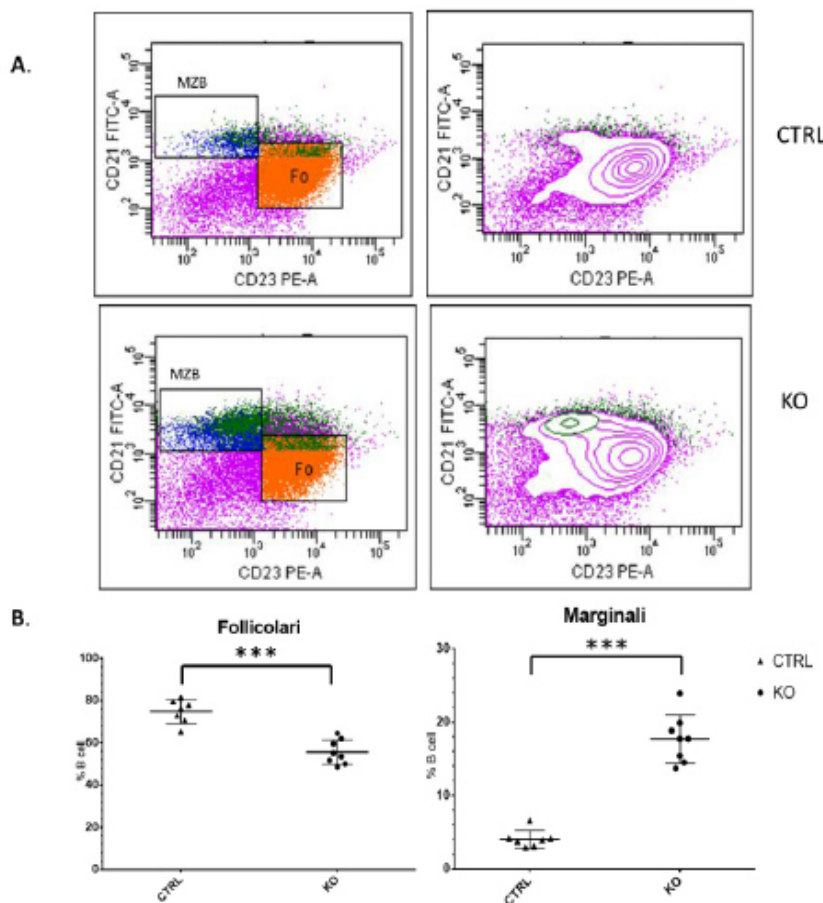

Fig.26: reduction of FOB and increase of MZB lymphocyte number in CK2β KO mice.
(A) Representative dot plot cytogram showing the stain for CD21 and CD23 used to characterize B lymphocyte populations. (B) Graphs summarizing FACS analysis of MZB and FOB in CTRL and KO mice. CK2β KO mice showed a marked reduction of FOB and a significant increase of MZB in the spleen. . Data representing mean +/- SD 8 CTRL and 8KO mice. *, $p < 0.05$; **, $p < 0.01$; ***, $p < 0.001$

After finding these differences, we performed a more accurate analysis to define all the population residing in the follicle ($CD23^+$, $CD21^-$) and analyze the precursors of MZB (MZP).

The markers used in this analysis were: CD19, B220, CD21, CD23 and IgM (**Fig.27**).

- CD19, B220 to identify B-cells;
- IgM to distinguish FoI (IgM^{low}) from other follicular populations expressing IgM^{high} (T2, FoII, MZP);
- CD23 to distinguish follicular populations ($CD23^+$) from the extrafollicolar populations $CD23^-$ (T1 and MZB);

- CD21 to discriminate, based on the intensity of the marker, between T1, T2 (CD21^{low}), FoB, FoI, FoII (CD21^{med}) and MZB, MZP (CD21^{high}).
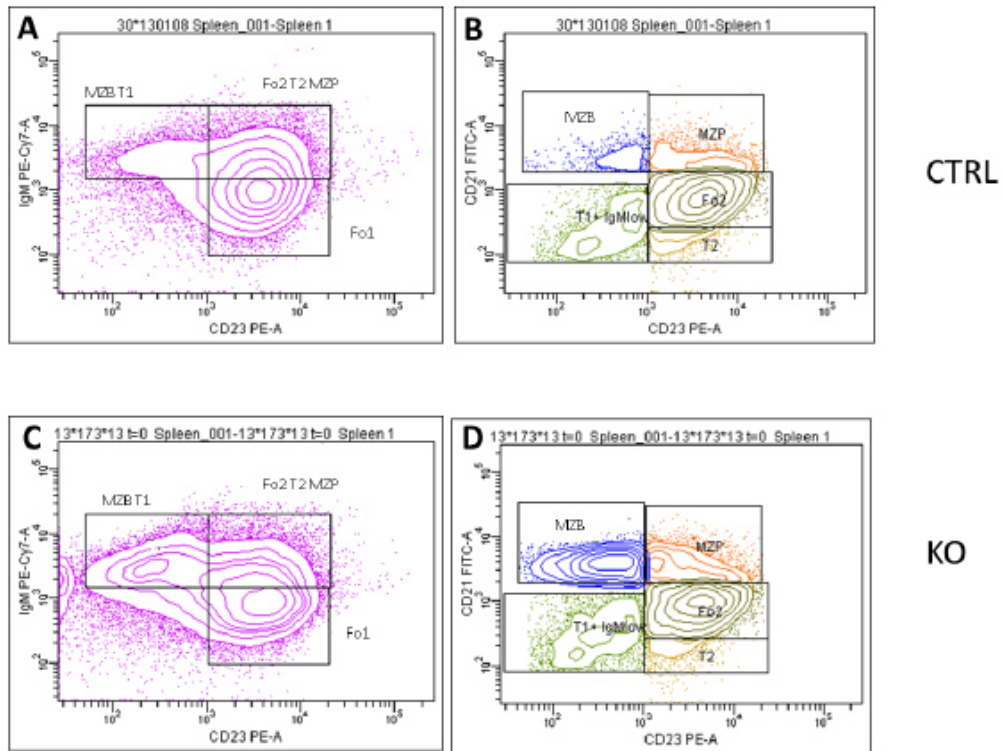

Fig. 27: cytograms of splenic B-cells population.
The analysis was performed on the gate of B-cells (CD19/B220) and, were identified by the expression of CD23 and IgM, the FoI and a large population that contains FoBII, T2, MZP (plot A-C). From this population, based on the expression of CD21, were distinguished the MZP, FoII and T2 (plot B-D). While T1 cells were identified as IgM^{+}/ CD21^{-} / CD23^{+}.

Analysis of the results show a several differences between KO and CTRL mice, indeed in KO mice there is an increase in MZB (CD19^{+}, B220^{+}, IgM^{+}, CD21^{high}, CD23^{-}), and an in precursors MZP (CD19^{+}, B220^{+}, IgM^{+}, CD21^{high}, CD23^{+}) (**Fig.27**).

Moreover IF analysis revealed a change of size/shape of spleen follicles and a significant expansion of the inter-follicular, marginal zone areas, which appeared to invade the follicle with larger cells (**Fig.28**).

Statistical analysis shows that in KO mice there is a significant increase of MZB and MZP, and a reduction of a follicular populations (FoI, FoII, T2) (**Fig.29**).
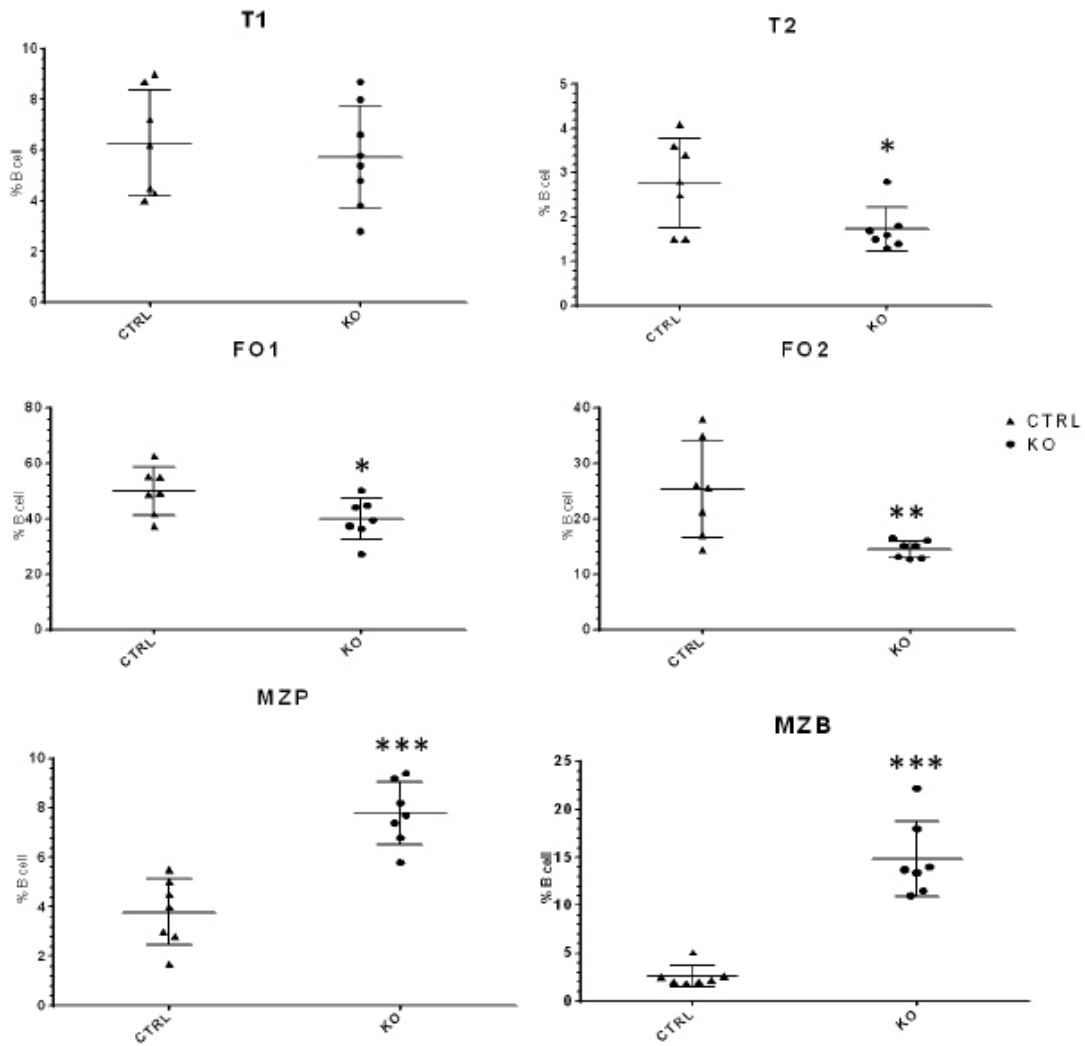

Fig.28:analysis of splenic B- cells population.
Graphs scatter representative cytometric analysis. Have compared the distributions of B subpopulations in KO and CTRL mice.. The graphs shows the mean ± SD. Mice analyzed: CTRL = 7, KO = 7. *** p <0.001, ** p <0.01, * p <0.05.
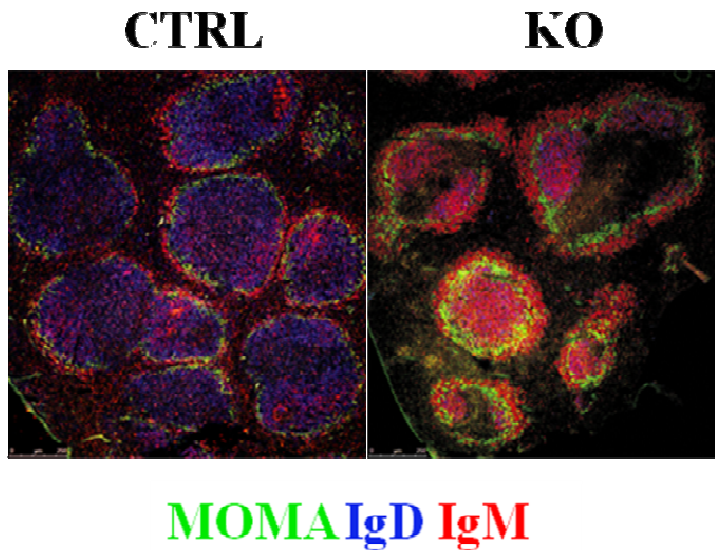
CTRL **KO**

MOMA IgD IgM

Fig. 29: IF staining of follicles in spleens of CTRL and KO mice.
IF analysis of frozen spleen sections from CTRL and KO mice, stained with anti-IgM , anti-IgD and MOMA to evaluate the morphological distribution of FO and MZ B-cells. Whereas spleens from CTRL mice had a precise distribution of FO and MZ B-cells with the IgD inside the FO zone, CK2β KO mice displayed a disorganization of such distribution, with the IgD staining redistributed in proximity of the marginal zone.

4.8 Functional analysis of GC

Having observed a clear reduction of FoB in KO mice, a study was performed to evaluate if these cells react to stimulus that induce isotype switching and proliferation. In this study we have used two approaches, *in vitro* and *in vivo*.

4.8.1 *In vitro* approach

Splenocytes were treated with LPS and LPS + IL4. LPS induces the proliferation and differentiation of B-cells into plasma cells (PC) secreting IgG3 (T-independent response). The stimulus LPS + IL4 induces differentiation in PC secreting IgG1 (T-dependent response). Splenocytes obtained from CTRL and KO mice were stimulated for 72 hours and analyzed by flow cytometry. Splenocytes were stained with anti-B220 and anti-IgG1 and IgG3. Results obtained demonstrate that in KO mice there is a

reduction in the number of IgG produced in presence of both stimuli, demonstrating the existence of anomalies that compromise isotype switching (**Fig.30**).

In addition, to assess the formation of PC, splenocytes were stained with anti-B220 and anti-CD138. Results showed that in KO mice there is a reduction of PC when compared to CTRL mice, after stimulation with LPS + IL4 (**Fig.31**).
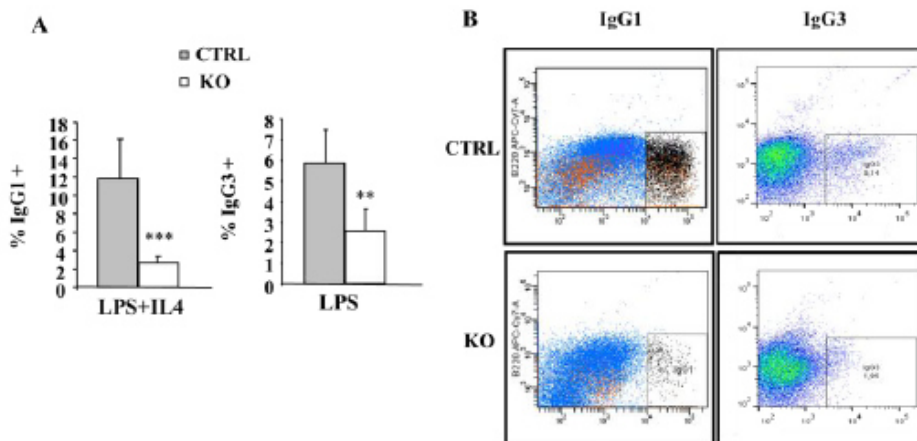

Fig.30: functional analysis of the GC reaction.
A.Histograms summarizing the FACS analysis of IgG1 and IgG3 expression of CD19$^+$ splenocytes from CTRL and KO mice treated for 72 hours with LPS (for IgG3) or LPS + IL-4 (for IgG1). Numerosity: IgG1 (CTRL = 8, KO = 6); IgG3 (CTRL = 5, KO = 4) *** p <0.001, ** p <0.01. Graphs show mean and SD. B. Representative dot plots are shown.
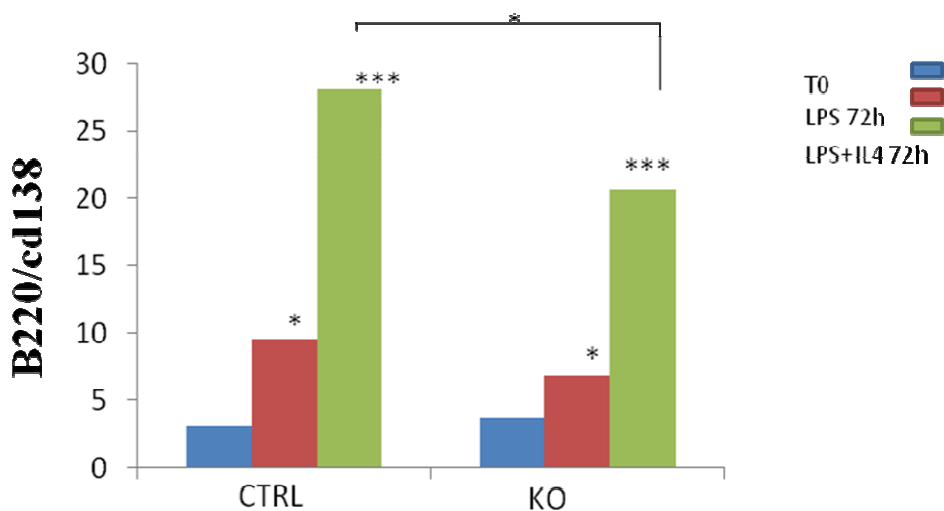

Fig.31: reduced production of PC in KO mice.
Histograms summarizing the FACS analysis of CD138 expression in CD19$^+$ splenocytes from CTRL and KO mice treated for 72 hours with LPS and LPS + IL-4 .Numerosity: (CTRL = 4, KO = 4); *** p <0.001 * p <0.05. Mean and SD are shown.

We then investigated the corresponding cultures throughout WB to assess the induction of the transcription factors Blimp1 and Irf4 [44], which are required for PC differentiation, we found out that CK2β KO showed a dramatically impaired up-regulation of BLIMP1 compared with CTRL mice (**Fig.32**).Conversely, IRF4, which in addition to PC differentiation regulates class switch recombination, was normally induced in CK2β KO mice.
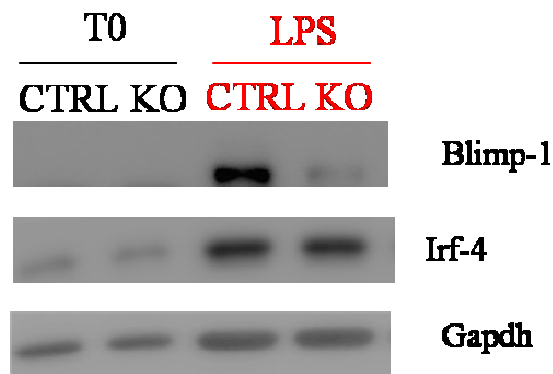

Fig. 32: CK2β is required for the generation of GC-derived PC.
Representative WB of purified B-cells stimulated or not for 3 days with LPS tu induce the expression of BLIMP1 and IRF4 proteins..

4.8.2 In vivo approach

To evaluate *in vivo* the GC reaction, we immunized CTRL and KO mice with SRBC to induce a T cell–dependent response. 14 days after immunization, the fraction of splenic CD95^{high}PNA^{high}/CD38 ^{low} GC B-cells in KO mice did not significantly differ from CTRL mice (**Fig.33**). Accordingly, histological analysis of spleen sections demonstrated a robust formation of BCL6+ GCs (**Fig.33**). Moreover, KO mice did show smaller follicles and expanded marginal/inter-follicular areas.
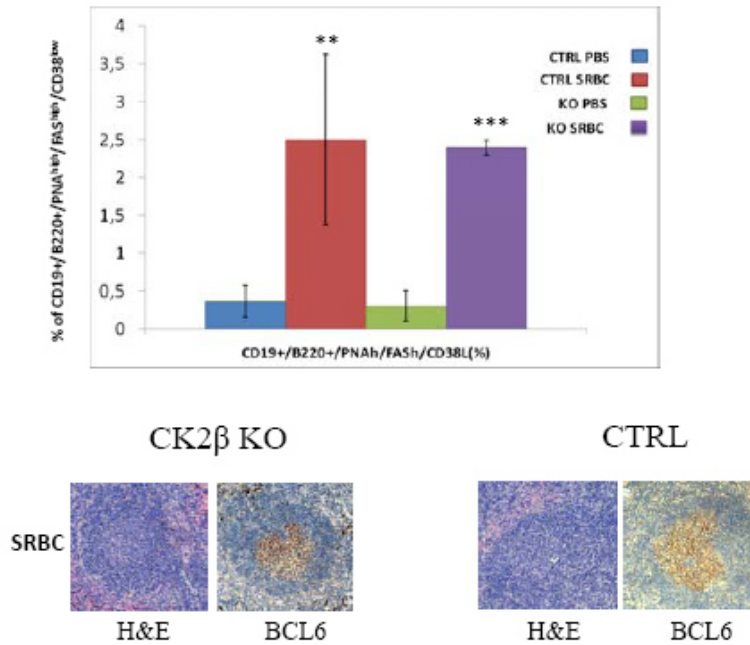
Fig.33: GC formation.

A. Flow cytometric analysis of splenic B-cells 14 days after inoculation of SRBC shows a conserved expression of GC markers, such as CD38, GL7 and PNA in CTRL mice and in KO mice.
B. histological analysis showed a conserved up-regulation of GC markers, such as BCL6. Nonetheless, the architecture of the reactive follicles was markedly changed.

4.9 Quantitation of Igs in mice sera

Since we have observed a reduction of FoB and an alteration of post-germinal center formation in CK2β KO mice, we assessed in the sera the production of different classes of immunoglobulins. This analysis was performed by ELISA test (**Fig.34**).

The results showed a marked reduction in the generation of antibody-producing cells (hypogammaglobulinemia) in CK2β KO compared to CTRL mice.
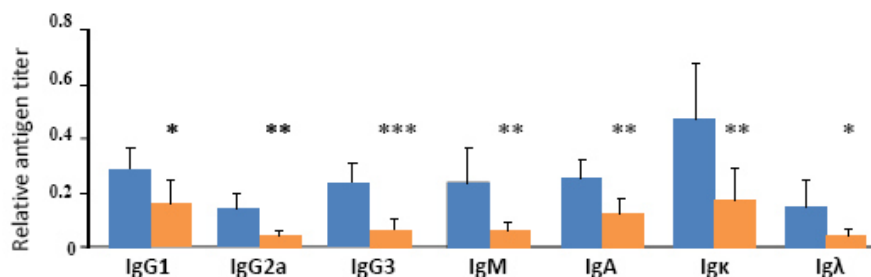

Fig.34: CK2β KO B lymphocytes display an impaired production of Igs

Basal levels of immunoglobulins detected in the sera of CTRL and KO mice (n=8 CTRL; n=6 KO).

4.10. CK2β-deficient B-cells show increased activation of the Notch2 pathway

The requirement of Notch2 for the generation of both precursor and mature marginal zone B-cells led to some intriguing insights about the follicular versus marginal zone B-cell transition. Notch2 is required for marginal zone B-cell development during B-cell maturation in the spleen[37]. Given these strong evidence, we analyzed the status of Notch2 and its target genes by WB and qRT-PCR. The qRT-PCR analysis also revealed a significant up-regulation of NOTCH target genes *hes1* and *deltex1*(**Fig.35**) in the CK2β KO compared with CTRL mice. WB analysis showed that Notch2 protein was strongly up-regulated in CK2β KO versus CTRL B-cells (**Fig.35**). Considering this result, we propose a CK2β involvment in Notch2 pathway.
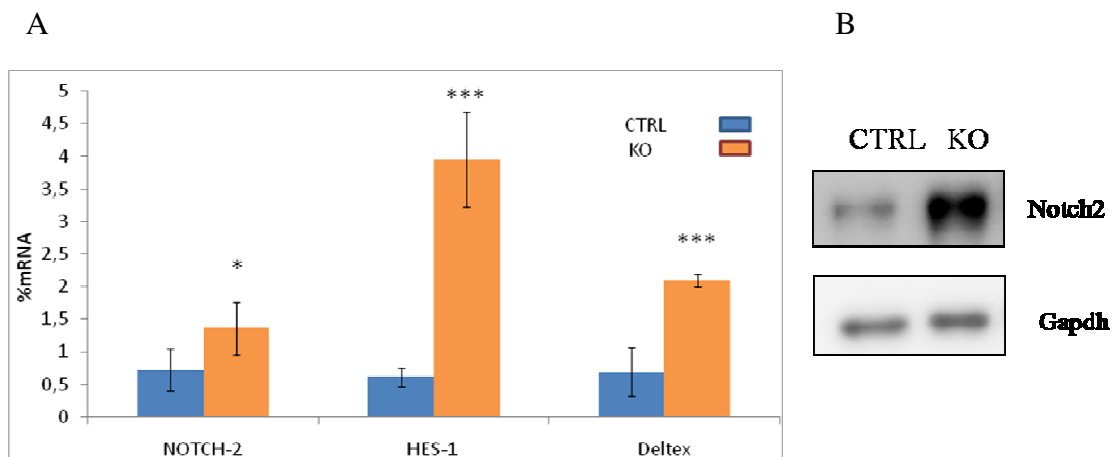

Fig.35: Elevated activation of Notch pathway in CK2β KO B-cells.

A CTRL (n=5) and KO (n=5) splenic B-cells were analyzed for the expression of *Notch* , *hes* and *dtx* by qRT-PCR. The expression was corrected for GAPDH levels and then normalized to CTRL. Statistical analysis was determined by student's t test (* p<0.05; *** p<0,001).

B. Notch2 2 expression in CTRL and KO splenic B-cells was analyzed by Western Blot.

Having established that in CK2β KO mice there is an increase of Notch2 pathway, to determine whether the accumulation of MZB is dependent on the activation of the Notch2 pathway, we blocked the Notch2 receptor *in vivo,* by the administration of a monoclonal antibody (a-NRR2, Wu et al., 2010). After 72h we analyzed the topography

of the MZ and FO areas in spleens and the amount of MZB and FOB in CTRL and KO mice (**Fig.36**) [44].
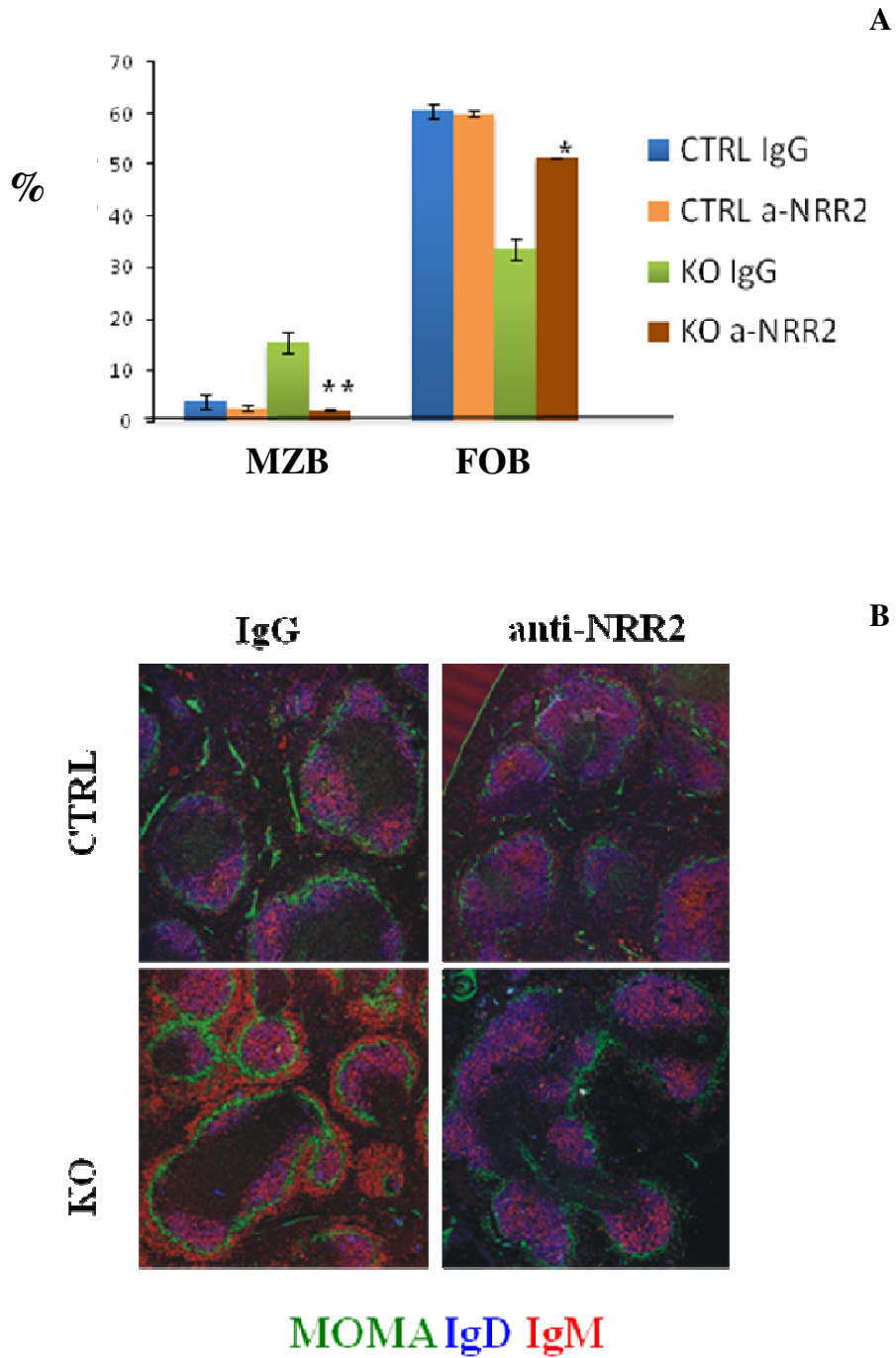

Fig.36: analysis of MZB and FOB population in CTRL and KO mice.

A. Graphs showing the flow cytometry analysis of MZB (CD21$^+$/CD23^{low}) and FOB (CD21$^-$/ CD23^{high}) after 72 h of treatment with a-NRR2 or IgG.
B. Spleen sections from CK2β KO and CTRL mice stained with a-IgM, a-IgD and a-MOMA after 72h of treatment with IgG or a-NRR2 antibody.

Figure 36 shows that after treatment with a-NRR2 there is a reduction of MZB cell number, and IF show a complete restoration of the architectural shape of the follicle in CK2β KO, suggesting a Notch2-dependent MZB expansion associated with CK2β loss.

4.11 RNA-seq

Mice phenotype determined by flow cytometry, IHC and IF prompted us to try to understand the molecular mechanism at its basis [15]. We performed an RNA-seq analysis, thanks to a useful collaboration, comparing mRNA extracted from purified B-cells of 3 KO and 3 CTRL mice (**Fig.37**).

Preliminary RNAseq analysis was also performed and revealed significant alterations in B-cells regulating pathways, such as NF-kB, cell adhesion molecule and signaling by Notch. Further analysis are ongoing in our laboratory to determine how these pathways could be implicated in the phenotypic alterations we observed in KO mice.
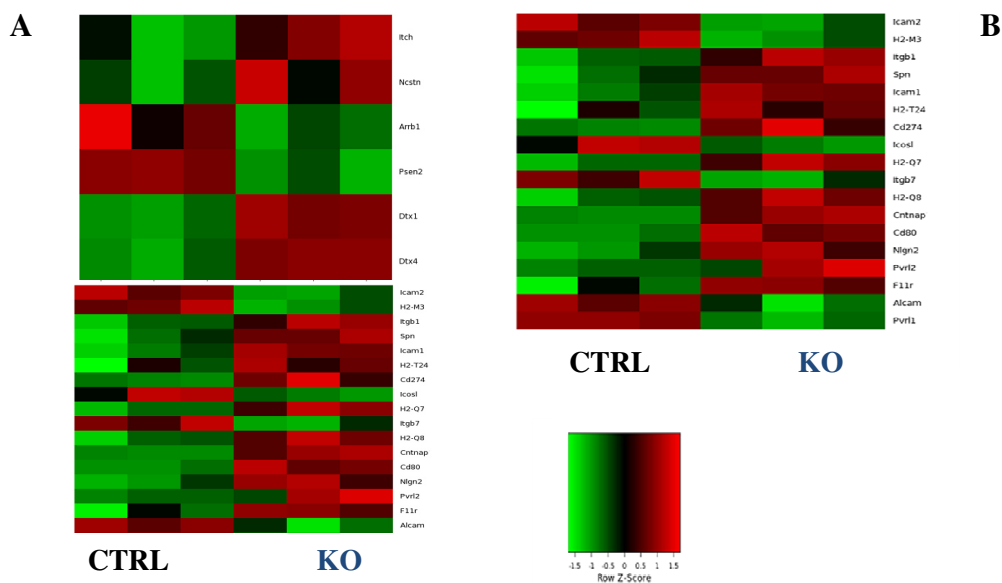

Fig. 37: CK2β KO fail to activate a set of genes involved in many cellular functions.
RNA was isolated from purified B-cells of, respectively, CTRL and CK2β KO mice and processed for hybridization on microarrays. B cell fractions were isolated separately from 3 mice per genotype and independently processed for microarray hybridization. Gene expression differences between B-cells from CTRL and CK2β KO mice were determined by supervised analysis. Color changes within a row indicate expression levels relative to the mean of the sample population. Values are quantified by the scale bar that shows the difference in the zge score relative to the mean (0). A. Rna seq showing the expression of cell adhesion molecules; B. Rna seq showing the expression of molecules involved in Notch signaling.

5. DISCUSSION

CK2 is a pleiotropic and evolutionary conserved serin-threonin kinase that is involved in several cellular processes. A number of studies revealed many mechanisms through which this kinase regulates cell cycle, apoptosis, cell survival and tumorigenesis.

However, despite all this data, little is known about the role of CK2 in B-lymphopoiesis and lymphomagenesis.

Considering this knowledge, we decided to investigate the role of CK2 using a conditional CK2β KO mouse model in B-cells.

To make this, we crossed homozygous mice for the *floxed Csnkb* allele with hemizygous mice for the *Cd19-Cre* transgene, in order to obtain the deletion of the *Csnk2b gene* only in B-cells.

The first thing we observed was a marked splenomegaly, derived by an increase in cellularity and weight of spleens in CK2β KO compared to CTRL mice.

WB and qRT-PCR analysis confirmed that in hematopoietic organs of KO mice, CK2β expression was significantly reduced and, in addition, splenocytes of KO mice presented a substantial reduction of CK2 kinase activity.

Flow cytometry analysis of BM, SP and PB-cells, demonstrated a remarkable reduction of total B-cells in CK2β KO compared to CTRL mice.

In bone marrow, B-lymphocyte reduction interested, in particular, recirculating B-cells, which reside only temporarily in the bone marrow, but, as their name suggests, they normally recirculate.

These results propose, for the first time, that CK2β subunit is necessary for the maintenance of the correct abundance of peripheral B lymphocytes.

Furthermore, these data were confirmed by the analysis of IgM and IgD immunoglobulins in naive B- (IgM$^+$ / IgD$^-$) and recirculating B-cells (IgM$^+$ / IgD$^+$) of bone marrow and spleen.

Analysis showed that there are no differences in the naive B-cell population, while there is a marked reduction of recirculating B-cells in bone marrow and spleen of KO compared to CTRL mice. These data support the idea that CK2 has a crucial role in determining the survival of peripheral B-cells, but not in the ontogeny of B-cells in the bone marrow.

Furthermore, the analysis of bone marrow precursors proB (B220 [+]/ IgM [-] /CKIT [+] / CD25 [-]) and preB (B220[+]/ IgM [-] / cKit [-] / CD25 [+]) showed no differences between KO and CTRL mice, reinforcing the idea that CK2 appears not to be essential for B-cell maturation in the bone marrow, but is critical for correct subsequent stages in B-cell development.

Since we observed a marked reduction of peripheral B-cells, we characterized this population, in particular we analyzed splenic B-cell subpopulations.

Flow cytometry analysis showed that spleens of CK2β KO mice are characterized by a reduction in FOB and an increase in MZB. Specifically, follicular populations are decreased (FoI, FoII, T2), while the marginal populations are increased (MZB, MZP).

This results suggest that CK2 may be involved in addressing immature cells to marginal or follicular differentiation. It is important to notice that there are no differences in T1 B-cells, which represent the peripheral B-cells more similar to the naive. These findings confirm the hypothesis that CK2 is principally involved in peripheral B-cell differentiation. Also histological and immunofluorescence analysis revealed a change in size/shape of splenic follicles and a significant expansion of the inter-follicular, marginal zone areas, which appeared to invade follicles with larger cells.

The requirement of Notch2 for the generation of both precursor and mature marginal zone B-cells led to some intriguing insights about the FOB versus MZB cell transition. Notch2 is required for MZB cell development during B-cell maturation in the spleen [37]. Given this evidence, we demonstrated a significant up-regulation of Notch2 target genes *hes* and *deltx* in CK2β KO compared with CTRL mice. WB analysis showed that Notch2 protein was strongly up-regulated in CK2β KO versus CTRL B-cells. Considering this result, we propose a role for CK2β in Notch2 pathway. In fact it was shown that CK2 phosphorylates Notch in serine 1901 and negatively regulates its functions by dissociating the complex from the DNA [53]. Considering this previous knowledge, we propose that the lack of the β subunit determines an increase of the Notch signal, leading to a prevalence of the marginal phenotype during splenic B lymphocyte differentiation. In addition, functional analysis of GC demonstrated an hypogammaglobulinemia, and, after stimulation, revealed that in KO mice there is a reduction in the number of IgG, demonstrating the existence of anomalies that compromise isotype switching. Among these alterations we also observed a dramatic impairment of BLIMP1 expression, a protein which is important for PC differentiation.

In vivo T-cell dependent response showed a conserved up-regulation of GC markers, such as CD38, GL7 and PNA. Nonetheless, the architecture of reactive follicles was found markedly changed. High throughput RNAseq analysis was also performed and revealed significant alterations in FOB and MZB-regulating pathways.

In conclusion these project shows that the β subunit of protein kinase CK2 is a novel regulator of peripheral B-cell differentiation. CK2β sustains a proper BCR signal, controls the GC reaction, class-switch recombination and somatic hypermutation. Moreover, it negatively regulates Notch2 signaling, acting as a master regulator of follicular/marginal zone architecture and terminal homeostasis of FOB and MZB-cells.

Additional studies are ongoing in our laboratory to elucidate the mechanistic role of CK2 in the physiology and pathobiology of B-cells to define its role in the development of various hematological malignancies.

These brand new findings could improve therapeutic strategies currently used in clinical procedures and pave the way to employ CK2 protein levels as a biomarker to discriminate between normal and malignant blood cells.

6. REFERENCES

1. Allman D., Lindsley R.C., DeMuth W., Rudd K., Shinton S.A., Hardy R.R. (2001). Resolution of three nonproliferative immature splenic B cell subsets reveals multiple selection points during peripheral B cell maturation. *The Journal of Immunology*. 167:6834-6840;

2. **Allman D., Pillai S.** (2008). Peripheral B cell subsets. *Current Opinion in Immunology*. 20:149-157;

3. **Araki K., Okada Y., Araki M., Yamamura K**. (2010). Comparative analysis of right element mutant lox sites on recombination efficiency in embryonic stem cells. *BMC Biotechnology*.10-29;

4. **Batts T.D., Machado H.L., Zhang Y., Creighton C.J., Li Y., Rosen J.M.**. (2011). Stem Cell Antigen-1 (Sca-1) Regulates Mammary Tumor Development and Cell Migration. *Plos*. 6(11):e27841;

5. **Buchou T., Vernet M., Blond O., Jensen H.H., Pointu H., Olsen B.B., Cochet C., Issinger O.G., Boldyreff B.** (2003). Disruption oft he regulatory β subunit of protein kinase CK2 in mice leads to a cell-autonomous defect and early embryonic lethality. *Molecular and Cellular Biology*. 908-915;

6. **Capecchi M.** (2001). Generating mice with targeted mutations. *Nature Medicine*. 7:1086-1090;

7. **Cariappa A., Boboila C., Moran S.T., Liu H., Ning Shi H., Pillai S.** (2007). The recirculating B cell pool contains two functionally distinct, long-lived, posttransitional, follicular B cell populations. *The Journal of Immunology*. 179: 2270-2281;

8. **Carsetti R, Rosado MM, Wardmann H.**(2004). Peripheral development of B-cells in mouse and man. *Immunol Rev.*197:179-91.;

9. Cerutti A., Cols M., Puga I. (2013). Marginal zone B cells: virtues of innatelike antibody-producing lymphocytes. *Nature Reviews Immunology*. 118-132;

10. Di Maira G, Brustolon F, Pinna LA, Ruzzene M. Dephosphorylation and inactivation of Akt/PKB is counteracted by protein kinase CK2 in HEK 293T cells. *Cell Mol Life Sci*. 2009;66:3363-3373

11. **Egawa T., Kawabata K., Kawamoto H., Amada K., Okamoto R., Fujii N., Kishimoto T., Katsura Y., Nagasawa T.** (2001). The earliest stages of B cell development require a chemokine stromal cell-derived factor/pre-B cell growth-stimulating factor. *Nature Reviews Immunology*. 15:323-334;

12. Gotz C, Wagner P, Issinger OG, Montenarh M. p21WAF1/CIP1 interacts with protein kinase CK2. *Oncogene*. 1996;**13**:391-398.

13. Guerra B, Issinger OG. (1999) Protein kinase CK2 and its role in cellular proliferation, development and pathology. *Electrophoresis*. 1999;**20**:391-408

14. **Hardy R.R., Carmack C.E., Shinton S.A., Kemp J.D., Hayakawa K.** (1991) Resolution and characterization of pro-B and pre-pro-B cell stages in normal mouse bone marrow. *The Journal of Experimental Medicine*. 173: 1213-1225; - 70 -

15. **Heise N, De Silva NS, Silva K, Carette A, Simonetti G, Pasparakis M, Klein U.** (2014). **Germinal center B cell maintenance and differentiation are controlled by distinct NF-κB transcription factor subunits**. *J Exp Med*. 183:5630-5643; 211 (10): 2103

16. Heriche JK, Chambaz EM. Protein kinase CK2alpha is a target for the Abl and Bcr-Abl tyrosine kinases. *Oncogene*. 1998;**17**:13-18

17. **Hoek K.L., Carlesso G., Clark E.S., Khan W.N.** (2013). Absence of mature peripheral B cell populations in mice with concomitant defects in B cell receptor and BAFF-R signaling. *The Journal of Immunology*. 183:5630-5643;

18. Homma MK, Li D, Krebs EG, Yuasa Y, Homma Y. Association and regulation of casein kinase 2 activity by adenomatous polyposis coli protein. *Proc Natl Acad Sci U S A*. 2002;**99**:5959-5964.

19. **Kanayama N., Cascalho M., Ohmori H.** (2005). Analysis of marginal zone B cell development in the mouse with limited B cell diversity: role of the antigen receptor signals in the recruitment of B cells to the marginal zone. *The Journal of Immunology*. 174:1438-1445;

20. Katsumoto T., Aikawa Y., Iwama A., Ueda S., Ichikawa H., Ochiya T., Kitabayashi I. (2006). Moz is essential for maintenance of hamopoietic stem cells. *Genes & Development*. 20:1321-1330;

21. **Kim J.E.** (2006). Functional study of gene using inducible Cre system. *Journal of Korean Endocrine Society*. 21:364-369;

22. Kim JS, Eom JI, Cheong JW, et al. (2007) Protein kinase CK2alpha as an unfavorable prognostic marker and novel therapeutic target in acute myeloid leukemia.*Clin Cancer Res*. 2007;**13**:1019-1028

23. **Kühn R., Torres R.M.** (2002).Cre/loxP recombination system and gene targeting, in *Methods in Molecular Biology*. Clarke AR ed. Humana Press Publ. Totowa. USA. 180:175-178;

24. **Litchfield D.W.** (2003). Protein kinase CK2: structure, regulation and role in cellular decisions of life and death. *Biochem Journal*. 369 (Pt 1): 1-15;

25. **Loder F., Mutschker B., Ray R.J., Paige C.J., Sideras P., Torres R., Lamers M.C., Carsetti R.** (1999). B cell development in the spleen takes place in discrete steps and is determined by the quality of B cell receptor-derived signals. *The Rockefeller University Press*. 75-89;

26. **Lund F.E., Randall T.D.** (2010). Effector and regulatory B cells: modulators of CD4+ T cell immunity. *Nature Reviews Immunology*. 236-247;

27. McDonnell MA, Abedin MJ, Melendez M, et al.(2008) Phosphorylation of murine caspase-9 by the protein kinase casein kinase 2 regulates its cleavage by caspase-8. *J Biol Chem*. 2008;**283**:20149-20158

28. **Martin F., Kearny J.F.** (2002). Marginal-zone B cells. *Nature Reviews Immunology*. 323-335;

29. Mebius R.E., Kraal G. (2005). Structure and functions of the spleen. *Nature Reviews Immunology*. 606-616;

30. **Mercier F. E., Ragu C., Scadden D.T.** (2012). The bone marrow at the crossroads of blood and immunity. *Nature Reviews Immunology*. 49-60;

31. **Merrell K.T., Benschop R.J., Gauld S.B., Aviszus K., Decote-Ricardo D.; Wysocki L.J.; Cambier J.C.** (2006). Identification of anergic B cells within a wild-type repertoire. *Nature Reviews Immunology*. 25:953-962; - 71 -

32. Meyer-Bahlburg A., Andrews S.F., Yu K.O.A., Porcelli S.A., Rawlings D.J. (2008). Characterization of a late transitional B cell population highly sensitive to BAFF-mediated homeostatic proliferation. *The Journal of Experimental Medicine*. 155-168;

33. Miyata Y, Nishida E. (2005) CK2 binds, phosphorylates, and regulates its pivotal substrate Cdc37, an Hsp90-cochaperone. *Mol Cell Biochem*. 2005;**274**:171-179.

34. **Murphy K.** *Janeway's Immunobiology*. 8th. Garland Science. 2012.

35. **Nagasawa T. (**2006). Microenvironmental niches in the bone marrow required for B-cell development. *Nature Reviews Immunology*. 107-116;

36. **Piazza F., Manni S., Ruzzene M., Pinna L.A., Gurrieri C., Semenzato G**. (2012). Protein kinase CK2 in hematologic malignancies: reliance on a pivotal cell survival regulator by oncogenic signaling pathways. *Leukemia.* 26 (6): 1174-1179;

37. **Pillai S., Cariappa A.** (2009). The follicular versus marginal zone B lynfocyte cell phate decision. *Nature Reviews Immunology*. 767-777;

38. **Pinna L.A., Allende J.E**. (2009). Protein kinase CK2: an ugly duckling in the kinome pond. *Cellular and Molecular Life Sciences.* 66 (11-12): 1797-1799;

39. **Saito T., Chiba S., Ichikawa M., Kunisato A., Asai T., Shimizu K., Yamaguchi T., Yamamoto G., Seo S., Kumano K.** (2003). Notch2 is preferentially expressed in mature B cells and indispensable for marginal zone B lineage development. *Nature Reviews Immunology*. 18:675-685;

40. Scaglioni PP, Yung TM, Cai LF, et al.(2006) A CK2-dependent mechanism for degradation of the PML tumor suppressor.*Cell*. 2006;**126**:269-283.

41. **Schäffer A.A., Salzer U., Hammarström L., Grimbacher B.** (2007). Deconstructing common variable immunodeficiency by genetic analysis. *Current Opinion in Genetics & Development*. 17: 201-212;

42. **Siebenlist U., Brown K., Claudio E.** (2005). Control of lymphocyte development by nuclear factor-κB. *Nature Reviews Immunology*. 435-445;

43. Silva A, Yunes JA, Cardoso BA, et al.(2008) PTEN posttranslational inactivation and hyperactivation of the PI3K/Akt pathway sustain primary T cell leukemia viability. *J Clin Invest*. 2008;**118**:3762-3774.

44. **Simonetti G, Carette A, Silva K, Wang H, De Silva NS, Heise N, Siebel CW, Shlomchik MJ, Klein U.** (2013). IRF4 controls the positioning of mature B cells in the lymphoid microenvironments by regulating NOTCH2 expression and activity. *J Exp Med*. 2013 2887-902;

45. **Srivastava B., Quinn III W.J., Hazard K., Erikson J., Allman D.** (2005). Characterization of marginal zone B cell precursors. *The Journal of Experimental Medicine*, 1225-1234;

46. **Tokoyoda K., Egawa T., Sugiyama T., Choi B.I., Nagasawa T.** (2004). Cellular niches controlling B lymphocyte behaviour within bone marrow during development. *Nature Reviews Immunity*. 20: 707-718;

47. **Trembley J.H., Wang G., Unger G., Slaton J., Ahmed K.** (2009). CK2: A key player in cancer biology. *Cellular and Molecular Life Sciences.* 66: 1858-1867;

48. Unger GM, Davis AT, Slaton JW, Ahmed K.(2004) Protein kinase CK2 as regulator of cell survival: implications for cancer therapy. *Curr Cancer Drug Targets*. 2004;**4**:77-84.

49. **Yan Wu, Carol Cain-Hom, Lisa Choy, Thijs J. Hagenbeek, et al..** (2010). Therapeutic antibody targeting of individual Notch receptors. *Nature.* 464, 1052-1057 ;

50. Zhang XK, Moussa O, LaRue A, Bradshaw S, Molano I, Spyropoulos DD, Gilkeson GS, Watson DK. (2008). The transcription factor Fli-1 modulates marginal zone and follicular B cell development in mice. *J Immunol.* 181(3):1644-54.

51. Zheng Y, Qin H, Frank SJ, et al. A CK2-dependent mechanism for activation of the JAK-STAT signaling pathway.*Blood*;118:156-166.

52. Ray A, Dittel BN. Isolation of mouse peritoneal cavity cells.(2010) *J Vis Exp.* 10.3791/1488.

53. Ranganathan P, Vasquez-Del Carpio R, Kaplan FM, Wang H, Gupta A, VanWye JD, Capobianco AJ. (2011) Hierarchical phosphorylation within the ankyrin repeat domain defines a phosphoregulatory loop that regulates Notch transcriptional activity. *J Biol Chem.* 286(33):28844-57

Publications

1)Protein Kinase CK2 Protects Multiple Myeloma Cells from ER Stress–Induced Apoptosis and from the Cytotoxic Effect of HSP90 Inhibition through Regulation of the Unfolded Protein Response.

Sabrina Manni, Alessandra Brancalion, Laura Quotti Tubi, Anna Colpo, Laura Pavan,Anna Cabrelle, Elisa Ave, Fortunato Zaffino, Giovanni Di Maira, Maria Ruzze, Fausto Adami,Renato Zambello, Maria Rita Pitari, Pierfrancesco Tassone, Lorenzo A. Pinna, Carmela Gurrieri, Gianpietro Semenzato, and Francesco Piazza.

(*Clin Cancer Res* 2012;18:1888-1900)

2)Protein Kinase CK2 Inhibition Down Modulates the NF-κB and STAT3 Survival Pathways, Enhances the Cellular Proteotoxic Stress and Synergistically Boosts the Cytotoxic Effect of Bortezomib on Multiple Myeloma and Mantle Cell Lymphoma Cells.

Manni S, Brancalion A, Mandato E, Tubi LQ, Colpo A, Pizzi M, Cappellesso R, Zaffino F, Di Maggio SA, Cabrelle A, Marino F, Zambello R, Trentin L, Adami F,Gurrieri C, Semenzato G, Piazza F.

(PLoS One. 2013 Sep 27;8(9):e75280).